THESIS

EQUINE BODY WEIGHT ESTIMATION USING THREE-DIMENSIONAL IMAGES

Submitted by

Kyung-nyer Ku

Department of Clinical Sciences

In partial fulfillment of the requirements

For the Degree of Master of Science

Colorado State University

Fort Collins, Colorado

Summer 2015

Master's Committee:

Advisor: Josie L. Traub-Dargatz
Co-Advisor: Mo Salman

David Alciatore
Tanja Hess

Copyright by Kyung-nyer Ku 2015

All Rights Reserved

ABSTRACT

EQUINE BODY WEIGHT ESTIMATION USING THREE-DIMENSIONAL IMAGES

Accurately estimating the body weight (BW) of a horse is important in order to make appropriate management and treatment decisions. Most field equine veterinarians and experienced equine people, however, visually estimate BW because large animal scales are impractical for field use due to the weight (>80 kg), size (length >200 cm), and cost (>$1,000). There are some alternative BW estimation methods such as a weight tape or BW estimation using a combination of heart girth and body length measurements. These methods, however, have 5 - 15% or even higher margin of error.

According to human studies, there is a high correlation between BW and body volume (BV). Correlation coefficient (R) between these two variables is 0.996-0.998. Our study was designed to develop methods to estimate the BW of horses by using 3D image based BV measurement. 3D imaging technology allows easy and accurate measurement of diverse indices of an object, including the volume. Recent development of Structure-light 3D scanning technology allows 3D scanning of an object as large as 3 by 3 square meter in a short time.

In this study, 3D images of 22 and 11 horses were obtained by using 3D scanning (3DScan) and photogrammetry (2Dto3D), respectively. BV and trunk volume (TV) of the horses were measured from the obtained 3D images. Measurements of BW using five conventional methods (visual estimation, 2 weight tapes (Purina, Shell), estimated BW by using heart girth and body length (Carroll's formula), and a large animal scale) were also conducted, and the data of body condition score (BCS), sex, coat color, and coat type of the horses were collected.

Linear regression models to estimate the BW of the horse based on the volume and other independent variables were developed using regression model stepwise selection procedures ($P<0.05$). Variables selected in 3DScan method were BV, sex, and coat type, and, in 2Dto3D method, BV (TV) was selected. The coefficient of determination of the developed regression models were 0.95 and 0.78-0.82, respectively, and the average percent errors of the predicted BW compared to the true BW of horses were 2.07 % and 2.67 %, respectively. The accuracy of the 3DScan method was significantly more accurate than WT, Carroll's formual, and VE ($P<0.05$).

3D image based BW measurement method had higher accuracy and convenience compared to conventional alternative BW measuring methods. Accurate and easy determination of BW using 3D images will allow for regular BW measurement in the field and allow optimal equine health management by equine stakeholders and practitioners. The 3D images obtained in this study were highly detailed. Further graphical analysis of the obtained 3D images will make it possible to use this technology on automatic evaluation of body condition score, equine conformation evaluation, breed registration, and the study of pharmacokinetics and dynamics of newly developed drugs. This research findings may also have utility for application to wild or zoo animals such as the elephant, rhinoceros, or even the tiger where hands on collection of body weight would be challenging.

ACKNOWLEDGEMENT

I would like to thank the Colorado Racing Commission: Peri-mutual Betting Receipts which provided financial support to conduct this project, and Gyeonggido Provincial Government in South Korea which gave me an amazing opportunity to study for a master's degree at Colorado State University in the USA.

Completion of this project was only possible because of the enormous support from my advisors, Dr. Josie L. Traub-Dargatz and Dr. Mo Salman, and my committee members, Dr. Tanja Hess and Dr. David Alciatore.

Thanks to my friends who gave me a great deal of help, Dana, Hugo, Steve, Sara, April, Samantha, Lei, Nicole, and Cayla. I would not have been able to even start my project without your help.

Thanks to my family, my parents (Chi-hwan Koo, Young-ran Park) and sisters (Kyung-ha Ku, Kyung-Jae Ku, brother-in-law, Jae-whan Kim, and my 7 month niece Sharon) who have always encouraged me to pursue dreams and always believed that I can accomplish my goal.

TABLE OF CONTENTS

LIST OF TABLES

LIST OF FIGURES

CHAPTER I.

LITERATURE REVIEW AND STUDY JUSTIFICATION

1.1. Importance of estimating body weight (BW) in horses

Determination of body weight (BW) is important in evaluating the health status of a horse. In juvenile horses, for example, regular measurement of BW is critically important because it gives fundamental information on the appropriate development of the horse. The development of a juvenile horse depends on adequate nourishment. Nutrition provided to the juvenile horse can affect the performance of the horse for its entire life. If juvenile horses are not provided with adequate nutrition they will fail to reach their full growth potential. If horses are overfed they are predisposed to devastating diseases such as developmental orthopedic diseases (Sillence et al., 2006). Regular measurement of BW is one part of the objective assessment of growth in juvenile horses.

Regular measurement of BW and record keeping over time is also important in adult horses. Estimating BW and monitoring the change in it are needed to determine the amount of feed and feed additives needed by each horse. This is also the basic information needed to calculate correct medication dosages when treatment is required or when a deworming product is administered. Over- or under-dosing of those medications may induce either treatment failure or drug resistance (Kaushal et al., 2001; Runciman and Walton, 2007; Powers, 2009).

A large part of equine management is conducted based on visual estimation of BW. Several epidemiological studies, however, have shown that visual estimation of BW has a large error associated with it (Ellis and Hollands, 1998). There are some substitutive methods to

approximate BW or, to evaluate the fat accumulation of a horse, such as weight tape or body condition score. Measuring BW using a weight tape has a wide margin of error and the accuracy is quite different depending on the breed or stage of growth of horses (Gharahveysi, 2012). Body condition scoring is also problematic because many owners do not accurately assign the BCS. According to several studies, horse owners have a strong tendency to underestimate their horses' weight especially when those horses are overweight (Geor, 2008; Wyse et al., 2008).

Excessive weight is not only a major health problem among people, but it is also a serious factor threatening animal health. Several studies have shown that, especially in developed countries, obesity in companion animals is a major health problem. Forty percent of the canine and feline populations were obese in mid-2000's (German, 2006). Wyse et al. reported that 45% of riding horses in Scotland are too fat (Wyse et al., 2008). Geor et al. also said around 19% of U.S. horses may be obese (Geor, 2008). Overweight horses are predisposed to several diseases and physical dysfunctions, for example, laminitis, osteochondrosis, lowered fertility, or dystocia (Alford et al., 2001; Geor, 2008; Wylie et al., 2012). Sudden BW change is also an important indicator of the change of health status. Sudden BW increase of pasture horses in spring is strongly associated with the occurrence of laminitis (Giles et al., 2014). Regular measurement of BW and adjusting the feeding plan based on the information is, therefore, very important to keep a healthy equine herd.

Regular measurement of BW is, however, not performed well in the field. Several epidemiological studies to estimate the relationship between important diseases of horses, such as laminitis, and BW or BCS have failed to find a link among those factors because there were too many missing values for the BW and BCS in the clinical veterinary records (Slater et al.,

1995; Alford et al., 2001). This finding illustrates how few large animal scales are being used to measure the horse's BW in the field setting.

There are some alternative methods to approximate equine BW such as weight tape or formulas that are based on heart girth and body length measurements. Advantages and disadvantages of those methods will be discussed further in this chapter.

1.2. Conventional BW measurement methods in horses

1.2.1. Large animal scale

A digital large animal scale is the most accurate tool to measure the BW of horses at present. Either 2,500 lb (1000 kg) or 5,000 lb (3000 kg) capacity scales are commonly used for equine BW measurement. These scales usually have 200-500 g display resolution and 0.1-0.3% standard deviation. Large horse facilities such as a veterinary teaching hospital or a stable with many horses may have the equipment but the majority do not have this equipment. One of the reasons that a large animal scale is not available at most horse farms is the high price. The price of a scale with 2,000 lb weighing capacity is more than 1,000 USD, and the price goes up as the model becomes more durable. Aside from the price, scales require a flat and dry space with available source of electrical power and many horse owners do not have that type of space to dedicate to a scale. In addition, the scales are large and heavy so are difficult to move. Ambulatory veterinary practitioners have to transport their equipment from farm to farm and the large size and weight of the large animal scale makes it impractical to move the scale to a horse farm. At least 2 people and a large vehicle are required to transport this equipment.

1.2.2. Combination of heart girth and body length measurement

Due to the cost and practical challenge associated with weighing horses on a large animal scale, several alternative methods have been developed to estimate the BW of horses. One of them is approximating the horse's BW using a formula including the heart girth and body length measurements. Many researchers have worked to develop the most accurate equation model using this method (Gibbs and Householder; Milner and Hewitt, 1969; Carroll and Huntington, 1988; Jones et al., 1989; Ellis and Hollands, 1998; Gharahveysi, 2012). Some examples of these equations are shown in Table 1.1. The reported error of the methods are an average of 5.6 - 10.6% of BW.

In this approach, heart girth is measured by determining the trunk circumference of a horse vertically at or just caudal to the withers. In some studies, half circumference (from the withers to the ventral midline) measurement, followed by doubling the value, was used instead of the entire trunk circumference measurement to minimize the measurement error which sometimes occur from the folding of a measuring tape on the opposite side of the horse from the operator.

This measurement method is known to have better accuracy compared to the weight tape method because the BW difference due to the body length is adjusted. There is, however, still a large error associated with this method e.g. more than 10% of the horse's true BW (Ellis and Hollands, 1998). The accuracy of the measurement is significantly affected by the type and breed of the horse. According to a study which compared the mean BW of 244 horses using several different measuring methods, significant differences were detected depending on the age of the horses and measurement methods. In this study, the mean BWs of horses varied by up to 230 Kg depending on the BW estimation formula used (Gharahveysi, 2012). Another disadvantage of this method is

that the application requires an assistant in order to perform the measurement e.g.one person needs to grasp one end of measuring tape (e.g. point of shoulder) while another person reads the body length on the point of the buttock.

This method, however, is widely used in diverse species of animals, for example, cattle and elephants (Hile et al., 1997). This method is thought to have better accuracy compared to the weight tape method.

1.2.3. Weight tape

Weight tape is a method used to estimate the BW based only on the measurement of heart girth of a horse. On a weight tape, the approximate weights of horses are marked based solely on the girth size. This method is easy to apply, compared to BW estimation using heart girth and body length measurements. Depending on the weight tape manufacturer, BW estimation using the weight tape compared to the true BW may be slightly different. The approximate BW is marked on some types of weight tapes, but other types of weight tape only show approximate BW ranges (figure1.1).

Weight tape method of estimating BW is known to have less accuracy than BW estimation using heart girth and body length measurements. According to several studies that measured the accuracy of weight tapes, the average error of this method is approximately 10.1-12% when compared to the true BW (Milner and Hewitt, 1969; Ellis and Hollands, 1998).

1.2.4. Visual estimation

Visual estimation of the horse's BW is the least accurate, yet it is the most commonly used method of estimating BW. According to an article in 1998 by Pagan et al., 96% of veterinarians and 68% of horsemen primarily use visual estimation to estimate the BW of horses. Many of the

horse BWs were underestimated, and no correlation between the years of experience of the estimator and the accuracy of visual estimation was observed (Pagan J.D.).

According Ellis and Hollands, the average error of the visual estimation was 20.1% when compared to the true BW (Ellis and Hollands, 1998). The amount of error increased up to 22.2% when the withers height of horses was taller than 15 hands. Johnson et al. reported in a short abstract that, among the 695 visual horse BW estimations performed by 139 horsemen or veterinarians, there were 12.5% overestimations and 87.5% underestimations of the BW. The average error was 92 lb in cases of overestimation and 186 lb in cases of underestimation in his study (Johnson et al., 1989).

1.2.5. Body Condition Score (BCS)

BCS was developed to estimate the fat accumulation of domestic animals such as cattle and goats. In horses, BCS is an important criterion to estimate the adequacy of body fat accumulation on broodmares before breeding (Henneke et al., 1981; Henneke et al., 1983). BCS is also an important tool to estimate the health status of horses or to assess the optimal nutritional plan and exercise management (Burkholder, 2000; Christie et al., 2006). BCS is also used in assessing the welfare of the horse in order to determine if there are cases of horse abuse.

The most commonly used BCS system in horses is a method developed by Henneke in 1981 for the purpose of studying the relationship between reproductive efficiency of mares and their body fat accumulations (Henneke et al., 1981). Horse BCS range in Henneke's method results in scoring horses 1-9. A horse that has a BCS 1 is an extremely emaciated horse and BCS 9 is an obviously fat horse (Figure 1.2, Table 1.2) (Henneke et al., 1983). Horses with a BCS of 4-6 are considered normal, but the normal range can depend on the breed and type of use of the horses.

For instance, the ideal BCS of a broodmare is 5.5-7.5, in contrast, the ideal BCS of a stallion is 4-6 (Mendell; Gibbs et al., 2005; McDonnell, 2005).

Besides the Henneke's BCS method, there is also a BCS system where a range of between 0-5 is used (Hardman, 1980). In this method, BCS 0 is very poor condition, BCS 5 is very fat, and BCS 2-3 is considered normal to good body condition. Henneke's method is more commonly used, but there are still equine veterinary practitioners and horsemen who use 0-5 scale BCS (Hardman, 1980). The use of more than one system often results in misinterpretation of the status of horses based on the BCS, even among experienced equine people.

1.2.6. Conclusion

Due to the cost and lack of portability of the large animal scale in the equine industry, there are several alternative methods used in the equine industry. The most commonly used method, visual estimation, has a large margin of error e.g. as high as 20% of the true BW. There are some methods such as weight tape or estimating BW based on the combination of heart girth and body length measurements, but these methods also have a large margin of error when compared to the true BW. BCS is useful to determine the adequacy of body fat accumulation and has been used to provide appropriate management of horses, but this method is inadequate in some cases, for example, calculation of the amount of nutrient supplements or medication to provide to the horse.

Accurate BW measurement is critical for the optimal management and treatment of horses and also for determination of the appropriate management of horses in training. In high performance horses, a slight BW change, for example, as little as a 30 lb change, results in the different ranking in a competition (Pagan J.D.). This means alternative BW measurement methods at

present are not accurate enough to replace a large animal scale since the error associated with these methods is too large to detect a slight BW change. In addition, the range of error of conventional horse BW measuring methods is amplified when a horse's conformation is out of normal range e.g. underweight or overweight. According to Gibbs and Householder, BW of an "extremely heavy fronted, deep hearted and light hipped" mare was 150 lb overestimated when they used the combined hearth girth and body length measurement method (Gibbs and Householder).

The requirement for the development of a new method which is easy to apply and accurate, therefore, is critically needed by the equine industry. In the next part of this chapter, correlation between BW and body volume (BV), and methods to measure the BV are discussed.

1.3. Body Volume (BV) as a method of BW measurement

1.3.1. Correlation between BW and BV

Accurate measurement of BV has long been an interest among various areas of medicine, for example, oncology and public health. Volume of the parts of the body, such as extremities is a useful criteria to measure edema (Clauser et al., 1969). This is important to monitor the existence of lymphedema in a patient of cancer chemotherapy (Sukul et al., 1993; Sander et al., 2002). In public health, BV is used to calculate body density and percentage of body fat. Estimating BV is essential to estimate the body density. Body density is used to estimate the percent of body fat with the least error (Rathbun and Pace, 1945; Ward, 1968).

Several different methods, such as geometric calculation, water displacement, and acoustic plethysmography, are used to measure the BV. Among these methods, water displacement and

acoustic plethysmography are highly accurate. In a study by Katch et al. in 1967, the underwater displacement method showed only 4-33ml variability (Katch et al., 1967). According these studies, the mean body density of a person is approximately 1.051. This value increases as the % body fat decreases, and decreases as the percent body fat increases since the fat density is lower than lean body density (Katch et al., 1967; Wakat et al., 1971).

Body density is required to estimate the percent body fat, but, interestingly, the variance of body density is very small, regardless of how fat or lean a person is. In the study by Katch et al., standard deviation of body density among 18 people was only 0.014 (Katch et al., 1967). In an animal study, body density of guinea pigs ranged from 1.021 to 1.096 when the weight of body fat was between 4 and 275 g (Rathbun and Pace, 1945). This means, regardless the value of body density and percnet body fat of each individual, there is a strong correlation between BW and BV. In fact, there is a strong linear relationship between BW and BV and their correlation coefficient (R) is 0.996-0.998 (Katch et al., 1967; Ward, 1968; Wakat et al., 1971).

1.3.2. BV measurement methods

1.3.2.1. Geometric calculation method

Geometric calculation method is a volume measuring method of an irregular shaped object using the geometric figure of the object. In human medicine, this method is usually used to estimate the volume of a simple shaped body part such as arms or legs. There are several applications for BV measurement using the geometric method (Figure 1.3). The most commonly used methods are the disk model method and the frustum sign model method. In the disk model method, several disks were drawn 3cm apart on an object and the sum of the volumes of all disks with 3cm height is estimated as the approximate volume of the object. In the case of the frustum sign

model method, a frustum is drawn based on the upper and lower surface areas of the object. The volume of the frustum becomes the approximate volume of the object (Sander et al., 2002).

According to the body extremity studies, the correlation of these methods with the true volume (water displacement method was used to measure gold standard values) was between 0.91-0.99. Even though the water displacement method is considered as a gold standard method to measure the volume of an object; in the clinical field, some believe that geometric calculation method has much higher practicability due to its simplicity and easy application. The water displacement method is more difficult to apply, and a mistake in application induces a large margin of error. Spilling of water, position change, or movement of the subject, for example, easily result in measurement error. There is also a danger of cross infection among patients when the water and the equipment are used without proper sanitization between applications (Deltombe et al., 2007).

1.3.2.2. Water displacement method

There are two approaches to measure the BV of an object using the water displacement method. One of them is placing the object into water and measuring the increased water volume. Increased water volume is the same as the volume of an object. Another method is hydrodensitometry. In this approach, the weight of an object is measured both outside and inside of the water. The weight difference between out of water weight and in water weight is the volume of an object (Behnke et al., 1942). To measure the accurate BW of a live object, not only the rigidness of an object during the measurement, but also synchronizing the temperature of water and an object is important. Angle and position of an object in the water also affects the accuracy of the measurement (King, 1993; Deltombe et al., 2007).

Water displacement method for measuring BV of people was well studied in mid 1900s and, at that time, a majority of the subjects were either athletes or military personnel. The results of those studies showed a high level of accuracy and the measurement variability was under several grams (Katch et al., 1967; Ward, 1968; Wakat et al., 1971). This method, however, has limited applicability. Only conscious adults are appropriate subjects for the use of this method. The method should not be used for measuring BV of an unconscious person, an infant, a child, a person who has hydrophobia, or one who has skin infection (Deltombe et al., 2007). In addition, a small disturbance on the water surface from a slight movement of a person causes errors in the measurement (Goldman and Buskirk, 1961). There is also a statistically significant difference of the measured volume depending on the temperature of water (King, 1993).

1.3.2.3. Acoustic plethysmography (air-displacement plethysmography)

The theory of acoustic plethysmography is similar to the water displacement method. Once a subject is introduced into a chamber, the volume of the subject displaces the air volume. In addition to the displaced volume measurement, in acoustic plethysmography, acoustic signal change is also measured to estimate the change of air density in the chamber.

In acoustic plethysmography, difference of the temperature between the subject and air, air pressure, and relative humidity cause error in the volume measurement. When this method was first developed, the approximate error was 2.5%. This amount of error in BV results in more than 10% change in the estimated percent body fat of the subject (Gnaedinger et al., 1963). This method was, therefore, considered to have too large a margin of error to be used in body composition studies and was barely used until late 1980 (Sheng et al., 1988). This method, however, was later adjusted to improve the accuracy. Since mid-1990, acoustic plethysmography has been considered to have, at least, the same level of accuracy as the water displacement

method (McCrory et al., 1995; Biaggi et al., 1999). In Dempster and Aikens's study in 1995, for example, the error of this method compared to the true BV was estimated at only 0.005-0.133% (Dempster and Aitkens, 1995). In a recent study, this method was successfully used to measure the air volume of the respiration of neonatal mice even though the tidal volume was only 12.6 μm (Daubenspeck et al., 2008).

In terms of application of acoustic plethysmography, this method has the same limitations as the water displacement method. The object is required to be at a standstill for accurate measurement, and the object should be located inside of a chamber for the measurement. These restrictions make it almost impossible to measure the volume of a live large animal using acoustic plethysmography.

1.3.2.4. 3D scanning

In the clinical field, there are several methods to measure the volume of a body or an organ using 3D images; for example, magnetic resonance imaging (MRI), computerized tomography (CT), or ultrasonography. These methods are, however, very expensive to use. 3D imaging of human body for BV measurement using a comparatively inexpensive 3D scanner has been studied since the early 2,000's.

Wells et al. showed 3D scanning as a method to measure BV. In his study, the accuracy of 3D scanning was slightly lower than water displacement, or acoustic plethysmography, but the standard error was low at 0.2-0.5%. This method was considered promising due to the ease of use and short time requirement to perform the measurement compared to other methods (Wells et al., 2000)(Wells et al., 2000)(Wells et al., 2000). 3D scanning, however, had some problems in a number of studies, for example, even minor extremity movement of an object induced error on

the 3D image and this error resulted in a corresponding error in the measured volume (Allen et al., 2003; Tong et al., 2012). Accuracy of 3D scanning, and error correction method, however, have rapidly improved through both the enhancement of the 3D scanners and the development of reconstruction techniques to correct errors on 3D images (Kazhdan et al., 2006; Izadi et al., 2011; Tong et al., 2012).

There are several brands of human body 3D scanning devices, and it takes under half a minute to perform the scanning (Istook and Hwang, 2001). These devices use 6 or more 3D scanners to decrease the time to obtain intact whole body 3D images. 3D images are obtained while the object is still, and acquired partial images from each scan are then assembled into a single image using imaging software.

Currently, 3D scanning of the human body is used to estimate percent body fat as well as to analyze the body composition, conformation, and local fat accumulation to give accurate and personalized dietary and exercise advice (www.bodyvolume.com). This method is also used to find previously unidentified human remains in forensic investigations. A 3D image of partial or the complete body provides useful data to estimate age, sex, and race of the person (Sholts et al., 2010).

1.3.3. Conclusion

The literature on BV measurement was to determine if BV measurement was an appropriate and easy method to estimate BW of horses and compare it to conventional methods of estimating equine BW. The correlation between BW and BV is very high, thus accurate estimation of BW can be obtained if the accurate BV measurement can be made (Katch et al., 1967; Wakat et al., 1971). The only remaining question was whether accurate BV measurement of horses was

feasible and also practical. Estimating BV for the purpose of determining BW would be worthless if the BV measurement is more difficult or more expensive than BW measurement using a large animal scale.

Even though the BV measurement methods which were discussed in this chapter have high accuracy, all of those methods except 3D scanning are impractical for field application. Both underwater displacement and acoustic plethysmography require the subject remain still while in a small enclosed space. In underwater displacement, for example, the subject has to be submerged completely in water. It is not feasible to place a horse underwater or in an acoustic plethysmography unit without using general anesthesia.

The 3D scanning studies reviewed in this chapter were conducted under optimal environmental conditions and included the use of several scanners to minimize the scanning time. The subjects were also people who followed instructions to remain stationary. A review of 3D scanning method showed that it may have a slightly lower accuracy compared with other methods of measuring BV but the error is very small. Based on the review of the literature it appears that the application of 3D scanning to horses will not be as easy as 3D scanning of people yet maybe feasible. The advantage of 3D scanning is the person performing the scanning does not need to intensively control the horse or the scanning environment. A horse can stand idle while the scanning is applied and the scanning can be conducted at any place. One other positive factor is, due to the rapid evolution within the 3D scanning industry, portable and inexpensive 3D scanners are now commercially available (Sansoni et al., 2009).

Accuracy of horse 3D scanning and estimated BV from that image may have a higher margin of error than human studies. The ease of application and the low price of 3D scanners, however,

make the study of 3D scanning of horses to estimate the BW worthwhile. The next section of this chapter explores the potential of using 3D scanners as a tool to estimate horse BV. Scanning theory, types of available 3D scanner, and the current use of this equipment are also reviewed.

1.4. 3D scanning

1.4.1. 3D scanning and the scanning theory

3D images provide true geometric information about an object. They minimize the inaccurate interpretation of the objects which happens quite often when reading 2D images to analyze 3D objects. There are several different methods for performing 3D scanning of an object, and each method has advantages and disadvantages (Table 1.3). Choice of a method should be based on several important considerations; such as the size, texture, type, or shape of an object in order to maximize the representativeness of obtained 3D images of the true object.

3D scanners are categorized into several types based on the type of light used, characteristics of the light projection, method for obtaining the image, and the algorithm of 3D image construction. The most commonly used 3D imaging technologies, at present, are structured light, laser triangulation, time-of-flight (ToF), and photogrammetry. Among these technologies, structured light, laser triangulation, and photogrammetry use triangulation algorithm to construct a complete 3D image. Time-of flight uses time-difference between projection and acquisition of light (Jecić and Drvar, 2003; Sansoni et al., 2009).

A structured-light 3D scanner uses projections of specifically designed light pattern to obtain the geometric map (3D image) of an object. At the beginning stage of this technology, the most commonly used light pattern was fringe pattern. Fringe patterned light and its distortion on the

surface of the scanning object is recorded by a camera. In addition, the size of triangles which were made from 3 points; a light projector, a point on the surface of the scanning object where the projected light met, and a camera, is calculated to measure the distance of an object from the 3D scanner and also to measure the geometric characteristics of the object (Figure 1.4). Consequently, a 3D image of the object is obtained. The most popular structured-light scanner at present is Kinect,[a] and some other scanners[b] that use the same 3D scanning technology as Kinect. In the scanner, Kinect, the light source is an infrared laser, and multiple dot patterns are projected from the scanner to an object (Figure 1.4). Depending on the distance and geometric angle of the 3D scanning object, the size, the level of blur, and shape of the projected dotted pattern through infrared (IR) projector is changed. The changed light pattern is acquired through an IR camera, and the acquired image is analyzed to build a 3D image of the object. Simultaneous 3D mapping is available with this technology (Ramos, 2012; Smisek et al., 2013).

There are several advantages of structured-light 3D scanners, for example, the price is low, the scanning speed is fast, and the size of the scanner is small. Before the development of this technology, 3D scanners were very expensive. Most of the 3D scanners were not available to individual customers, but only used for quality control in the manufacturing industry. There were some comparatively low cost 3D scanners such as NextEngine 3D scanner[c], but the range of scanning was less than 50cm, and it also was very time consuming to use. The price of structured-light 3D scanners such as Kinect[a] or Structure Sensor[b] is less than $400. The unit is small and easy to handle. It includes the software that allows the scanning of an object while

[a] Kinect, Microsoft corporation, Redmond, Washington, USA
[b] Structure Sensor, Occipital Inc., San Francisco, CA and Boulder, CO, USA; PrimeSense 3D Sensor, PrimeSense, Israel.
[c] 3D Scanner HD, NextEngine Inc., 401 Wilshire Blvd., Ninth Floor, Santa Monica, California 90401

moving the 3D scanner. There are commercial 3D scanning devices that allow imaging of the human body based on this technology. Only a short time is required to perform the 3D scanning of a complete human body e.g. between 7-30 seconds (Istook and Hwang, 2001).

The ideal 3D scanning range of Kinect from the object is between 40cm-3m, and, practically, it is recommended to be between 1-3m from the object. In this given range, the error in 3D image is less than 2cm. The range of error multiplies as the distance from the object increases, and once the distance is over 5m, the acquired image loses most of its 3D characteristics, almost flat (Khoshelham, 2011). The amount of error is different depending on the surface texture, light reflexion, and the movement of the object. Structured light 3D scanners intrinsically have error since the empty space between dots or fringe patterns is not scanned. Missing parts from this intrinsic error are reconstructed through approximate estimation (Cui and Stricker, 2011). This 3D scanning technology is known to have less accuracy compared to laser triangulation 3D scanners. Laser triangulation 3D scanners have less than 1 mm error, and have millimicron level of accuracy.

The theory of 3D image acquisition using laser triangulation technology is basically the same as that for structured light 3D scanners. Laser triangulation 3D scanners use a single or a few dots or lines to obtain depth information of an object. The advantage of this technology is its high accuracy. The accuracy of a fixed 3D laser scanner is high enough to be used for quality control in the manufacturing industry. The error is less than 1 mm (Wang et al., 2006b). Even inexpensive laser 3D scanners such as NextEngine[c] have only 1-2mm of error (Polo and Felicísimo, 2012). Another advantage of a laser 3D scanner is that the quality of 3D image is less compromised by the texture and light reflection on the surface of the object than structured light 3D scanners (Jecić and Drvar, 2003). This type of 3D scanners are, however, very expensive if

an object as large as a horse is to be scanned. The price range can easily go over $10,000. There are some inexpensive models, but the machines can only accurately scan small solid objects such as a toy (Polo and Felicísimo, 2012; Munkelt et al., 2014).

Time-of-flight (ToF) 3D scanners calculate the time difference between the projection and acquisition of returned light after the light is reflected from the object of 3D scanning. This method is used to scan a wide area or a large object, for example, geometry mapping or 3D modeling of a large building, and the scanning range is between several hundred meters to kilometers. The most famous ToF 3D scanners in the field are the FARO laser tracker[d] and Leica Scan Station[e]. These models scan 100-300m of space in several minutes and the error of surface precision of an object is less than 2mm according to the fact sheets.[f] These high-end ToF scanners, however, are even more expensive than the laser triangulation 3D scanners, for example, the retail price of Leica Scan Station is over $100,000. The major disadvantage of the ToF scanning is that its accuracy is comparatively low when this method is applied on 3D mapping of a small object located nearby to the scanner. Since this method measures the time difference of light reflection, and the speed of light is faster than 200,000 km/s, even a small error in the time measurement induces a large error on 3D mapping of an object. This method, therefore, has not been used often in scanning of small, nearby objects such as a statue or a person. Recent development of reconstruction technology improved the quality of acquired 3D image after an additional image correction process (Wulf and Wagner, 2003; Cui et al., 2013).

[d] FARO laser tracker, FARO, Lake Mary, FL, USA
[e] Leica Scan Station, Leica, Wetzlar, Germany.
[f] http://hds.leica-geosystems.com

Photogrammetry builds a 3D image based on several 2D images (photographs). In this method, triangulation algorithm is used to build a 3D image. Several identical points of the object are detected from its 2D images which are obtained from different angles and largely overlapped with each other. Those identical points are located in a hypothetical space based on the least sum of squares algorithm and geometric figure of the object is analyzed based on the potential geometric locations of those identical points in order to minimize the probability of error. Consequently, the most probable 3D figure was drawn based on the finalized 3D locations of the identical points. This process is conducted by specially designed software. Examples of current, free reconstruction software is 123D Catch[g] and Visual SFM.[h]

The advantage of photogrammetry is the fact that the application of this method does not require the purchase of a 3D scanning device. Photographs taken from a cellular phone are adequate for use in photogrammetry. The number of photographs required differ depending on the software used. As few as 18 photographs are used to build a 3D image when using 123D Catch software. Eighteen photographs, however, maybe inadequate to build a complete 3D model of an object. In addition, 3D construction using photogrammetry can fail if there are not distinct points on the object. 3D construction of monotone spherical shape ball, for example, may not produce a 3D image in photogrammetry because the several identical points in photographs taken from different angles will not be recognized as distinct aspects of this object. Lastly, this method does not have a function to measure the absolute value of an object. The size of a constructed 3D image should be adjusted using a reference object with known size if this method is applied for the purpose of volumetric, or other size measurements.

[g] 123D Catch, Autodesk, San Rafael, CA, USA
[h] Changchang Wu, http://ccwu.me/vsfm/

Recent technological developments have made it possible to build a 3D model in an easy and inexpensive way. There are many different types of 3D scanners now available. Inexpensive 3D scanners usually have a higher margin of error compared with high-end, expensive 3D scanners. Development of reconstruction and error correction algorithms such as Poisson reconstruction, volumetric reconstruction methods, or global non-rigid alignment has made it possible to correct the missing parts or an error of raw 3D images (Wilhelms and Van Gelder, 1992; Curless and Levoy, 1996; Kazhdan et al., 2006; Brown and Rusinkiewicz, 2007). There are now software packages with a built-in reconstruction function that use these algorithms. These methods are still improving and are becoming more user-friendly. KinectFusion[i], for example, makes it possible to accurately 3D scan a moving object (Izadi et al., 2011). The various types of 3D scanners and software differ in their accuracy, applicability, scanning time, and scanning field. The selection of a 3D scanner should be made based on, e.g., the purpose of 3D scanning, required resolution, available budget to purchase the equipment and size of the object to be scanned.

1.4.2. Categories of 3D scanner use

3D scanners are used in diverse industries and the diversity of uses is continuously expanding. Imaging modality is being used in art, the apparel industry, manufacturing, cultural reservation, forensic science and medicine (Sansoni et al., 2009). Depending on the purpose and required 3D scanning speed, different types of 3D scanners are chosen based on their accuracy, speed, and scanning range.

[i] Kinect fusion, Microsoft corporation, Redmond, Washington, USA, https://msdn.microsoft.com/en-us/library/dn188670.aspx

In 2000, for example, there was the “digital Michelangelo project” described by Levoy et al. A portable laser 3D scanner was used to build fine and accurate 3D images of several statues of Michelangelo. The team succeeded in obtaining 3D images of those statues in 0.25mm accuracy, but it was a labor intensive project that required several months to complete and required the efforts of many art and engineering experts (Levoy et al., 2000). This and similar projects make it possible to produce replicas of art products with only micron level error. These methods can be used for education and also for the reconstruction of damaged pieces of art. 3D imaging and iterative closest point (ICP) algorithm are, for example, used for reassembling fractured objects. This method is very useful not only in the art industry, but also in forensic science (Huang et al., 2006).

Laser 3D scanning with its high accuracy, is used for quality control and detection of defective products in the manufacturing industry. In terms of quality control of products, there has been an attempt to monitor the quality and potential defects of agricultural products such as pears using 3D scanning (Uyar and Erdoğdu, 2009). 3D scanning and consequent 3D modeling are very useful in the building of molds and samples in diverse industries (Wang et al., 2006a).

Until early 2000, 3D scanning was a slow and laborious procedure. With the advent of structured-light 3D scanner and laser range scanner, there has been a marked change in technology. This technologic advances along with the use of reconstruction software to correct the errors have made it possible to scan a large object in a short time. Some examples of using these type of scanners are 3D mapping of the outside and inside of a building, cave mapping for mine development, and analyzing the pattern of tree growth in a forest (Hubert et al., 1983; Magnusson et al., 2007; Seidel et al., 2011; Henry et al., 2012; Taylor, 2012). The fast and inexpensive structured-light 3D scanner have made it possible to image human bodies on a mass

production scale in the areas of medicine and apparel industry (Istook and Hwang, 2001; Yu et al., 2003). The scanning of a large number of people has allowed human body pattern analysis. Extensive efforts on human body 3D scanning and accumulated data for more than a decade made it possible to estimate the body shape of people while they are in attire (Hasler et al., 2009).

In addition, photogrammetry has its own future potential. Since building a 3D image using photogrammetry is based only on photographs, there is no limitation on the size of the object in this technology. Photogrammetry not only allows for 3D imaging of a small object but also makes it available to build a 3D image of large objects such as a large historic building or even a mountain if a set of high resolution photographs are obtained for the process (Liu and Kang; Martín et al., 2013).

1.4.3. Use of 3D scanning in human medicine and veterinary medicine

3D scanning has many diverse uses in human medicine and veterinary medicine. One major example of that use is 3D construction of internal organs by using one of the following modalities: magnetic resonance imaging (MRI), computed tomography (CT), or ultrasonography with consequent analysis of the volume, flow, and normality/abnormality of these imaged organs (Hatcher and Aboudara, 2004). It is now feasible to obtain accurate geometric map and depth data of the human or animal body by using these state-of-the-art technologies. These methods are, however, very expensive so they are only used when more conventional and inexpensive imaging method such as radiographs fail to result in a diagnosis.

3D imaging using inexpensive 3D scanners has been applied in human medicine for almost a decade. This has resulted in accurate 3D images of the human body (Wells et al., 2000; Yu et al.,

2003). 3D images of human body can be used to measure the body density and percent body fat and they provide useful data to tailor an individualized diet and health plan. 3D imaging of a human body also makes it possible to measure the partial or the entire body surface area of the subject accurately and easily. Those data can be used to calculate the exact dosage of chemotherapy, topical medications, or estimate the amount of tissue required for skin transplantation. In addition, the volume measurement of the body extremity using 3D scanning can be a useful tool to diagnose lymphedema in cancer patients as previously discussed in this chapter. The estimation of accurate body surface area or BV was very difficult in the past but 3D scanning makes them easier and more accurate (Wells et al., 2000; Yu et al., 2003).

There have been no studies applying 3D scanning of animals except CT, MRI, and ultrasonography. There could be multiple reasons why 3D scanning has not been applied to veterinary subjects but one likely reason is concern that the animal may not remain still while being scanned. Remaining stationary while 3D scanning is performed is fundamental part of the scanning process in order to obtain an accurate 3D image. Even a slight movement of an object can induce a large error in the resulting image (Tong et al., 2012).

1.4.4. Feasibility of 3D scanning for the estimation of BW of horses.

Studies using 3D scanning of the human body showed high accuracy in both BV and body surface area measurement (Yu et al., 2003). According to a study by Wells et al., the standard error when measuring the human BV using 3D scanning was under 0.5% (Wells et al., 2000)(Wells et al., 2000)(Wells et al., 2000). In case of Kinect, if a 2 by 2 by 2m size object is scanned at 2m distance with the 3D scanner, up to 1.05% of error will be observed when the volume is measured from the 3D image (Khoshelham, 2011). If an accurate BW is estimated from BV, this margin of error is still very low compared to the error associate with other

conventional equine BW measuring methods (Carroll and Huntington, 1988; Gharahveysi, 2012). Even if the error that is associated with 3D images of a live horse is larger than that reported for a human, there still is a high probability that 3D imaging will be much more accurate than conventional equine BW measuring methods.

Another advantage of developing 3D scanning method to estimate the BW of horses is ease of use in the field setting. A 3D scanner such as Structure Sensor[b] is a very small device which is highly portable and easy to use. The device currently costs only $340. It is very affordable even for a small scale stable owner. Once the method for measuring equine BW is developed, it will have a great utility and can be used in diverse areas of equine industry.

1.4.5. Conclusion

There can be some obstacles to apply 3D scanning on the live horse, such as the lack of stationary position of the horse during scanning; but 3D scanning of live animals such as horses would hypothetically be feasible if a 3D scanner had a short scanning time and reconstruction methods is used. A structured-light 3D scanner e.g. Kinect[a] or Structure Sensor[b], likely is an optimal scanner to use to obtain 3D images of live animals. In terms of other 3D scanning methods, laser scanners have higher accuracy but are comparatively slow and more expensive than the structured-light 3D scanner. Taking a longer time to create images than the structured-light 3D scanner would likely induce a large error if used to scan a live animal. In addition, the price of a laser scanner is higher than the cost of the large animal scales currently available and it makes laser scanners less feasible to be used to measure the equine BW rather than that of a large animal scale (Polo and Felicísimo, 2012). ToF 3D scanners have a large error when the object is near to the scanner and highly accurate ToF scanners are extremely expensive (Sansoni et al., 2009; Cui et al., 2013). In the case of photogrammetry, this method is intriguing because the

equipment needed (a camera or a cellular phone) would be readily available to most equine owners and equine veterinary practitioners but it may be difficult to obtain an intact 3D image from 2D photographs if only one photography device is used because it is likely that movement of the horse will occur while obtaining the 2D photographs.

Structured-light 3D scanners have lower accuracy compared to laser triangulation scanners and lower size of 3D scanning field compared to ToF scanners. Distance between a structured-light 3D scanner and the scanning object should be kept less than 4 m because the scanned image losses its 3D characteristics once the distance gets larger. It means scanning an object larger than 3.5-6m is not possible all at once using this 3D scanner since the angle of the field of view is only 45°-58°. The error of the volume measurement of an object using the 3D image obtained using a structured-light 3D scanner would be up to 1.03% if the object is being scanned at a distance of 2m from the 3D scanner (Khoshelham, 2011). Two meter is a distance which we are considering as a required distance between a structured-light 3D scanner and a horse to obtain an entire horse 3D image all at once. Expected margin of error and the field of view of structured-light 3D scanners can be a disadvantage depending on the field of use but are not limitations for the purpose of equine 3D scanning and consequently BW measurement using the 3D images. The high 3D scanning speed of the structured-light 3D scanner is an advantage because the 3D image is more likely to be obtained before a horse moves (Istook and Hwang, 2001; Yu et al., 2003).

A goal of this thesis project is to perform 3D scans of horses using an inexpensive and hand-held structured-light 3D scanner and determine the correlation between horse BW and estimated BV using 3D scanning technology.

1.5. Tables and figures

Table 1.1. Summary of heart girth and body length based methods for estimation of equine BW.

Author	Year published	Measurement	# of horses	Formula	Error/Accuracy
Miller and Hewitt	1969	Girth (behind the withers) Body length (point of shoulder to point of hip)	108	$\text{BW (lb)} = \frac{\text{Girth}^2 \times \text{Length (inch)}}{228.1}$	5.6% (Average absolute % error)
Gibbs and Householder	-	Girth (highest point of the withers), body length (point of shoulder to point of buttock)	12	$\text{BW (lb)} = \frac{\text{Girth}^2 \times \text{Length (inch)}}{330}$	Average 24 lb (data were not clearly given)
Carroll and Huntington	1988	Heart girth Body length (point of shoulder to tuber ischii)	372	$\text{BW (kg)} = \frac{\text{Girth}^2 \times \text{Length (cm)}}{11877.4}$	R^2=0.9*
Jones et al.	1989	Umbilical girth Body length (elbow to tuber ischii)	53	$\text{BW (kg)} = \frac{\text{Girth}^{1.78} \times \text{Length}^{0.97}\ \text{(cm)}}{3011}$	Error of 53% of horses was under ∓20 kg. 94% were under ∓60 kg error. No horse had over ∓100 kg error
Ellis and Hollands	1998	Carroll and Huntington's Formula	600	$\text{BW (kg)} = \frac{\text{Girth}^2 \times \text{Length (cm)}}{11877.4}$	% error 10.6**
Ellis and Hollands	1998	Spillers weight tape	600	Weight tape	% error 9.3**
Ellis and Hollands	1998	Dalton weight tape	600	Weight tape	% error 8.1**
Ellis and Hollands	1998	Visual estimation	100	Visual estimation	% error 20.1**
Miller and Hewitt	1969	Master Feeds tape	108	Weight tape	10.9% (Average absolute % error)
Miller and Hewitt	1969	AGWAY tape	108	Weight tape	10.1% (Average absolute % error)

* True BW vs. Predicted BW using the formula

** Percentage error compared to the true BW

Table 1.2. The method to determine the Body Condition Score (BCS) by Henneke et al. (1983). The method for estimating the BCS on horses is well described in the Henneke's study and is summarized below.

Score	Status	Vertebrae	Ribs	Tailhead	Withers	Shoulders	Neck
1	Poor: extremely emaciated	Prominent projection of bony structure	Prominent projection of bony structure	Prominent projection of bony structure	Bone noticeable	Bone noticeable	Bone noticeable
2	Very thin: emaciated	Prominent projection of bony structure (slight fat covering on the base of the spinous, transverse process)	Prominent projection of bony structure	Prominent projection of bony structure	Faintly discernable	Faintly discernable	Faintly discernable
3	Thin	Body structure is Easily discernable. Transverse processes are not felt.	Easily discernable Slight fat cover	Prominent but not visually identifiable of each vertebrae	Accentuated	Accentuated	Accentuated
4	Moderately thin	Negative crease	Faint visible outline	Fat is felt around	Not obviously thin	Not obviously thin	Not obviously thin
5	Moderate	Level	Not visible but easily felt	Fat spongy feeling	Round over spinous process	Blend smooth into body	Blend smooth into body
6	Moderately fleshy	Slight crease down the back	Fat felt spongy	Soft fat feeling	Fat deposition along the side	Fat deposition on behind	Fat deposition sides
7	Fleshy	Crease down the back	Ribs can be felt but fat filling is noticeable	Soft fat feeling	Fat deposition along withers	Fat deposition on behind	Fat deposition along the neck
8	Fat	Crease down the back	Difficult to feel	Very soft fat	Fat deposition along withers	Behind is filled with fat	Noticeable thickening
9	Extremely fat	Obvious crease down the back	Patchy fat accumulation	Fat bulged	Fat bulged	Fat bulged	Fat bulged

Adopted from Henneke et al., 1983

Table 1.3. Imaging characteristics of four different 3D image construction methods.

Method	3D image construction algorithm	Type of projected light used	Scanning range	Approximate Cost in US dollar	Strength	Weakness
Structured light	Triangulation	Patterned (e.g. fringe pattern) visible lay or laser	Medium: 40cm-4m (ideally 1-3m)	$400	easy and fast	Lower accuracy than laser triangulation
Laser triangulation	Triangulation	Dotted or lined laser	Small: > 40cm	$10,000	High accuracy	Comparatively slow scanning speed
Time-of-flight	Time difference**	Laser	Large: 100-300m	$100,000	Best for 3D scanning a large object	Accuracy is low in 3D scanning of a small, and short distanced*** object
Photogrammetry	Triangulation	Photography	Small-large	Zero	Inexpensive No limitation due to the size of the object	3D image acquisition may fail No object size representation (reference is required)

* Scanning range varies even among the scanners of the same method. Scanning range written in this table is based on 3D scanners which represent the type of the scanners listed (structured light: Microsoft Kinect, Laser triangulation: NextEngine 3D Scanner HD, Time-of-flight: Leica Scan Station).

** Time difference between the projection and acquisition of the light.

*** Short distance between the object and the origin of the light projection/acquisition.

1.1.a

1.1.b

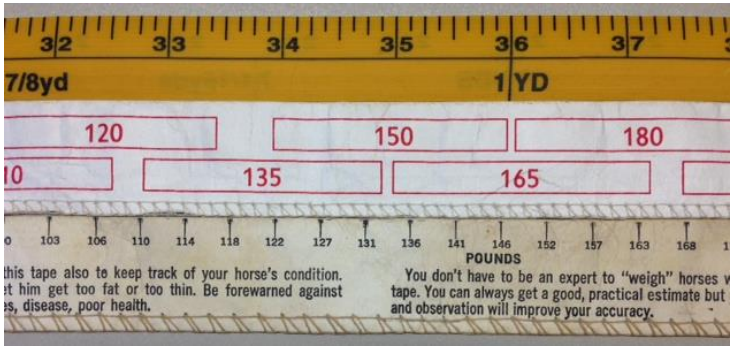

1.1.c

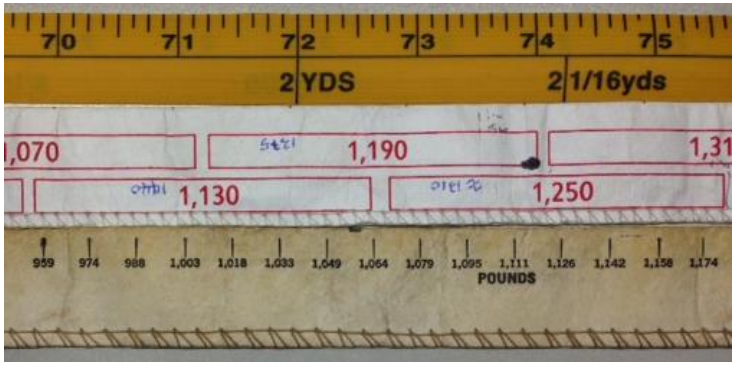

Figure 1.1. Measuring tape and weight tape.

Most of the commercially available measuring and weight tapes in the USA provide an inch/hand height or lb BW as the outcome (Figure 1.1.a). For weight tapes, the estimated outcome is approximate BW of horses in lb. Some tapes provide an approximate range for the estimated BW (Figure 1.1.b. The tape in the middle). In other types of weight tape, approximate BW is indicated with the weight (Figure 1.1.b. The tape at the bottom). Estimated BW for the same horse varies based on which weight tape is used. This difference gets larger as the circumference of the heart girth increases. Approximate BW estimation from use of the two weight tapes illustrated in this figure, are not identical. In a horse with heart girth 71-74 inches, the estimated BW differs by 125 lbs (Figure 1.1.c).

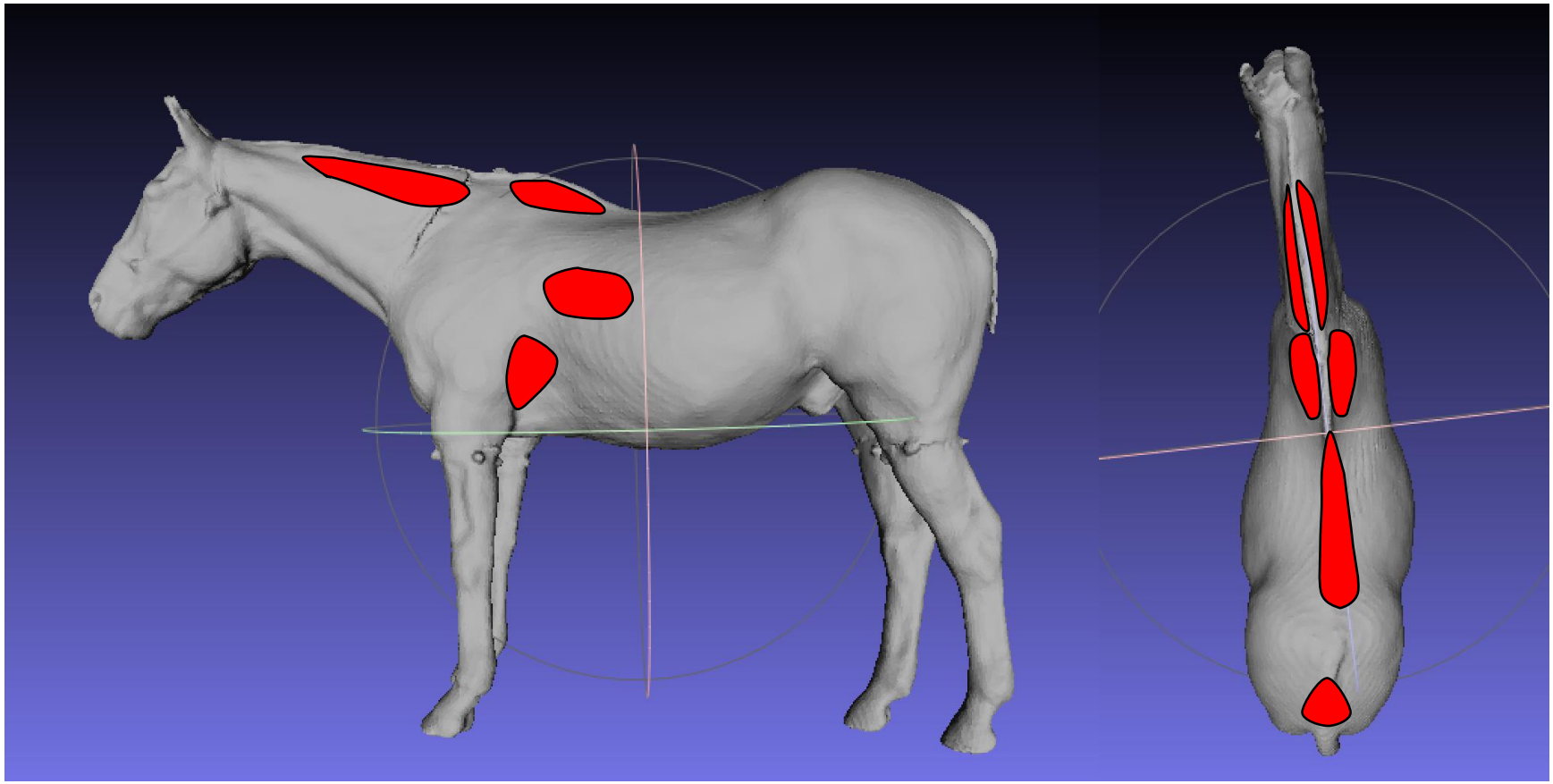

Figure 1.2. The method to determine the Body Condition Score (BCS) by Henneke et al. (1983). This figure shows the six locations of the horse's body (Along the neck, the withers, crease down back, tailhead, ribs, and behind the shoulder) used to determine the body fat accumulation of the horse and thus to determine the BCS of the horse.

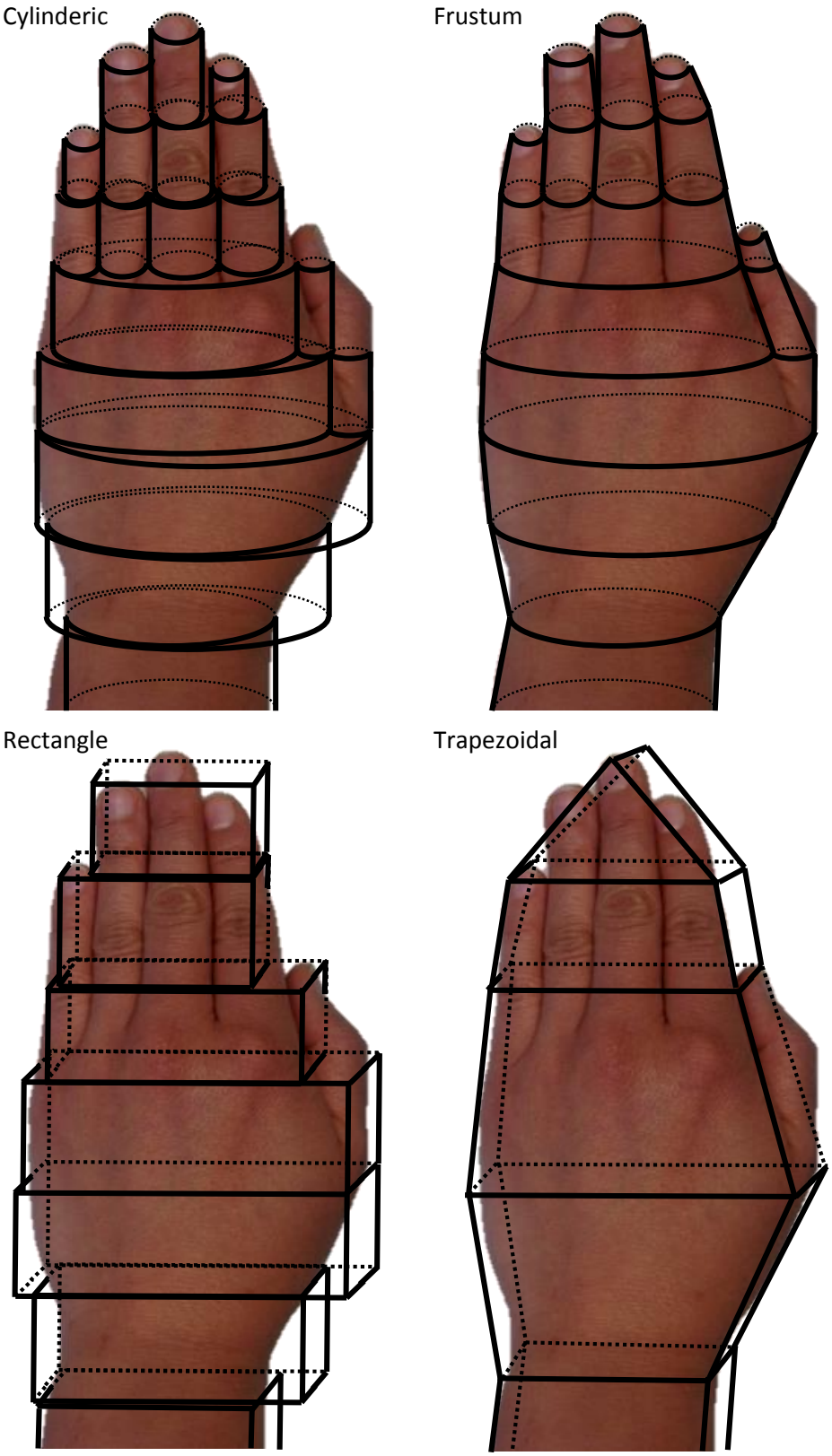

Figure 1.3. Several types of geometric calculation methods. These methods are used to estimate the volume of hand and arm. Cylinderic and Frustum methods are most commonly used.

1.4.a. principle of triangulation

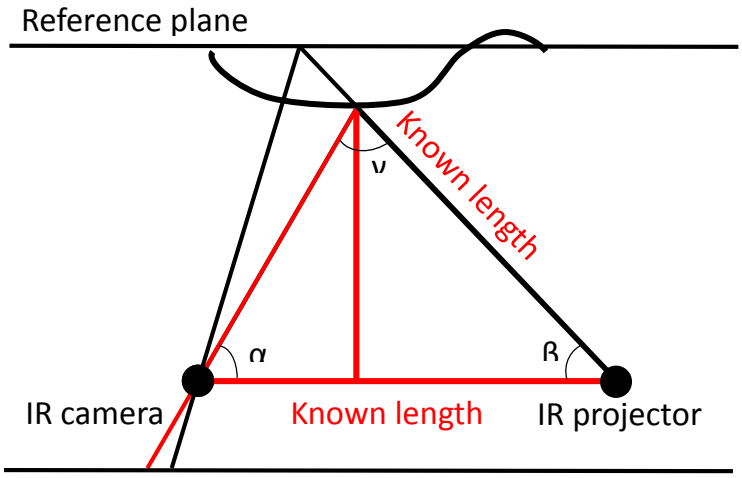

1.4.b. principle of geometric and depth measurement of a fringe pattered structured-light 3D scanner.

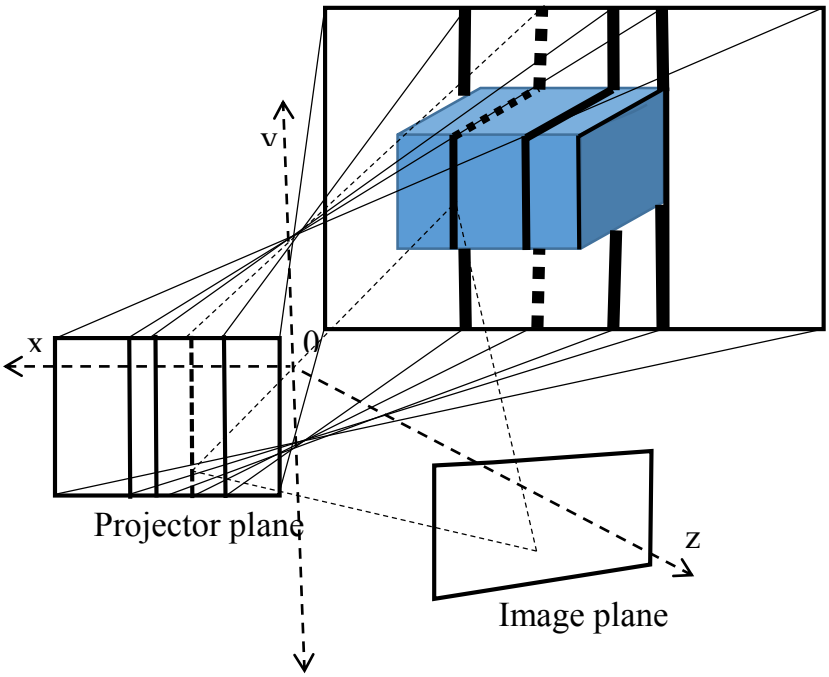

Figure 1.4. The principles of 3D scanning. Figure 1.4.a shows the principle of triangulation. In Structured-light 3D scanners, numbers of fringe or dotted patters are projected. This make it available to scan a large object in a short time. The figure 1.4.b shows the principle of geometric and depth measurement of a structured-light 3D scanner with several fringe patterns.

REFERENCES

Alford, P. et al. 2001. A multicenter, matched case-control study of risk factors for equine laminitis. Prev. Vet. Med. 49: 209-222.

Allen, B., B. Curless, and Z. Popović. 2003. The space of human body shapes: reconstruction and parameterization from range scans. In: ACM Transactions on Graphics (TOG). 22: 587-594.

Behnke, A., B. Feen, and W. Welham. 1942. The specific gravity of healthy men: body weight÷ volume as an index of obesity. JAMA 118: 495-498.

Biaggi, R. R. et al. 1999. Comparison of air-displacement plethysmography with hydrostatic weighing and bioelectrical impedance analysis for the assessment of body composition in healthy adults. Am. J. Clin. Nutr. 69: 898-903.

Brown, B. J., and S. Rusinkiewicz. 2007. Global non-rigid alignment of 3-D scans. ACM Transactions on Graphics (TOG) 26: 21.

Burkholder, W. J. 2000. Timely Topics in Nutrition. Use of body condition scores in clinical assessment of the provision of optimal nutrition. J. Am. Vet. Med. Assoc. 217: 650-654.

Carroll, C., and P. Huntington. 1988. Body condition scoring and weight estimation of horses. Equine Vet. J. 20: 41-45.

Christie, J. L. et al. 2006. Management factors affecting stereotypies and body condition score in nonracing horses in Prince Edward Island. Can. Vet. J. 47: 136.

Clauser, C. E., J. T. McConville, and J. W. Young. 1969. Weight, volume, and center of mass of segments of the human body, DTIC Document.

Cui, Y., S. Schuon, S. Thrun, D. Stricker, and C. Theobalt. 2013. Algorithms for 3d shape scanning with a depth camera. IEEE Trans. Pattern. Anal. Mach. Intell. 35: 1039-1050.

Cui, Y., and D. Stricker. 2011. 3d shape scanning with a kinect. In: ACM SIGGRAPH 2011 Posters. p 57.

Curless, B., and M. Levoy. 1996. A volumetric method for building complex models from range images. Proc. 23rd annual conf. Computer graphics and interactive techniques. p 303-312.

Daubenspeck, J. A., A. Li, and E. E. Nattie. 2008. Acoustic plethysmography measures breathing in unrestrained neonatal mice. J. Appl. Physiol. 104: 262-268.

Deltombe, T. et al. 2007. Reliability and Limits of Agreement of Circuferential, Water Displacement, and Optoelectronic Volumetry in the Measurement of Upper Limb Lymphedema. Lymphology 40: 26-34.

Dempster, P., and S. Aitkens. 1995. A new air displacement method for the determination of human body composition. Med. Sci. Sports Exerc. 27: 1692-1697.

Ellis, J., and T. Hollands. 1998. Accuracy of different methods of estimating the weight of horses. Vet. Rec. 143: 335-336.

Geor, R. J. 2008. Metabolic predispositions to laminitis in horses and ponies: obesity, insulin resistance and metabolic syndromes. J. equine Vet. Sci. 28: 753-759.

German, A. J. 2006. The growing problem of obesity in dogs and cats. J. Nutr. 136: 1940S-1946S.

Gharahveysi, S. 2012. Compare of Different Formulas of Estimating the Weight of Horses by the Iranian Arab Horse Data. JAVA 11: 2429-2431.

Gibbs, P., and D. Householder. Estimating Horse Body Weight with a Simple Formula. http://www.aspcapro.org/sites/pro/files/estimating_horse_body_weight.pdf (Accessed 4 April 2015). Texas A&M.

Gibbs, P. G., G. D. Potter, and M. Vogelsang. 2005. Nutritional and Feeding Management of Broodmares. http://scholar.google.com/scholar?q=Nutritional+and+Feeding+Management+of+Broodmares&btnG=&hl=en&as_sdt=0%2C6 (Accessed 4 April 2015).

Giles, S. L., S. A. Rands, C. J. Nicol, and P. A. Harris. 2014. Obesity prevalence and associated risk factors in outdoor living domestic horses and ponies. Peer J. 2: e299.

Gnaedinger, R. et al. 1963. Determination of body density by air displacement, helium dilution, and underwater weighing. Ann. N. Y. Acad. Sci. 110: 96-108.

Goldman, R., and E. Buskirk. 1961. Body volume measurement by underwater weighing: description of a method. Techniques for measuring body composition: 78-89.

Hardman, A. C. L. 1980. Equine nutrition. Michael Joseph.

Hasler, N., C. Stoll, B. Rosenhahn, T. Thormählen, and H.-P. Seidel. 2009. Estimating body shape of dressed humans. Computers & Graphics 33: 211-216.

Hatcher, D. C., and C. L. Aboudara. 2004. Diagnosis goes digital. Am. J. Orthod. Dentofacial Orthop. 125: 512-515.

Henneke, D., G. Potter, and J. Kreider. 1981. Rebreeding efficiency in mares fed different levels of energy during late gestation. Proc. 7th Eq. Nutr. Physiol. Symp. Virginia State Univ. p 101-104.

Henneke, D., G. Potter, J. Kreider, and B. Yeates. 1983. Relationship between condition score, physical measurements and body fat percentage in mares. Equine Vet. J. 15: 371-372.

Henry, P., M. Krainin, E. Herbst, X. Ren, and D. Fox. 2012. RGB-D mapping: Using Kinect-style depth cameras for dense 3D modeling of indoor environments. Int. J. Robot. Res. 31: 647-663.

Hile, M. E., H. F. Hintz, and H. N. Erb. 1997. Predicting body weight from body measurements in Asian elephants (Elephas maximus). J Zoo. Wildl. Med.: 424-427.

Huang, Q.-X., S. Flöry, N. Gelfand, M. Hofer, and H. Pottmann. 2006. Reassembling fractured objects by geometric matching. ACM Transactions on Graphics (TOG) 25: 569-578.

Hubert, H. B., M. Feinleib, P. M. McNamara, and W. P. Castelli. 1983. Obesity as an independent risk factor for cardiovascular disease: a 26-year follow-up of participants in the Framingham Heart Study. Circulation 67: 968-977.

Istook, C. L., and S.-J. Hwang. 2001. 3D body scanning systems with application to the apparel industry. JFMM 5: 120-132.

Izadi, S. et al. 2011. KinectFusion: real-time 3D reconstruction and interaction using a moving depth camera. Proc. 24th annual ACM symposium on User interface software and technology. p 559-568.

Jecić, S., and N. Drvar. 2003. The assessment of structured light and laser scanning methods in 3D shape measurements. Proc. 4th International Congress of Croatian Society of Mechanics. p 237-244.

Johnson, E., R. Asquith, and J. Kivipelto. 1989. Accuracy of weight determination of equids by visual estimation. Proc. 11th ENPS. Stillwater, Oklahma. p 240.

Jones, R., T. Lawrence, A. Veevers, N. Cleave, and J. Hall. 1989. Accuracy of prediction of the liveweight of horses from body measurements. Vet. Rec. 125: 549-553.

Katch, F., E. D. Michael, and S. M. Horvath. 1967. Estimation of body volume by underwater weighing: description of a simple method. J. Appl. Physiol. 23: 811-813.

Kaushal, R. et al. 2001. Medication errors and adverse drug events in pediatric inpatients. JAMA 285: 2114-2120.

Kazhdan, M., M. Bolitho, and H. Hoppe. 2006. Poisson surface reconstruction. Proc. of the fourth Symp. Geom. Process.

Khoshelham, K. 2011. Accuracy analysis of kinect depth data. In: ISPRS workshop laser scanning. p W12.

King, T. I. 1993. The effect of water temperature on hand volume during volumetric measurement using the water displacement method. J. Hand Ther. 6: 202-204.

Levoy, M. et al. 2000. The digital Michelangelo project: 3D scanning of large statues. In: Proceedings of the 27th annual conference on Computer graphics and interactive techniques. p 131-144.

Liu, Y., and J. Kang. Application of Photogrammetry: 3D Modeling of a Historic Building. In: Construction Research Congress 2014 at Construction in a Global Network. p 219-228.

Magnusson, M., A. Lilienthal, and T. Duckett. 2007. Scan registration for autonomous mining vehicles using 3D-NDT. J. Field Robot. 24: 803-827.

Martín, S., H. Uzkeda, J. Poblet, M. Bulnes, and R. Rubio. 2013. Construction of accurate geological cross-sections along trenches, cliffs and mountain slopes using photogrammetry. Computers & Geosciences 51: 90-100.

McCrory, M. A., T. D. Gomez, E. M. Bernauer, and P. A. Molé. 1995. Evaluation of a new air displacement plethysmograph for measuring human body composition. Med. Sci. Sports Exerc. 27: 1686-1691.

McDonnell, S. M. 2005. Techniques for Extending the Breeding Career of Aging and Disabled Stallions. Clin. Tech. Equine. Pract. 4: 269-276.

Mendell, C. A Better "Weigh". http://homesforhorses.org/wp-content/uploads/BCS.pdf (Accessed on April 4 2015).

Milner, J., and D. Hewitt. 1969. Weight of horses: improved estimates based on girth and length. Can. Vet. J. 10: 314.

Munkelt, C., B. Kleiner, T. Torhallsson, P. Kühmstedt, and G. Notni. 2014. Handheld 3D Scanning with Automatic Multi-View Registration Based on Optical and Inertial Pose Estimation. Fringe 2013. p 809-814. Springer.

Pagan J.D., J. S., Duren S. What does your horse weigh? www.ker.com/library/advances/113 (Accessed April 29 2015).

Polo, M.-E., and Á. M. Felicísimo. 2012. Analysis of uncertainty and repeatability of a low-cost 3d laser scanner. Sensors 12: 9046-9054.

Powers, J. H. 2009. Risk perception and inappropriate antimicrobial use: yes, it can hurt. Clin. Infect. Dis. 48: 1350-1353.

Ramos, E. 2012. Kinect Basics Arduino and Kinect Projects. p 23-34. Springer.

Rathbun, E. N., and N. Pace. 1945. Studies on body composition I. The determination of total body fat by means of the body specific gravity. J. Biol. Chem. 158: 667-676.

Runciman, B., and M. Walton. 2007. Safety and ethics in healthcare: a guide to getting it right. Ashgate Publishing, Ltd.

Sander, A. P., N. M. Hajer, K. Hemenway, and A. C. Miller. 2002. Upper-extremity volume measurements in women with lymphedema: a comparison of measurements obtained via water displacement with geometrically determined volume. Phys. Ther. 82: 1201-1212.

Sansoni, G., M. Trebeschi, and F. Docchio. 2009. State-of-the-art and applications of 3D imaging sensors in industry, cultural heritage, medicine, and criminal investigation. Sensors 9: 568-601.

Seidel, D., F. Beyer, D. Hertel, S. Fleck, and C. Leuschner. 2011. 3D-laser scanning: A non-destructive method for studying above-ground biomass and growth of juvenile trees. Agr. forest Meteorol. 151: 1305-1311.

Sheng, H.-P., A. L. Adolph, and C. Garza. 1988. Body volume and fat-free mass determinations by acoustic plethysmography. Pediatr. Res. 24: 85-89.

Sholts, S. B., S. K. Wärmländer, L. M. Flores, K. W. Miller, and P. L. Walker. 2010. Variation in the measurement of cranial volume and surface area using 3D laser scanning technology. J. Forensic Sci. 55: 871-876.

Sillence, M., G. Noble, and C. McGowan. 2006. Fast food and fat fillies: the ills of western civilisation. Vet. J. 172: 396-397.

Slater, M. R., D. Hood, and G. Carter. 1995. Descriptive epidemiological study of equine laminitis. Equine Vet. J. 27: 364-367.

Smisek, J., M. Jancosek, and T. Pajdla. 2013. 3D with Kinect Consumer Depth Cameras for Computer Vision. p 3-25. Springer.

Sukul, D. K., P. T. den Hoed, E. Johannes, R. Van Dolder, and E. Benda. 1993. Direct and indirect methods for the quantification of leg volume: comparison between water displacement volumetry, the disk model method and the frustum sign model method, using the correlation coefficient and the limits of agreement. J. Biomed. Eng. 15: 477-480.

Taylor, M. W. 2012. 3D surface modeling of a giant redwood trunk. The magazine of the native tree society No. 2. p 101.

Tong, J., J. Zhou, L. Liu, Z. Pan, and H. Yan. 2012. Scanning 3d full human bodies using kinects. Visualization and Computer Graphics, IEEE Trans. Pattern. Anal. Mach. Intell. 18: 643-650.

Uyar, R., and F. Erdoğdu. 2009. Potential use of 3-dimensional scanners for food process modeling. J. Food Eng. 93: 337-343.

Wakat, D. K., R. E. Johnson, H. J. Krzywicki, and L. I. Gerber. 1971. Correlation between body volume and body mass in men. Am. J. Clin. Nutr. 24: 1308-1312.

Wang, J. et al. 2006a. Validation of a 3-dimensional photonic scanner for the measurement of body volumes, dimensions, and percentage body fat. Am. J. Clin. Nutr. 83: 809-816.

Wang, Y.-C., M.-S. Wei, Y.-Y. Jiang, Y.-H. Chang, and Y.-H. Fan. 2006b. Automatic Measurement System using a Laser Scan Instrument for Ceramic Bearings. Laser and Fiber-Optical Networks Modeling, 8-th International Conference on Laser and Fiber-Optical Networks Modeling. p 66-69.

Ward, C. L. 1968. Obese or overweight? Aerosp. Med. 39: 680-682.

Wilhelms, J., and A. Van Gelder. 1992. Octrees for faster isosurface generation. ACM Transactions on Graphics (TOG) 11: 201-227.

Wulf, O., and B. Wagner. 2003. Fast 3D scanning methods for laser measurement systems. In: International conference on control systems and computer science (CSCS14). p 2-5.

Wylie, C. E., S. N. Collins, K. L. Verheyen, and J. R. Newton. 2012. Risk factors for equine laminitis: a systematic review with quality appraisal of published evidence. Vet. J. 193: 58-66.

Wyse, C., K. McNie, V. Tannahil, J. Murray, and S. Love. 2008. Prevalence of obesity in riding horses in Scotland. Vet. Rec. 162: 590.

Yu, C.-Y., Y.-H. Lo, and W.-K. Chiou. 2003. The 3D scanner for measuring body surface area: a simplified calculation in the Chinese adult. Appl. Ergon. 34: 273-278.

CHAPTER II.

DEVELOPMENT OF AN EQUINE BW MEASUREMENT METHOD USING THREE-DIMENSIONAL SCANNING TECHNOLOGY

2.1. Introduction

2.1.1. Background

Accurately measuring body weight (BW) is a fundamental part of best management practices for horses. BW is a key component for nutritional planning, determining growth status and detecting the presence of disease. For the equine veterinarian this information is also important for accurate calculation of dosage of medications. Over- or under-estimation of BW results in medication errors that carry the potential hazard of inducing drug related intoxication, antibacterial or anthelmintic drug resistance, or treatment failure (Kaushal et al., 2001).

Accurate measurement of equine BW, however, has long been a difficult task since large animal scales are not readily available in the field due to their price, size, and lack of easy portability. Therefore, methods that give approximate BW, such as a weight tape or a formula based on combined girth and body length measurements, have long been used. Studies have shown, however, that these methods have an average of 6-11% error compared to the true BW (Milner and Hewitt, 1969; Carroll and Huntington, 1988). The large error associated with the use of conventional alternative methods of estimating equine BW makes it difficult to monitor equine BW accurately over time; this may result in delayed medical evaluation and corrective action for sick or undernourished horses. Therefore, an accurate and easily portable method to determine a horse's BW is needed.

BW is highly correlated with body volume (BV) and their relationship was well documented in human studies. The correlation coefficient (R) between BV and BW was found to be 0.996-0.998 (Katch et al., 1967; Wakat et al., 1971). In those studies, BV was measured using a water displacement method, but Wells showed that measurement of BV using 3D scanning was also highly accurate (Wells et al., 2000). If the volume of horses can be accurately measured using 3D scanning, these data can be used to then calculate BW.

3D scanning is widely used in diverse industries such as automobile manufacturing, architecture, and in textiles (Wells et al., 2000; Tikuisis et al., 2001; Uyar and Erdoğdu, 2009; Sholts et al., 2010; Seidel et al., 2011). Cutting-edge 3D scanners can detect even micron-level differences in the scanned object, but these instruments are very expensive and lack portability. On the other hand, there are 3D scanners[j] that are inexpensive and can be hand-held (Wells et al., 2000; Munkelt et al., 2014). Inexpensive 3D scanners have lower resolution compared to their counterparts but still have millimeter-level accuracy and are user friendly. Once a 3D image is obtained, it is easy to measure the diverse indices of the scanned item such as volume, surface area, height, length and width. 3D scanning, therefore, has the potential to be a very convenient, accurate and portable method to estimate the horse BW, something that could easily be used in field situations.

This study was designed to develop a method of determining equine BW using an inexpensive handheld 3D scanner. This method is expected to overcome the limitations of conventional methods of measuring equine BW. The use of a handheld 3D scanner to calculate equine BW

[j] Some examples of these hand-held 3D scanners are Structure Sensor® (Structure Sensor, Occipital Inc., San Francisco, CA and Boulder, CO, USA, http://structure.io/) or Sense® (3D systems, Rock Hill, SC, USA, http://www.geomagic.com/en/)

eliminates the limitations experienced with large animal scales in terms of high price and lack of convenience in the field. In addition, the high accuracy of 3D scanning overcomes the inaccuracies of conventionally used equine BW measurement methods (Gibbs and Householder; Ellis and Hollands, 1998; Gharahveysi, 2012). The method developed through this research will, in consequence, help to decrease the potential for malpractice or poor equine management and improve the welfare of horses.

2.1.2. Hypothesis

A. Equine BW measurement using 3D scanning is accurate, inexpensive, and easy to use compared to conventional methods for estimating equine BW.

2.1.3. Objectives

A. To obtain accurate 3D images of horses using an inexpensive handheld 3D scanner.

B. To estimate the volume of horses using the obtained 3D images.

C. To develop a linear regression model to estimate the BW of horses based on body volume (BV) as estimated from the 3D images.

2.2. Materials and methods

2.2.1. Sample size and target population

Sample size was determined based on the power and sample size calculation of a regression model. Expected power was 0.9, expected minimum correlations between predictor variables and dependent variable was set to 0.7, and the maximum number of predictor variables was set as five. A statistics package[k] was used for the sample size determination. The determined sample size was twenty-one. In this study, twenty-two horses were used. Twenty of these horses were

[k] SAS, version 9.3, SAS Institute Inc., Cary, NC, USA

owned by Colorado State University (CSU) as education/study horses and two horses were privately owned horses residing in Fort Collins, Colorado. This study group included ten polo horses, six therapeutic riding horses, three research horses from the Equine Reproduction Laboratory, one dressage horse and two pleasure riding horses. There were fifteen mares and seven geldings. The breeds included mostly American Quarter Horse or Thoroughbred-Quarter Horse crosses and one Hanoverian. These horses were selected based on their availability during the planned study dates.

The number of horses used as well as the study procedure were approved by the institutional animal care and use committee (IACUC) at CSU. An animal use plan for this study was properly documented and examined. Animals used in this study were neither tranquilized nor anesthetized. Data collected for this study was obtained between September and December 2014.

2.2.2. 3D scanning

2.2.2.1. Preparation of horses

All of the study horses owned by CSU were kept in square paddocks with sheds for shading, and average of 3-4 horses were housed in each paddock. On a study day, two horses from the same paddock were brought into an indoor arena using a rope halter and lead to handle the horses. The horses were loosely tied to hitching rail poles in a tie area located on the west side of the building. The horses were tied 4-5 m apart. The horses were then lightly groomed and their tails were wrapped using an elastic bandage. In addition, 21 small white cylindrical markers were placed on the body. Five markers were placed around the lower neck and four were placed on each leg between the shoulder and carpus or the between the stifle and tarsus (Figure 2.1). The

markers were approximately 2 cm in diameter and 2 cm in height and were secured on the body using an elastic band and/or tape.

2.2.2.2. Measurement of BW and BCS

The BW of each study horse was measured using a digital large animal scale.[l] This scale has a capacity of up to 1500 kg and the display resolution of 0.5 kg. The previous calibration date of the scale was February 6, 2014. The scale had not been moved since that time and this study was conducted 7-10 month from the calibration date. The BW measurement was conducted three times for each horse. Among those three measurements the median value was considered as a true BW (i.e.; gold standard BW).

The body condition score (BCS) for each horse was determined by three people who used Henneke's method (Figure 2.2, Table 2.1) (Henneke et al., 1981; Henneke et al., 1983). These people were either experienced horsemen or a veterinarian, and their understanding of the procedure was refreshed through informational brochures.[m] Each person estimated the BCS once per horse; therefore each horse had three independent BCS estimation. The median value among those three values was considered as the true BCS of the horse.

For each horse all the BW and BCS measurements were conducted primarily on the same day as the 3D scanning. In rare instances one or two people conducted the BCS measurement either a day prior or after the 3D scanning as fit their schedule. Even though the same measurement date

[l] Model 700, True-test, Mount Wellington, New Zealand, http://group.tru-test.com/en
[m] Equine body condition score poster, The Horse Media Group LLC, http://www.thehorse.com/free-reports/30154/equine-body-condition-score-poster

was preferred, a difference of one day was considered acceptable since the BCS was not likely to change in a day.

In addition to the BW and BCS measurements, sex (mare, gelding), coat type (summer, winter), and coat color (light, dark) of each horse was also recorded. For coat color black, sorrel, bay or chestnut was recorded as dark, and appaloosa, roan, or paint was recorded as light.

2.2.2.3. 3D scanning

3D scanning of the horses was conducted in an open space (approximate size 5.5m×14m) in front of the tie area (Figure 2.3). 3D scanning was conducted 3 times on each horse as other measurements and all three 3D scanning was conducted on the same day.

After each horse was prepared as described above, the handler led it to an open space. The horse and the handler stood in the middle of that space while the 3D scanning was conducted. The handler stood on the left side of the horse at a location between the neck and shoulder and approximately 30cm lateral to the horse. The handler held the lead rope loosely. Occasionally when a horse moved and caused several instances of 3D scanning failure, the handler shortened the lead rope and tried to calm the horse and minimize its movement. Horses were allowed to stand in their natural standing position.

A handheld structured-light infrared light scanner Structure Sensor[n], was used for the 3D scanning. Structure Sensor[n] requires a connection to a mobile device to scan an object. For this study, an iPad[o] was connected to the 3D scanner and a mobile device application[p] was used to

[n] Structure Sensor, Occipital Inc., San Francisco, CA and Boulder, CO, USA, http://structure.io/
[o] iPad, Apple Inc., Cupertino, CA, USA, https://www.apple.com/
[p] Scanner, Occipital Inc., San Francisco, CA and Boulder, CO, USA, https://itunes.apple.com/us/app/scanner-structure-sensor-sample/id891169722?mt=8

3D scan each horse. Scanning of four body segments, body, head/neck, both forelimbs, and both hindlimbs was conducted separately.

Before the scanning of a horse began, the field of scanning was set to include 5-21 cylindrical markers in each body segment for 3D scanning. The head/neck 3D scanning field was set to include 5 markers placed on the neck, the trunk scanning field was set to include all 5 neck markers and 16 leg markers, the forelimb scanning field was set to include 8 markers placed on the forelimbs, and the hindlimb scanning included 8 hindlimb markers. Once the scanning field was well set, the operator started the scan. Since the scan was displayed real time on the iPad screen, the operator walked around the scanning area while simultaneously adjusting the scanning speed and distance between the horse and the scanner. Distance between the scanner and the horse was maintained at approximately 0.5-2m.

3D images of the trunk, head, forelimbs, and hindlimbs were obtained, and every scan was repeated three times per horse. When a 3D scan of a body region was completed, the 3D image file was e-mailed as an attachment to the lead investigator before another scan was begun. All those files were later saved on a computer hard drive. Each set of segmental body 3D images (a set included an image of the head, trunk, forelimbs, and hindlimbs) was grouped and assembled into a whole body 3D image. Three sets of partial body 3D images were obtained per horse, thus the total number of sets was 66 for 22 horses.

2.2.2.4. Process of the scanned 3D image

The four partial body 3D images were imported together into a 3D image software, Meshlab[q], and point-based gluing alignment was conducted to create a whole body 3D image of each horse (Cignoni et al., 2008). The markers included in the scans were used as gluing alignment points.

Once a well-aligned 3D image of a horse was obtained, the partial images were merged to create a complete image (Figure 2.4). During this process, any 3D image of a non-horse part, for example a knot of the halter, part of a tie pole, or a hand of the handler, was erased. The whole body 3D image was then transferred to Blender.[r] Using Blender, small faces (particles of 3D images) which were created due to scanning noise but were not part of the main image, were deleted. The cleaned image was transferred to Meshlab, and Poisson surface reconstruction was applied to fill any holes and missing parts in the 3D image to create a watertight 3D image of each horse (Kazhdan et al., 2006). For this process the octree depth was set as 11 (Wilhelms and Van Gelder, 1992). After a waterproof complete horse 3D image was obtained, that image was rescaled to 1000 times the original image. Rescaling was conducted because scanning creates an image that is exactly 0.001 times smaller than the true object.

Lastly, the face number of the reconstructed horse 3D image was reduced by 100,000 times to shrink the file size without losing much of the image detail. The quadric edge collapse decimation tool in Meshlab was used for this process. The original file size was 150 megabytes and the number of faces was around 1,000,000, but the file size was decreased to less than 2Mb after the face reduction procedure. In this process the volume of the 3D image was slightly

[q] Meshlab, Istituto di Scienza e Tecnologie dell'Informazione (Institute of Information Science and Technology), Italian National Research Council (CNR), Pisa, Italy, http://meshlab.sourceforge.net/
[r] Blender 2.71, Blender Foundation, Amsterdam, Netherland, http://www.blender.org/

decreased, too, but the level was only around 60ml (40-80ml). The face-reduced 3D images were saved as a final model and used in the next steps.

From the complete equine 3D image, trunk 3D images were also created. To create a trunk image, a complete 3D image was cut and processed so that only the trunk was retained. The original image was cut at the thoracic inlet, dorsally at the withers, ventrally at the lowest point of the belly, and at the point of buttocks. The head, neck, legs and tail separated from the original 3D image during this process were deleted, and the remaining trunk 3D image was saved as a separate file.

2.2.3. Volume measurement

Volume measurement using the 3D images was conducted using either Meshlab or Netfabb Basic.[s] Complete body volume (BV), and trunk volume (TV) were both measured. The volume of each horse was recorded in liters down to the ml level.

2.2.4. Statistical analysis

Multiple linear regression models were developed to predict the BW of horses using volume (BV or TV) and/or other variables. A statistics package[t] was used for all statistical analyses. In the regression model selection procedure, true BW was set as a response variable (i.e., dependent variable, Y), and volume (either BV or TV), sex, BCS, coat type and coat color were used as potential predictor variables (i.e. independent variable. X_n). Among independent variables, volume was a numeric variable. BCS, sex, coat type and coat color were originally categorical variables, but were treated as numeric variables (BCS= 4-8.5. 0.5 span, sex (mare=0, gelding=1),

[s] Netfabb Basic, Netfabb company, Lupburg, Germany, http://www.netfabb.com/
[t] SAS, version 9.3, SAS Institute Inc., Cary, NC, USA

coat type (summer coat=0, winter coat=1), coat color (dark=0, light=1). Models were developed using a function, Proc GLMselect, in the statistics package, SAS, with stepwise selection. Criteria for the addition or removal of the variable as well as the statistical significance was $P<0.05$.

2.3. Results

2.3.1. 3D scanning

Movement of the horse during 3D scanning caused image distortion or 3D scanning failure, but many quality 3D images were obtained without any movement (Figure 2.5). When the image distortion was minimal, the image was corrected using 3D image software, e.g., Meshlab or Geomagic Studio[u] (Figure 2.6). The most difficult body part to scan was the head and neck because some horses constantly moved their head toward the 3D scanning operator while the scanning was conducted. Overall, there was no case where 3D scanning of a horse failed.

Total sixty-six highly detailed 3D images were obtained using the 3D scanning and image processing procedure (Figures 2.7). The image quality was high, clear, and reflected true 3D information for each horse. Even very slight variations on the body such as the spinous processes of thoracic and lumbar vertebrae, rib cage, muscle bundles and their divisions, and joints were well detailed in the 3D images.

[u] Geomagic Studio, 3D systems, Rock Hill, SC, USA, http://www.geomagic.com/en/

2.3.2. BW, BCS, and BV measurement

Mean BW and standard deviation (SD) of the 22 horses based on the large animal scale was 525.61 ± 60.73 kg. Mean BCS$\pm$SD of those horses was 5.95 ± 1.06. Mean BV of the horses measured from the 3D images was 555.58 liters and the SD was 64.82 liters. In the case of trunk volume (TV), mean and SD was 477.74 ± 58.84 liters.

2.3.3. Multiple linear regression model

Selected independent variables in the multiple regression model using stepwise procedure were BV, coat type, sex, and coat color. Coat color, however, was not included in the final model because the effect of this variable was minimal, and also because it also could be easily misclassified since there are so many varieties of coat color of horses. An equation to estimate the BW from the developed regression model is below. Coefficient of determination (R^2) of this model is 0.95 (Figure 2.8). This model shows that horses with a winter coat averaged 30.3 liters greater volume than horses with a summer coat when the values of BV and sex were held constant, and geldings were 14.23 kg heavier than mares of the same volume when the coat type was held constant.

$$\text{BW} = 12.76284 + 0.92984 \times \text{BV} - 30.34523 \times \text{coat type} + 14.22675 \times \text{sex}$$

A multiple linear regression model using trunk volume (TV) instead of BV was also developed. The variable selection procedure was the same with the BV-based regression model. The developed model is below. R^2 of the developed model is 0.9315. The R^2 of the TV-based regression model was slightly smaller than BV-based model, but the accuracy was still higher compared to other conventional methods (Miller and Hewitt, 1969; Carroll and Huntington, 1988).

$$\mathrm{BW} = 52.201 + 0.991 \times \mathrm{TV} - 23.564 \times \text{coat type} + 19.829 \times \text{sex}$$

The mean BW and SD estimated from the developed regression models were 525.62 ± 58.29 kg and 525.62 ± 57.71 kg in the BV and TV multiple regression models, respectively. Mean % error of both methods was calculated as below. In the equation shown, "true BW" is a median value among three measurements using a large animal scale. The mean % error of the multiple regression model with variables BV, sex, and coat type was 2.07%; and 2.32% in the model with variables TV, sex, and coat type.

$$\sum_{\iota=1}^{n} \frac{|predicted\ BW\ from\ the\ regression\ model - true\ BW|}{true\ BW} \div n \times 100$$

2.4. Discussion

To our knowledge, obtaining 3D images of live animals using a 3D scanner has not been studied in any animal science area, even though human body 3D scanning and its use have been studied for the last two decades. This lack of animal studies likely is related to the challenge of keeping the animals still enough to obtain a high-quality image. As a result, this process has not been considered feasible in a majority of animals. This study was conducted understanding the risk that movement of the horses might cause the study to fail. Horses were considered to be ideal subjects for this study since most will stand relatively still compared to other animal species. In addition, the physical characteristics of most horses, such as the hair length, are similar, even across breeds. In addition, the current technological developments for structured-light 3D scanning and diverse error correction algorithms make it possible to obtain 3D images of a large object, such as a horse, and to correct minor errors due to slight movement. It was, therefore,

assumed in this study that obtaining high quality live animal 3D images using 3D scanning technology was possible. Since in most situations a large animal scale is not available, development of an accurate equine BW measurement method that can be used in the field will improve overall equine management and well-being of the horses.

Due to horse movement and its effect on the 3D images while conducting a preliminary study, the plan for equine 3D scanning in the initial study was changed slightly from the original plan. In our original plan, the entire body (from head to tail) was to be 3D scanned all at once; instead, four body segment 3D images of each horse were obtained separately and those partial images were assembled into one whole body image using 3D image software. Highly detailed equine 3D images were obtained because the decreased scanning time due to obtaining small segment of 3D image at once reduced the likelihood of movement. The resolution was also improved due to the decreased size of the scanning field. Even though for this study partial 3D images were obtained and later assembled, it does not necessarily mean that it is not possible to obtain a whole body horse 3D image in one scan. There are several commercially available 3D scanners that are more accurate and faster than the 3D scanner that was used in this study, Structure Sensor. If a faster 3D scanner was used, it would have been possible to obtain a highly accurate large animal 3D image in one scan. The Structure Sensor was chosen for this study instead of the high-end 3D scanners because the goal of this study was to develop an equine BW measuring method using an inexpensive (The price of Structure Sensor is $340) and small hand-held 3D image device. The results from this small 3D scanner more than exceeded our expectations as it worked very well to create detailed equine 3D images (Figure 2.7).

The development of 3D imaging technology has been progressing rapidly during the last several years, so it is very likely that faster and more accurate 3D scanners than the Structure Sensor will

soon be available at a more affordable price in the near future. In addition, the development of a new image-processing algorithm always goes together with advancements in the device. One example of the outstanding software development is Kinect fusion[v] which makes it possible 3D imaging of a moving object. (Izadi et al., 2011)

Overall the 3D image quality and accuracy of the measured volume were very satisfactory in this study. Even though there was not a true gold standard BV value to compare with our measurements, there was only 3.93 liters on average within-horse volume measurement error compared to the mean value. It was only 0.71% of the mean BV (555.58 liters). According to Kinect-based studies, the standard deviation of the scanning of an object located 1-3 meters away from the scanner (and the size of an object is similar to the distance) was approximately 0.25-1.5 cm (Khoshelham, 2011). If there are two objects which sizes are 1 m^3 and 3^3 m^3(similar to the 3D scanning field size of this study), then the volume of the 3D images will be estimated as 0.9975^3-1.0025^3 and 2.985^3- 3.015^3 m^3, respectively, when the error is taken into account. The % error of the estimated volume compared to the true volume of the object would be 0.75%-1.51% in this case. In this study, we had expected larger margin of error than 1.51% because of the potential error inducing factors such as hair, mane and tail of the horse. We were very impressed with only 0.71% within-horse error on the BV measurement in this study.

The mean measurement error of the equine BW estimation using the developed multiple linear regression model was only 2.07-2.32 % of the true BW. The accuracy was lower than for the large animal scale (average error of the large animal scale was 0.1%), but is exceptionally more accurate than a weight tape or a formula based on combined girth and body length measurements

[v] Kinect fusion, Microsoft corporation, Redmond, Washington, USA, https://msdn.microsoft.com/en-us/library/dn188670.aspx

where the average errors are between 6-11% (Milner and Hewitt, 1969; Carroll and Huntington, 1988; Ellis and Hollands, 1998). Due to its high level of accuracy and portability, a 3D image based BW measuring method has tremendous potential for practical use in the equine industry. Developed regression models have three variables: volume, coat type and sex. This equation is very easy to apply since the equation is simple, and two of the variables, coat type and sex, have only two variances, 0 or 1. Data are not included in this paper, but R^2 of a simple linear regression model (independent variable = BV, dependent variable = BW) was 88% and the average error was 3.05%. This means even the simple regression model with only one independent variable, BV, outperformed the accuracy of a weight tape or a formula based on combined girth and body length measurements.

The overall accuracy was slightly decreased in the regression model using TV instead of BV. This method, however, has great potential to be an easier method to measure the equine BW since only the trunk 3D scan is required. High correlation between the true BW and TV (coefficient = 0.93) shows how well the horse 3D images represent all aspect of their true bodies. Many conventional BW measuring methods estimate the BW of horses using heart girth or heart girth and body length. Even though both approaches estimate the equine BW based on values measured from the trunk of the horse, a 3D image based BW estimation has much lower error compared to those methods (2.3% vs. 6-11% average error) (Milner and Hewitt, 1969; Ellis and Hollands, 1998).

One variable, coat color, was excluded in the final regression model due to high probability of misclassification. T-test was conducted (data are not included in this paper) to check if there was a difference in the error of the predicted BW between “dark” and “light” coat color sub-groups. The results showed that there was 8.97 kg of deviation difference between these two groups and

the coat color difference was statistically significant (P=0.033). In our study, there were 18 dark and 4 light coat colored horses. Since the size of the two groups was not equivalent it is difficult to generalize the results. However there is an indication from this study that coat color may affect 3D scanning. There is some agreement among structured-light 3D scanner users that 3D scanning of a black object under direct sunlight results in poor 3D imaging or may even cause the scan to fail because infrared light (IR) is absorbed on the surface of the object and compromises the acquisition of the surface reflected light pattern through the IR camera[w]. In our study, no failure was observed in 3D scanning even when scanning a dark colored horse (e.g. seal brown) in direct sunlight. The effect of color and light strength in 3D scanning should be carefully considered and studied through follow-up studies. A possible and reasonable explanation for our success in 3D scanning of dark colored horses might be that our dark colored horses were not true blacks but a variety of somewhat lighter colors such as brown, bay or chestnut.

At the beginning of the regression model development, an interaction between coat type and BV was included in the model because the volume difference between summer and winter coats is greater for large horses than small horses since body surface area increases as BW increases (Tikuisis et al., 2001). In a tested regression model selection procedure with a coat type×BV interaction term, the interaction term was selected in the stepwise selection. This interaction term, however, was not included in the final model because it was observed that the two linear graphs which reflected predicted BW of summer-coated horses and winter-coated horses crossed over at the point of predicted BW of 450 kg. Estimated BW of horses of the same volume is smaller in a winter-coated horse than a summer-coated horse when the BW is higher than 450 kg,

[w] Structure Sensor Forum. http://forums.structure.io/login

but the trend is opposite when the horse's BW is under 450 kg, according to this regression model. This unexpected result which was observed in the model with BV×coat type interaction term is likely due to the influence of 3D scanning errors of a few horses, probably low BW horses with winter coats. Among our study horses, we had only six with winter coats, and only two of them had BW lower than 450 kg (430.5 kg and 436.4 kg in each). In addition, the BW variance in our study horses was very narrow. All of the study horses were in the BW range between 430.46 kg -635.48 kg. In this study setting, even a small error may induce a large difference in the slope of the developed regression line. The multiple linear regression models developed in this study showed high correlation with the true BW of the horses, but it is still too early to say that this model can be applied to the general horse population. For that purpose, adjustment of the model with larger and more diverse study population is required.

In conclusion, this pilot study to estimate the BW of horses using 3D images obtained from an inexpensive hand-held 3D scanner was successful. The average % error of this method was much lower than the reported error of conventional equine BW measurement methods. An exciting discovery from this study is the proof that live animal 3D scanning can be practically achieved without extreme physical restraint or the use of sedatives.

Movement of the head was a minor obstacle for obtaining a high-resolution whole body image in a single scan, therefore, the method of the 3D scanning had to be modified. In addition, our study did not follow a statistically random selection procedure for the horses; this may have induced some questions regarding the applicability of 3D scanners for the general horse population. Moreover, we intentionally excluded one candidate horse that had Cushing's disease; it was assumed that his hairliness would bias the results. Despite these concerns the overall project result was very successful. The highly detailed 3D images obtained in this study showed that 3D

scanning can be used not only for BW measurement but also potentially in additional ways such as BCS estimation, conformation evaluation, evaluating of saddle fit, customized horse shoe design, or analyzing conformation over time.

2.5. Tables and figures

Table 2.1. Determination of the Body Condition Score (BCS) by Henneke et al (Henneke et al., 1983).

Score	Status	Vertebrae	Ribs	Tailhead	Withers	Shoulders	Neck
1	Poor: extremely emaciated	Prominent projection of bony structure	Prominent projection of bony structure	Prominent projection of bony structure	Bone noticeable	Bone noticeable	Bone noticeable
2	Very thin: emaciated	Prominent projection of bony structure (slight fat covering on the base of the spinous, transverse process)	Prominent projection of bony structure	Prominent projection of bony structure	Faintly discernable	Faintly discernable	Faintly discernable
3	Thin	Body structure is easily discernable. Transverse processes are not felt.	Easily discernable Slight fat cover	Prominent but not visually identifiable of each vertebrae	Accentuated	Accentuated	Accentuated
4	Moderately thin	Negative crease	Faint visible outline	Fat is felt around	Not obviously thin	Not obviously thin	Not obviously thin
5	Moderate	Level	Not visible but easily felt	Fat spongy feeling	Round over spinous process	Blend smooth into body	Blend smooth into body
6	Moderately fleshy	Slight crease on the down back	Fat felt spongy	Soft fat feeling	Fat deposition along the side	Fat deposition caudal	Fat deposition sides
7	Fleshy	Crease the down back	Ribs can be felt but fat filling is noticeable	Soft fat feeling	Fat deposition along withers	Fat deposition caudal	Fat deposition along the neck
8	Fat	Crease the down back	Difficult to feel	Very soft fat	Fat deposition along withers	Caudal area filled with fat	Noticeable thickening
9	Extremely fat	Obvious crease down back	Patchy fat accumulation	Fat bulging	Fat bulging	Fat bulging	Fat bulging

Figure 2.1. A horse ready for 3D scanning. A horse was groomed and the tail was wrapped with an elastic band. Twenty-one cylindrical markers were placed on the body. The markers were secured using elastic bands and tape.

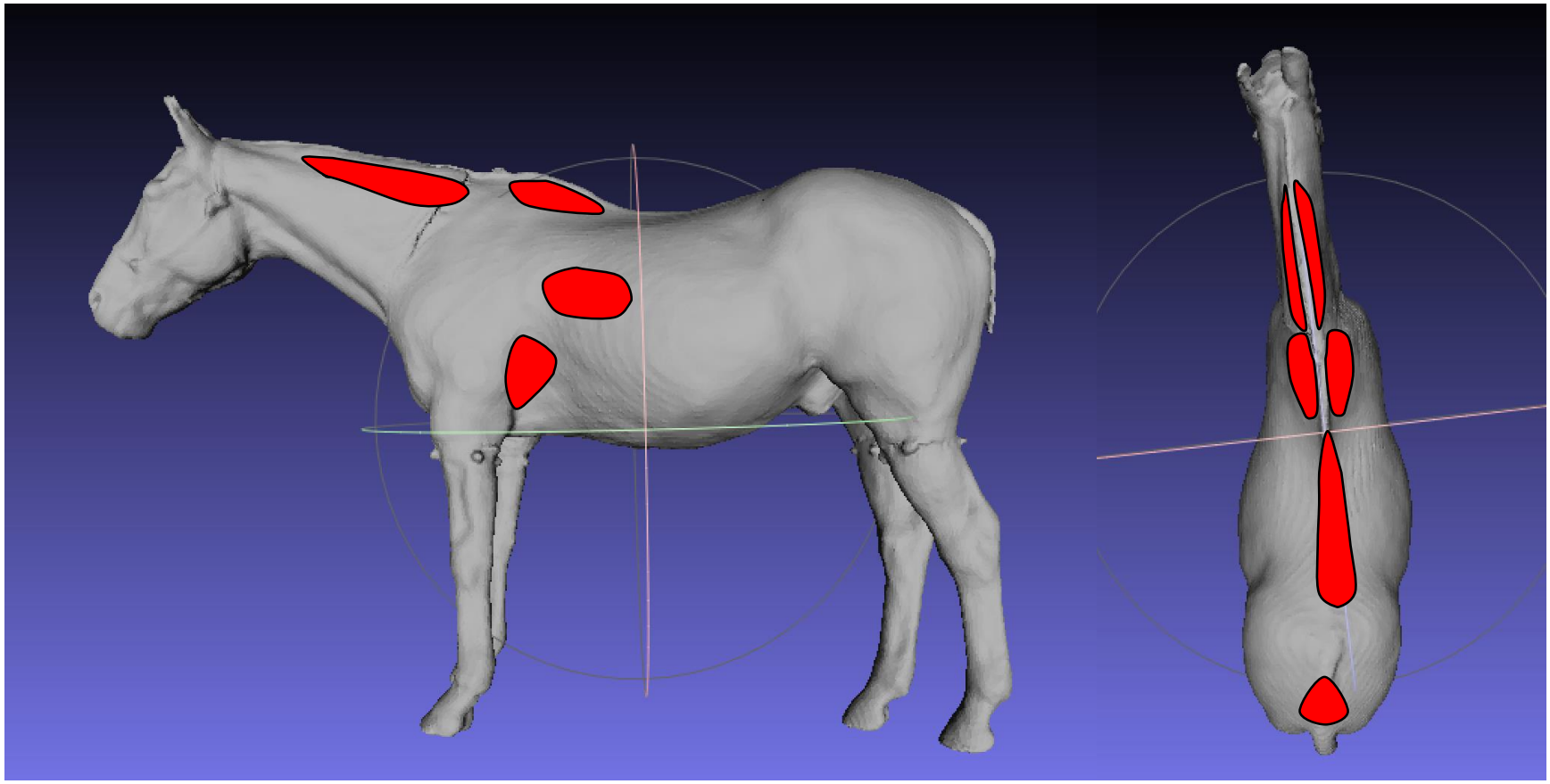

Figure 2.2. Determination of the Body Condition Score (BCS) based on the six locations of the horse body by Henneke et al. (Henneke et al., 1983). Six locations of the horse's body (Along the neck, the withers, crease down the back, tailhead, ribs, and behind the shoulder) are examined to determine the body fat accumulation of the horse in order to determine the BCS of the horse. The detailed description to estimate the BCS of horses based on these six locations is in Table 2.1.

2.3.a

2.3.b

Figure 2.3. The location where the 3D scanning of horses were conducted. Two horses were brought into an indoor arena and placed in a tie area approximately four poles apart (figure 2.3.a). One side of the tie area was covered with rubber mats and another side was a large empty space (figure 2.3.b). 3D scanning was conducted within the space.

2.4.a

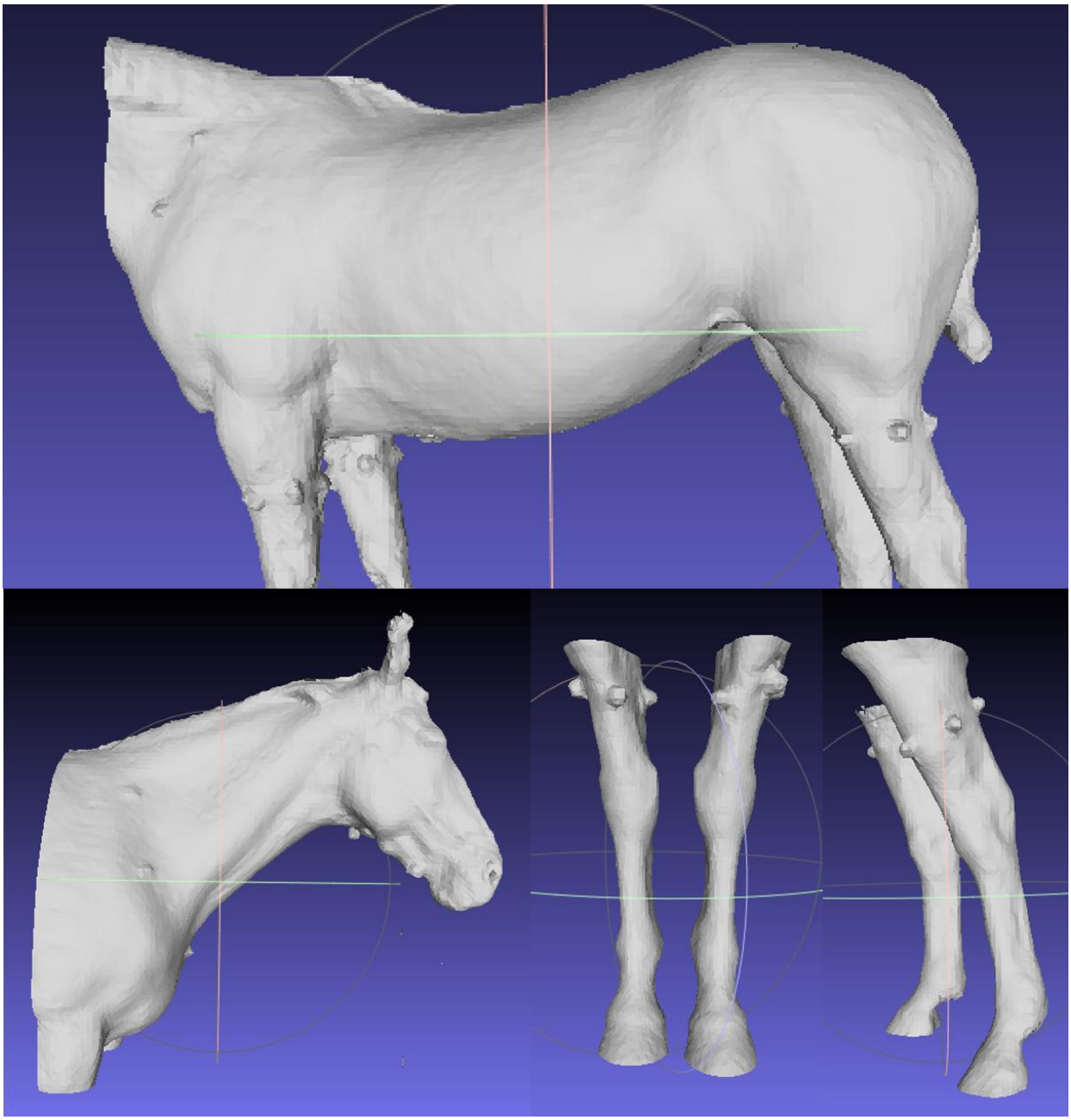

2.4.b

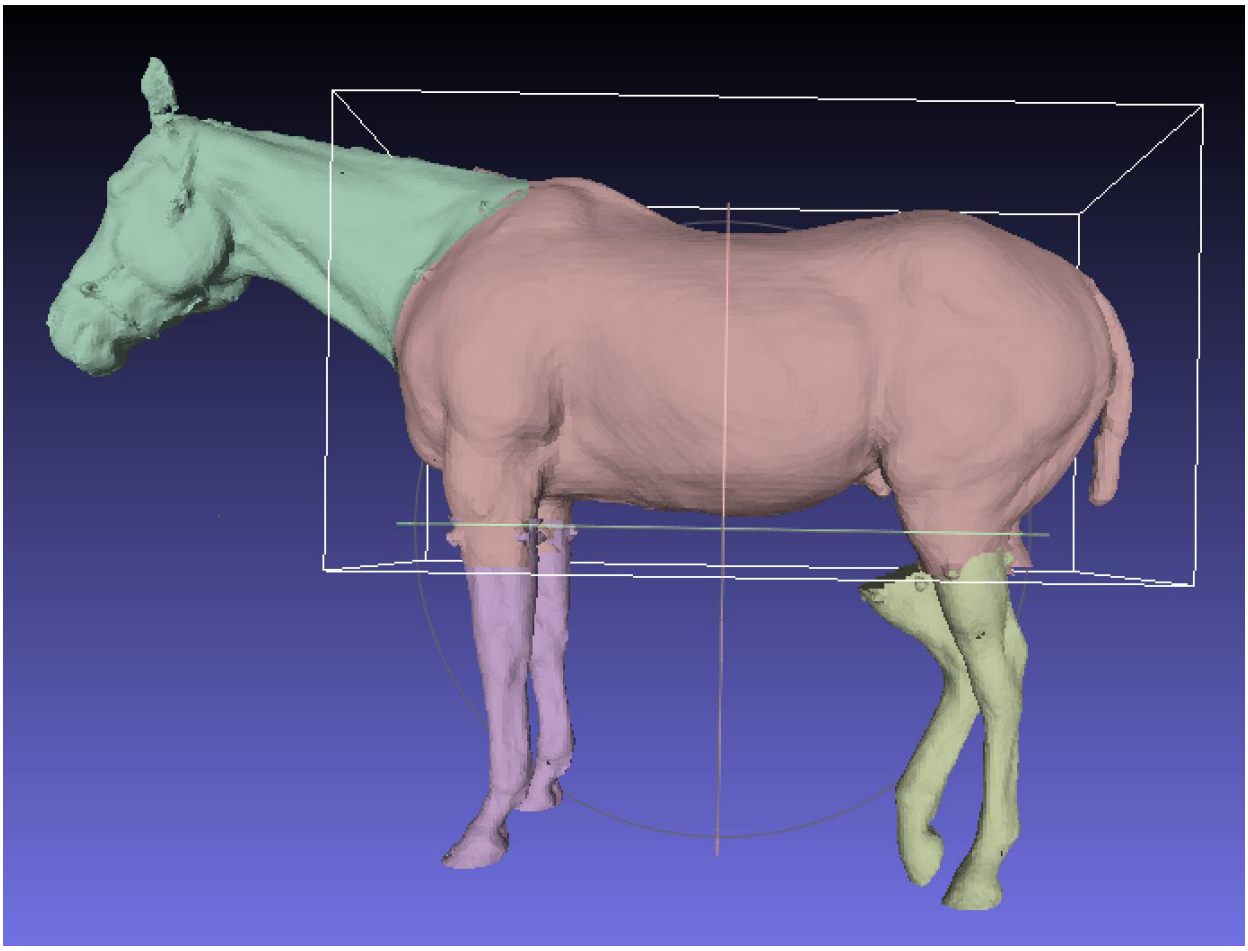

Figure 2.4. Four 3D images of body segments and assembly of those images into an entire body horse 3D image. Twenty one markers placed on the horse were readily viewable on the segmented horse 3D images (Figure 2.4.a). Markers represented in the 3D images were used for the point-based gluing process to assemble four partial 3D images into a whole body 3D image (Figure 2.4.b).

2.5.a

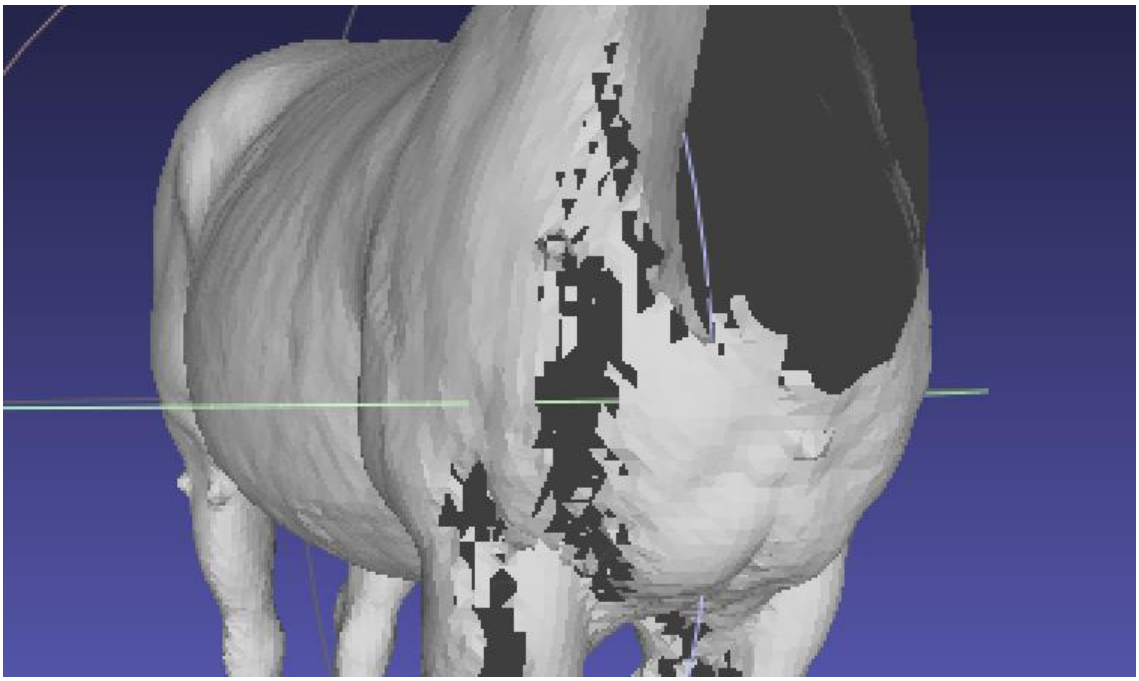

2.5.b

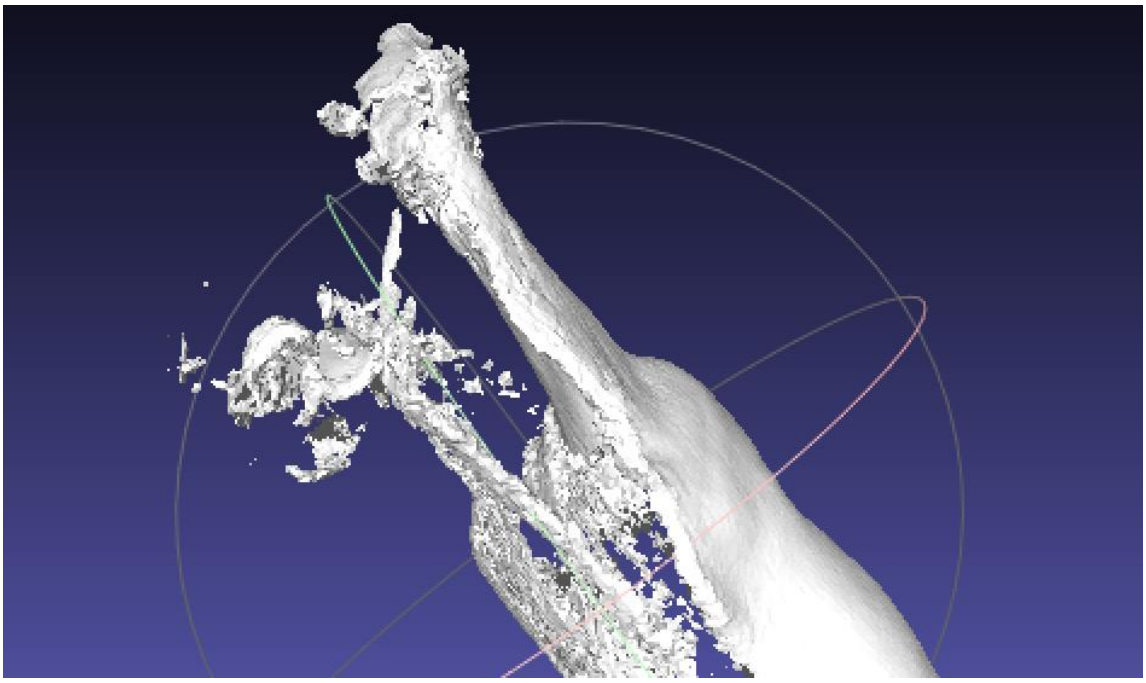

Figure 2.5. Examples of 3D imaging failure due to the horse movement. 3D image distortion was observed when a horse made a movement during the 3D scanning. Even when the movement was subtle, slight image distortion occurred and it caused a mismatch between the 3D scanning start point and the end point (Figure 2.5.a). 3D scanning failed when a horse moved a large part of the body (Figure 2.5.b).

2.6.a 2.6.b 2.6.c

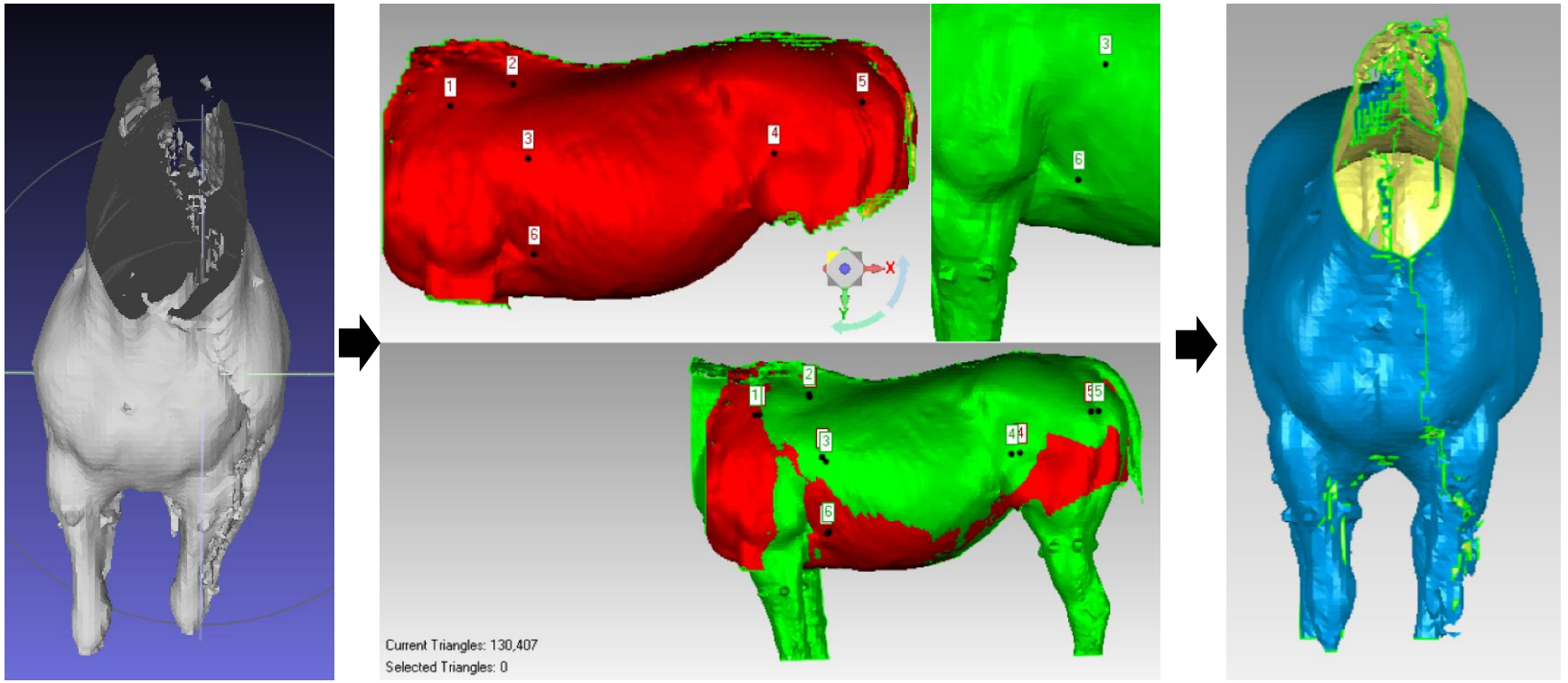

Figure 2.6. Image correction procedure to fix the minor distortion of the equine 3D image. When the image distortion was minimal, the image was corrected using 3D image software, e.g., Meshlab or Geomagic Studio. Image correction was conducted using point based alignment and global alignment (Figure 2.6.b). Figure 2.6.a is a raw trunk 3D image with image distortion from the left neck to the left forelimb. Figure 2.6.b shows the alignment process, Figure 2.6.c is the result of the alignment procedure. A distortion observed in the original trunk 3D image was corrected in this image

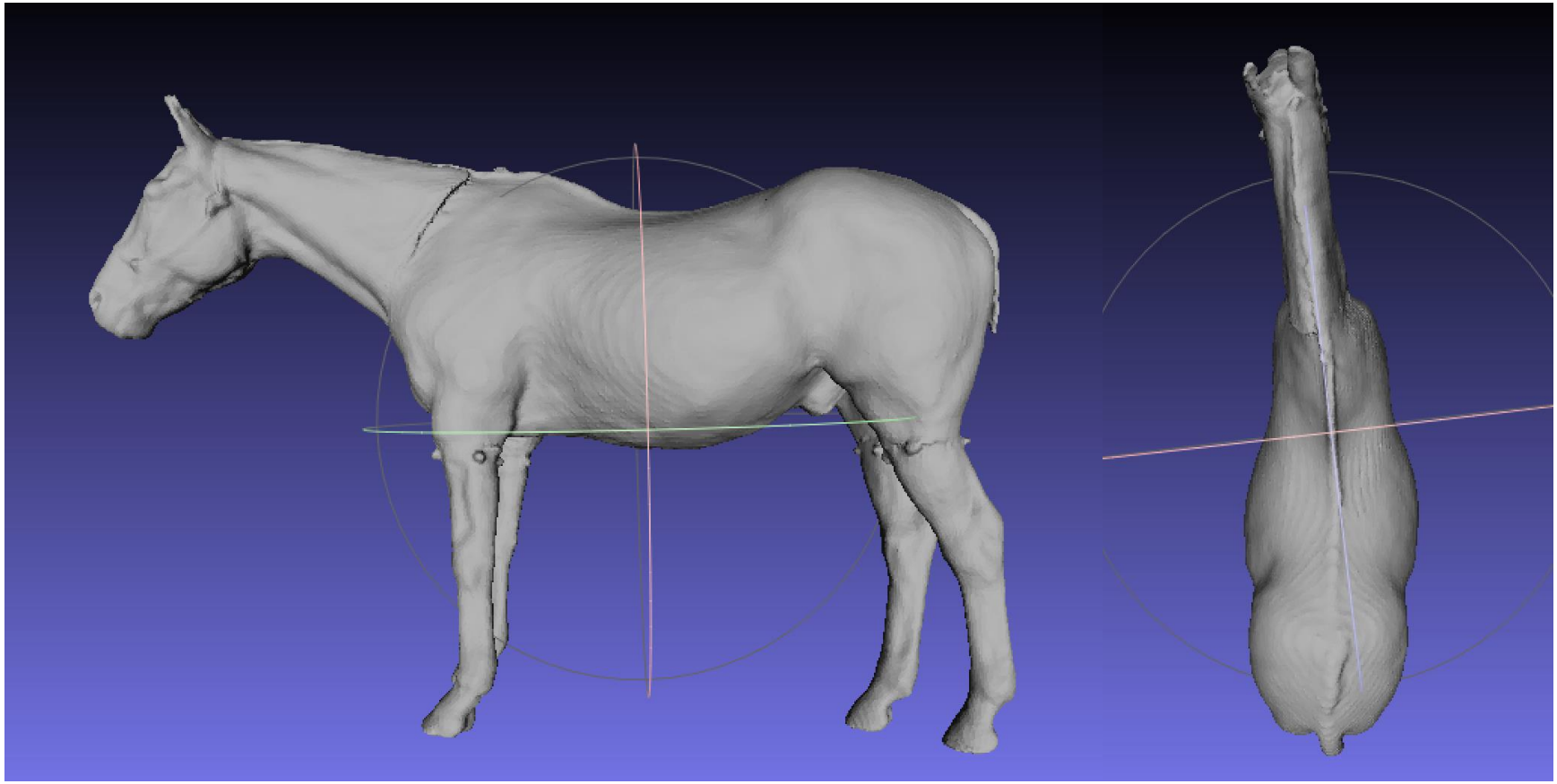

Figure 2.7. An example of a competed 3D image of a horse. Left lateral view (left) and dorsal view (right). 3D imaging makes it possible to observe areas of a horse that are not easily seen when viewed with naked eye (e.g. dorsal view).

2.8.a

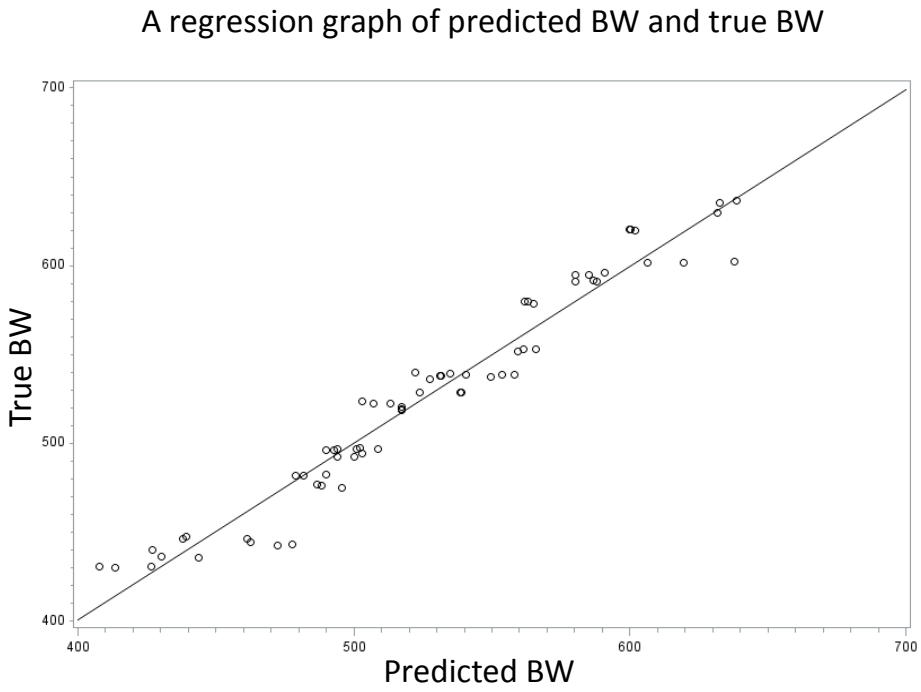

2.8.b

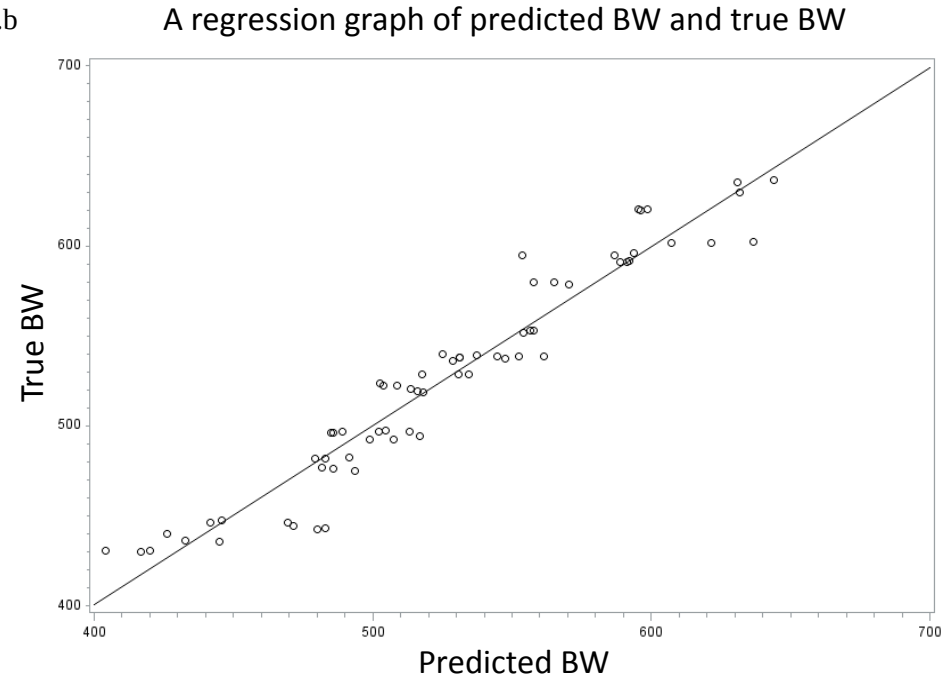

Figure 2.8. Regression graphs of predicted BW and the true BW of horses which were drawn based on the multiple linear regression model with independent variables BV, sex, and coat type (Figure 2.8.a), and TV, sex, and coat type (Figure 2.8.b).

X-axis is predicted values and Y-axis is true BW. Both models showed strong linear correlation between the predicted BW and true BW. The R^2s are 0.95 and 0.93 in Figure 2.8.a and 2.8.b, respectively. Figure 2.8.a has slightly more scattered plot than Figure 2.8.b.

REFERENCES

Carroll, C., and P. Huntington. 1988. Body condition scoring and weight estimation of horses. Equine Vet. J. 20: 41-45.

Cignoni, P., M. Corsini, and G. Ranzuglia. 2008. Meshlab: an open-source 3d mesh processing system. Ercim news 73: 45-46.

Ellis, J., and T. Hollands. 1998. Accuracy of different methods of estimating the weight of horses. Vet. Rec. 143: 335-336.

Gharahveysi, S. 2012. Compare of Different Formulas of Estimating the Weight of Horses by the Iranian Arab Horse Data. JAVA 11: 2429-2431.

Gibbs, P., and D. Householder. Estimating Horse Body Weight with a Simple Formula. http://www.aspcapro.org/sites/pro/files/estimating_horse_body_weight.pdf (Accessed 4 April 2015). Texas A&M.

Henneke, D., G. Potter, and J. Kreider. 1981. Rebreeding efficiency in mares fed different levels of energy during late gestation. Proc. 7th Eq. Nutr. Physiol. Symp., Virginia State Univ. p 101-104.

Henneke, D., G. Potter, J. Kreider, and B. Yeates. 1983. Relationship between condition score, physical measurements and body fat percentage in mares. Equine Vet. J. 15: 371-372.

Izadi, S. et al. 2011. KinectFusion: real-time 3D reconstruction and interaction using a moving depth camera. Proc. 24th ACM Symp User interface software and technology. p 559-568.

Katch, F., E. D. Michael, and S. M. Horvath. 1967. Estimation of body volume by underwater weighing: description of a simple method. J. Appl. Physiol. 23: 811-813.

Kaushal, R. et al. 2001. Medication errors and adverse drug events in pediatric inpatients. JAMA 285: 2114-2120.

Kazhdan, M., M. Bolitho, and H. Hoppe. 2006. Poisson surface reconstruction. Proc. 4th Eurographics symposium on Geom. Process.

Khoshelham, K. 2011. Accuracy analysis of kinect depth data. ISPRS workshop laser scanning. 133-138.

Milner, J., and D. Hewitt. 1969. Weight of horses: improved estimates based on girth and length. Can. Vet. J. 10: 314.

Munkelt, C., B. Kleiner, T. Torhallsson, P. Kühmstedt, and G. Notni. 2014. Handheld 3D Scanning with Automatic Multi-View Registration Based on Optical and Inertial Pose Estimation. Fringe. 2013. p 809-814. Springer.

Seidel, D., F. Beyer, D. Hertel, S. Fleck, and C. Leuschner. 2011. 3D-laser scanning: A non-destructive method for studying above-ground biomass and growth of juvenile trees. Agr. forest Meteorol. 151: 1305-1311.

Sholts, S. B., S. K. Wärmländer, L. M. Flores, K. W. Miller, and P. L. Walker. 2010. Variation in the measurement of cranial volume and surface area using 3D laser scanning technology. J. Forensic Sci. 55: 871-876.

Tikuisis, P., P. Meunier, and C. Jubenville. 2001. Human body surface area: measurement and prediction using three dimensional body scans. Eur. J. Appl. Physiol. 85: 264-271.

Uyar, R., and F. Erdoğdu. 2009. Potential use of 3-dimensional scanners for food process modeling. J. Food Eng. 93: 337-343.

Wakat, D. K., R. E. Johnson, H. J. Krzywicki, and L. I. Gerber. 1971. Correlation between body volume and body mass in men. Am. J. Clin. Nutr. 24: 1308-1312.

Wells, J. C., I. Douros, N. J. Fuller, M. Elia, and L. Dekker. 2000. Assessment of body volume using three-dimensional photonic scanning. Ann. N. Y. Acad. Sci. 904: 247-254.

Wilhelms, J., and A. Van Gelder. 1992. Octrees for faster isosurface generation. ACM Transactions on Graphics (TOG) 11: 201-227.

CHAPTER III.

COMPARISON OF A 3D SCANNING-BASED EQUINE BW ESTIMATION METHOD TO CONVNETIONAL BW MEASUREMENT METHODS

3.1. Introduction

3.1.1. Background

Accurately estimating the body weight (BW) of a horse and detecting any change is important in order to make appropriate management and treatment decisions. A large animal scale is an accurate tool for measuring BW; however, it is expensive and lacks portability, thus BW measurement is rarely conducted in field situations. Instead, most equine veterinarians and horsemen visually estimate the BW of horses. There are some alternative conventional methods for determining equine BW, such as a weight tape or a formula using a combination of heart girth and body length measurements. These methods, however, have a 6 - 12% or even higher margin of error(Gibbs and Householder; Ellis and Hollands, 1998) and so are often unreliable in detecting changes in weight that can accompany disease processes or poor nutritional management. There is, therefore, a need to develop an accurate and convenient equine BW measurement method, one that can be easily used in the field.

3D scanning is widely used in diverse industries, and one of its important applications is for measuring the volume of an object (Wells et al., 2000; Tikuisis et al., 2001; Sholts et al., 2010; Seidel et al., 2011). Traditionally, 3D scanning has been conducted only on rigid inorganic materials, but some studies used human bodies as the study subject. According to those studies,

the error of measured body volume (BV) of the 3D images was only 0.2-0.5% of true BV (Wells et al., 2000). We hypothesized that BV measurement using 3D scanning can result in an accurate BW estimation because the correlation coefficient (R) between BV and BW is 0.996-0.998 (Katch et al., 1967; Wakat et al., 1971). The high R in the human studies suggests this technology may have applicability for horses. If the result of the horse study is similar to the human-based studies, then the 3D scanning method would be an easy way to more accurately determine equine BW in the field due to low price and ease of use (due to the small size) of some commercially available 3D scanners.

Our pilot study to develop a method to measure equine BW using an inexpensive and handheld 3D scanner showed high accuracy. The coefficient of determination (R^2) between a developed multiple linear regression model with variables: BV, coat type and sex, and true BW, was 95%. In addition, the average error of the developed equation to estimate equine BW compared to the true BW was only 2%. This is a much lower margin of error than have been found with conventional equine BW measurement methods. The reported average error of conventional equine BW measurement methods was at least 5.6% (Milner and Hewitt, 1969). This error difference, however, cannot be used as a direct proof of the advantage of the 3D scanning based equine BW measurement method (3DScan) in its accuracy compared to conventional equine BW measurement methods. Design of previous studies to estimate the accuracy of the alternative conventional equine BW estimation methods were different from our pilot study, e.g. number of horses studied, breed, sex, type, and the season. Different study design and study population with different characteristics results in different outcomes due to the association between the unaccounted for variables and outcome of the study (Rothman et al., 2008; Gharahveysi, 2012).

The study described in this chapter was designed to compare the accuracy of the newly-developed 3D scanning based equine BW measurement method with conventional equine BW measurement methods in the same study population. This design of the statistical comparisons minimizes biases in the study results that can be induced when the characteristics (variables) of study population are diverse among compared study groups (Rothman et al., 2008; Gharahveysi, 2012). Our study design allows for the comparison of equine BW measurement methods in a quantitative and statistically accurate manner.

3.1.2. Hypothesis

A 3D scanning based measurement method (3DScan) is more accurate than conventional measuring methods for determining equine BW.

3.1.3. Objectives

A. To measure equine BW using 3DScan, a large animal scale, and conventional equine BW measurement methods (weight tape, calculated BW based on girth and body length measurements, and visual estimation) in the same study population.
B. To compare the accuracy of measured BW by those equine BW measurement methods.

3.2. Materials and methods

3.2.1. Target population

Twenty-two horses were included in this study. The sample size was determined based on the power and sample size calculation using a statistics package.[x] In the sample size calculation, the

[x] SAS, version 9.3, SAS Institute Inc., Cary, NC, USA

expected mean % error of 3DScan method was set at 2% and, in case of a conventional method, it was set at 4%. Standard deviation of the samples was set to 2, and the expected power was 0.99. Calculated minimal number of samples was 21 but the total 22 horses were used in this study.

Horses were randomly selected but the selection did not follow statistical random selection procedure because the complete list of the source population was not available, and horse availability was different depending on the study date. Among these 22 horses, Colorado State University (CSU) owned 20 and two were privately owned horses. In terms of horse type, ten were polo horses, six were therapeutic riding horses, three were Equine Reproduction Laboratory (ERL) CSU-owned research mares, one was a dressage horse and two were pleasure riding horses. The study group included fifteen mares and seven geldings. The majority of these horses were either American Quarter Horse or Thoroughbred-American Quarter Horse cross but there were also other breeds such as a Hanoverian.

The study procedure was approved by the institutional animal care and use committee (IACUC) at CSU in 2014 and the study was conducted accordingly. All of the animal use portions of this study were conducted between September and December of 2014.

3.2.2. BW measurements

BW measurement of 22 study horses was conducted using six different methods: a digital large animal scale[y], a 3D scanning based equine BW measurement (referred as 3DScan, an equation from a multiple regression model described in chapter 2 of this study for which a structured light

[y] Model 700, True-test, Mount Wellington, New Zealand, http://group.tru-test.com/en

3D scanner[z] was used), two types of equine weight tapes, one from Purina[aa] and other from Shell[bb] (WT Purina, WT Shell), a formula to estimate the equine BW using heart girth and body length measurements (Carroll's formula), and visual estimation (VE) (Carroll and Huntington, 1988). The equation for 3DScan method and Carroll's formula are as below. In 3DScan method, values of coat type is winter coat is 1 and summer coat is 0, and, in sex, gelding is 1 and mare is 0. All six methods were applied on the same day on the same horse and all of the measurements were repeated three times for each horse. The measured value was recorded as either lb or kg, but lb was later converted to kg prior to the data analysis so only metric unit BW was used in the following analysis. To change the lb BW into kg BW, lb were multiplied by 0.453592.

3DScan: $\text{BW (kg)} = 12.76 + 0.93 \times \text{BV (liter)} - 30.35 \times \text{coat type} + 14.23 \times \text{sex}$

Carroll's formula: $\text{BW (kg)} = \frac{\text{Girth (cm)}^2 \times \text{Length (cm)}}{11877.4}$

Prior to all other types of BW measurement, each horse was weighed using a digital large animal scale. A horse was brought on to the scale, stood square in the middle, and the BW was recorded after the value on the screen was constant for 2-3 seconds. The BW measurement in the scale was conducted three times, and each time the horse was taken off the scale and then led back on. The median value among the three weights was considered as the true BW of the horse. Once the BW measurement using the large animal scale was finished, the horse was brought to the study area. In the study area horses were lightly groomed prior to conducting other BW measurements. Horses were handled using a rope halter and a lead.

[z] Structure Sensor, Occipital Inc., San Francisco, CA and Boulder, CO, USA, http://structure.io/
[aa] Purina, St. Louis, Missouri
[bb] Shell, The Hague, Netherlands. Weight tape by Shell is no longer commercially available.

A small (119.2 mm × 27.9 mm × 29 mm) hand-held 3D Scanner was used to 3D scan each horse. The scanning range of this device is 0.4-3.5 m and the precision is 0.15 (0.4m) -1 (3m) % according to the manufacturer's description. 3D scanning and BW measurement from the obtained 3D images were conducted as described in chapter 2 of this thesis. 3D scanning was conducted three times for each horse; therefore, three values of estimated BW per horse were obtained using 3DScan.

BW measurement using the conventional equine BW measurement methods of Carroll's formula, WT Purina, WT Shell, and VE was also conducted three times for each horse. Each repetition of these methods was conducted by a different individual because it was obvious that if the measurements were repeated by the same person, any previous measurements would compromise the neutrality of the next measurement. Therefore, three people, either veterinarians or experienced equine people, conducted the conventional equine BW measurements. Each person applied VE, WT Purina, WT Shell, and heart girth and body length measurements only once per method on each horse. The order of the measurement was strictly followed the order of VE → heart girth and body length measurements → weight tape measurement, and the true BW of a horse was not informed to them until all of these equine BW estimations were finished.

While measurements were conducted, a horse handler kept the horse standing square and also assisted the measurement operator. Heart girth was measured using a measuring tape.[cc] The measuring tape was placed on the withers of the horse and the circumference of the heart girth was measured in inches. This unit was later converted to cm by multiplying the measured value by 2.54. Body length was measured from the point of the shoulder to the point of the buttock.

[cc] Tailor Craft Flexible Ruler Tape, China

Weight tape measurement methods were the same as for heart girth measurement. A weight tape was placed encircling the heart girth of a horse vertically from the withers and the approximate BW as marked on the weight tape was recorded. In some horses, the circumference of the heart girth was larger than the maximum reading limit of the weight tapes. In this case, the distance between both ends (from the weight reading mark to the last marked approximate BW) of the weight tape was measured and an approximate BW was estimated based on the length-BW relationship at lower values on the weight tape. Once all of these measurements were completed, the operator was told the true BW of the horse. The possibility of the increased accuracy of VE over time due to offering the true BW information to the operators was considered inconsequential because all of the BW estimation was conducted on only 9 days during the study period and some of the horsepersons or a veterinarians who conducted the VE changed throughout the study.

Prior to the BW, heart girth, and body length measurements, the veterinarians and experienced equine people were asked to estimate the BCS of the horse as described by Henneke et al. (Henneke et al., 1981; Henneke et al., 1983). Three of them conducted BCS estimate once in each horse, therefore, there were 3 BCS estimations in each horse. The median value of the three BCS estimations was considered as the true BCS of the horse.

3.2.3. Statistical analysis

The accuracy of the six equine BW measurement methods was compared with the true BW and with each other using pairwise comparisons. First, the modified absolute deviation (AbsDev) of measured BW using each method was calculated as below. Percentage proportion of the mean

AbsDev of each BW measurement method from the mean true BW was considered as the average % error of each method.

$$\text{absolute deviation (AbsDev)} = |\text{BW measured by the method used} - \text{true BW}|$$

$$\text{average \% error of a BW measurement method} = \frac{\text{mean AbsDev}}{\text{mean true BW}} \times 100$$

Secondly, ANOVA and pairwise-comparisons were conducted to compare the mean AbsDev of different BW measurement methods. Prior to conducting ANOVA, natural logarithmic change of AbsDev was accomplished to normalize the residuals. In addition, Levene's test was conducted to check the homogeneity of variance of the distribution of $\log_e$ (AbsDev) of all equine BW measurement methods except the large animal scale. ANOVA and pair-wise comparisons were then conducted using the value of $\log_e$ (AbsDev).

Lastly, horses were sub-grouped depending on their BCS and BW. Regarding BCS, horses with a BCS of 4-6 were in one group, and horses with a BCS of less than four or higher than six were in another group. In case of BW, horses equal to or lower than the mean BW (525.6 kg) were placed in one group, and horses higher than the mean BW were in the other group. The mean and variance of AbsDev of horses in different categories in each equine BW measurement method were compared using T-test and Levene's test. Since the values in this study were AbsDev, mean difference in the T-test means the difference of the measurement error, and significance in Levene's test means the variance difference. Criteria for the statistical significance was $P<0.05$. All of the statistical analyses were conducted using a statistical package.[dd]

[dd] SAS, version 9.3, SAS Institute Inc., Cary, NC, USA

3.3. Results

Among all 66 sets of data obtained from 22 horses, one from an Appaloosa horse was excluded because this dataset was an outlier, therefore, the total number of samples used in the analysis was 65. The excluded sample showed too much error from the true BW in Carroll's formula and WT Purina. The values were overestimated by 239.5 kg and 201.3 kg in WT Purina and Carroll's formula, respectively. The % error from the true BW (601.9 kg) was 39.8% and 33.4%, respectively. The values of studentized residual and cook's distance of this horse's estimated BW of Carroll's formula were -4.043 and 3.090, respectively, and, in case of WT Purina, -3.656 and 2.161. The exact reason for this error is not clearly understood, but folding of the tape while conducting BW measurements was suspected.

The mean true BW and SD (BW±SD) of the 22 study horses was 525.6±60.73 kg and the BCS range was 4.5-8.5. The measured BW and SD (BW±SD) of 65 samples from six measurement methods was 524.39±59.23 kg for the large animal scale, 524.37±57.86 kg for the 3DScan, 518.42±59.12 kg for the Carroll's formula, 531.67±69.76 kg for WT Purina, 496.20±61.02 kg for WT Shell, and 528.64±59.63 kg for VE. There was -28.24-7.22 kg of error compared to the true BW on the mean BW depending on the method. The largest error was observed with WT Shell (-28 kg), and this method was the only conventional method that showed statistically significant mean difference with true BW ($P<0.0001$).

Levene's test was conducted to test if the variances of $\log_e$(AbsDev) in different BW measurement method groups were significantly different. This test was conducted on five BW measurement method groups excluding the large animal scale group because the large animal scale had too small variance compared to other methods, so it was assured that the Levene's test

result will be significant if this group is included in the analysis regardless the homogeneity of variance among other groups. The test result showed that even among the other five groups variance difference existed (P-value = 0.0302). This means that for at least one group the variance was different from the other groups. ANOVA, in which one of the assumptions for the analysis is equal variance, was, however, conducted because the diagnostic plot of the variance of $\log_e$(AbsDev) showed comparatively equal distribution of variances among those groups even though their variance distribution difference was not statistically insignificant.

The mean AbsDev and Log_e(AbsDev) and 95% Confidence Limits (CL) of the six equine BW measurement methods are shown in Table 3.1 and Figure 3.1. Those methods were categorized into four different groups based on their 95% CL: the large animal scale, 3DScan, Carroll's formula + WT Purina + VE, and WT Shell. The most accurate method was the large animal scale (mean AbsDev = 0.55 kg) followed by 3DScan (10.80 kg), Carroll's formula (24.29 kg), WT Purina (27.57 kg), VE (29.20 kg), and WT Shell (38.16 kg). 3DScan was significantly more accurate than Carroll's formula, WT Purina, WT Shell, and VE. AbsDev of 3DScan was only 28.3%-44.5% of those conventional equine BW measurement methods (except the large animal scale). The mean % error of these six methods from the mean true BW of the horses were 0.1%, 2.05%, 4.6%, 5.26%, 5.57%, and 7.28% for the digital large animal scale, 3DScan, Carroll's formula, WT Purina, VE, and WT Shell, respectively.

The results of BW and BCS sub-group comparisons are shown in Table 3.2 and Figure 3.2. T-test to compare the mean AbsDev of the lower than average and higher than average BW groups showed that the mean AbsDev was not significantly different between the two groups for the large animal scale, 3DScan and Carroll's formula methods, but showed a significant mean difference for the WT Purina and WT Shell. In VE, the initial comparison of AbsDev didn't

show any mean difference. Comparison for the deviation was conducted instead on VE method of the lower than average and higher than average BW groups and the result showed clear mean difference (P value=0.0037). VE method, the BW of horses was 18.18 kg overestimated in the lower than the average BW group and 10.21 kg underestimated in the higher than the average BW group.

In the comparison of BCS groups (BCS 5-6=normal BCS group, BCS<5 or BCS>6=out-of-normal BCS group), a significant difference was clearly observed. This time, the digital large animal scale and 3DScan methods did not show significant difference on the mean and variance of AbsDev of the two BCS groups, but Carroll's formula, WT Purina, and WT Shell showed significant difference in either the mean or variance. The mean and AbsDev and the variance were large in the out-of-normal BCS group. In the case of VE, statistically significant difference was again observed in the comparison of deviation rather than AbsDev.

3.4. Discussion

To compare the accuracy of equine BW measurement methods, absolute deviation was used instead of BW or deviation. Mean BW comparison itself may be important because the mean BWs predicted using different equine BW measurement methods can be up to 230 kg different (Gharahveysi, 2012). Direct comparison of either BWs or deviations from the true BW, however, can result in misinterpretation of data, for example, if there are two values that the direction of the error is opposite, the conclusion would be no error since the value of the sum of those two errors is smaller than the original errors. For instance, if there are two values with 10 and -10

from the true value, respectively, the sum of these is zero, and the analysis will show that there is no error.

Nevertheless, the decision to use absolute deviation instead of deviation should be made very carefully when it comes to the comparison of two groups. Using absolute values may induce an inaccurate result due to the loss of the directional information. For instance, if the measurement error of two groups occurs in opposite direction from each other and absolute deviation is used to compare those groups, the result may show that there is no difference when there is actually a large difference between these groups. One example of this in our study is the result of the comparison of the measurement accuracy in the two VE groups. When the comparison of the two VE groups using either BCS or BW was conducted on AbsDev, no difference of the measurement error was observed between the two groups. The comparison of deviation, however, showed a clear mean difference between the two groups. This happened because the direction of error in VE in the two groups were opposite but the absolute values were similar.

Pair-wise comparison showed that the 3DScan method was superior in its accuracy compared to alternative conventional methods. 3DScan was not as accurate as the digital large animal scale, but still the mean error was only 2.05% (10.8 kg) of equine BW. When it is considered that a 30 lb (13.6 kg) change in BW can affect the performance of equine athletes(Pagan J.D.), a BW measurement method with more than this level of error would not be a good alternative to a large animal scale. In the comparison of the five methods for estimating equine BW, 63 samples among the total 65 predicted BW (96.9%) by 3DScan showed less than 30 lb of error, but in Carroll's formula, WT Purina, VE, and WT Shell, the % of the estimations which were under a 30 lb error were only 70.77%, 66.15%, 63.08% and 33.85%, respectively.

Even though their error was larger than the 3DScan, Carroll's formula, WTs, and VE in this study showed higher accuracy than in other studies (Milner and Hewitt, 1969; Carroll and Huntington, 1988; Ellis and Hollands, 1998). According to previous articles, Carroll's formula method had approximately 6-10% error, 9-11% error for the WT methods and up to 20% error for the method of VE, but the error for all three of these methods was 4.6-7.3% in this study. One of the reasons is that most of our study horses had average BW and BCS, and their variances were narrower than previous studies. Horse BW in this study was between 430 kg -636 kg and the BCS was 4.5-8.5. Among those horses, only three had a BCS higher than 7. Horse conformation affects the accuracy of conventional methods and the error gets larger as the conformation becomes out of normal (e.g. wide or narrow chest, long body length) (Gibbs and Householder). Since almost all of the horses in our study were in the normal BW, BCS range, and conformation, there was a smaller error in the BW estimation of the conventional equine BW measurement methods than in other studies. In addition, exclusion of data from the Appaloosa horse where the measurements using for the WT Purina and Carroll's formula methods were suspected as outliers contributed to the decreased average error of conventional equine BW measurement methods.

In spite of the seemingly clear accuracy difference between 3DScan and conventional methods, the statistically significant variance difference of AbsDev among groups may bring into question the reliability of the result of ANOVA in this study. Even though the variance difference was significant, the p-value of homogeneity test (Levene's test) was not extremely small (P-value=0.0302). A diagnostic plot of residuals and predicted value of Log_e(AbsDev) did not show large variance difference. The ANOVA is a robust method to accurately compare the mean of

more than two groups if their variances are not extremely different even if the difference of variances of the residuals among groups is statistically significant (Box, 1953).

A limitation of this study is the fact that one person conducted the 3DScan, but three different people conducted the conventional methods. It is a common theory that within-person variance is smaller than between-person variance in any type of quantitative measurement. Since one person conducted the 3DScanning, an argument could be made that this method had less variance because of the study design. This within and between- person error effect does not impact the result of our study because we used modified AbsDev to be certain the values represented the difference of equine BW measurement methods but not the within-horse variance. This was possible because AbsDev was estimated by subtracting true BW from each measurement instead of the traditional method of measuring the absolute deviation (|measured BW−mean BW of each method|). Since the measurement error could occur in either direction, decrease or increase in error, the effect of within and between-person variance difference on the comparison of accuracy of equine BW measurement methods did not pertain to our study.

An advantage of 3DScan method is its consistent accuracy regardless of the horse's conformation. Our study showed that BW or BCS difference changes of accuracy of Carroll's formula, weight tapes and visual estimation methods. The error became larger when the horse's BCS was outside of normal range. The 3DScan method, however, did not show any such trend and its accuracy was consistent regardless of the BW or BCS of the horses. This result strongly suggests the high accuracy of 3DScan method compared to conventional equine BW measurement methods in equine populations with wider varieties of BW and BCS than the horses included in this study.

In this study, we divided horses into only two BW or BCS sub-groups for analysis purposes, but it would also be meaningful if data from a larger number of horses with multiple levels of stratification could be analyzed; for example, nine groups with horses that were in BCS 1 to 9 categories. The comparison of accuracy in horses of different ages, breeds, color, sex, and height may also bring interesting and useful results. The consistent accuracy of 3DScan method regardless of the BW or BCS difference also suggest the possibility that this method can be used to estimate the BW of pregnant horses, horses with injuries, or down horses.

In conclusion, the results of pair-wise comparison of five different equine BW measurement methods to true BW showed that the 3DScan method had much higher accuracy than the conventional methods. The average % error of 3DScan method compared to true BW was only 2.07%. This margin of error was under the BW change that can affect the performance of equine athletes. 3DScan method also showed consistent accuracy regardless of the BW (lower than the average BW vs. higher than the average BW) or BCS (normal BCS vs. out-of-the normal BCS) of the study horses. In contrast, conventional methods showed statistically significant differences in the accuracy of measured values depending on the BW, BCS, or both.

3.5. Tables and figures

Table 3.1. Absolute deviations (AbsDev) of six equine BW estimation methods: large animal scale, 3DScan method, Carroll's formula, WT Purina, WT Shell, and VE. The data were organized from the smallest AbsDev to the largest AbsDev. Natural log transformation was conducted for homogeneity of variances among groups. BW estimation methods were categorized into different groups when there was a statistically significant mean difference (p-value<0.05)

Methods	Log_e(AbsDev)		AbsDev	
	mean	95% CL*	mean	95% CL*
Large animal scale	0.32^{A}	0.10-0.55	0.55^{A}	-4.28-5.37
3DScan	2.24^{B}	2.02-2.46	10.80^{B}	5.98-15.63
Carroll's formula	2.81^{C}	2.59-3.03	24.29^{C}	19.46-29.12
WT Purina	2.88^{C}	2.66-3.10	27.57^{C}	22.74-32.40
VE	2.93^{C}	2.71-3.15	$29.20^{C, D}$	24.37-34.02
WT Shell	3.42^{D}	3.20-3.64	38.16^{D}	33.33-42.99

* CL: Confidence Limit

Table 3.2. The comparison of groups categorized by BW or BCS. The number of the observations is 65. In BW groups, group 1 is horses with the BW <524.4 kg and group 2 is BW greater than or equal to 524.4 kg. In BCS groups, group 1 is horses with BCS 5-6 and group 2 is horses outside of this BCS range (BCS<5 or BCS>6). In BW groups, the number of observations in Group 1 was 33 and the number in Group 2 was 32. In the BCS groups, the number of observations in Group 1 was 42 and Group 2 was 23. T-test and Levene's test were conducted on the values of AbsDev.

Methods	BW					BCS				
	Mean AbsDev			P-value		Mean AbsDev			P-value	
	|Difference|	Group1 <524.4 kg	Group2 ≥524.4 kg	t-test	Levene's test	|Difference|	Group1 5-6	Group2 <5 or >6	t-test	Levene's test
Scale	0.09	0.5	0.59	0.701	0.356	0.28	0.45	0.73	0.274	0.163
3DScan	1.19	10.22	11.41	0.542	0.623	2.09	10.06	12.15	0.305	0.866
Carroll's Formula	4.71	21.97	26.68	0.369	0.228	11.80	20.12	31.91	0.029	0.059
WT Purina	14.82	20.27	35.10	0.015	0.003	22.04	19.77	41.81	0.0004	0.002
WT Shell	19.77	28.43	48.19	<0.0001	0.160	23.38	29.88	53.26	<0.0001	0.193
VE (AbsDev)	9.23	33.74	24.51	0.184	0.013	4.37	30.74	26.37	0.549	0.097
VE (Dev)	28.39	18.18	-10.21	0.004	0.060	21.29	11.74	-9.55	0.041	0.218

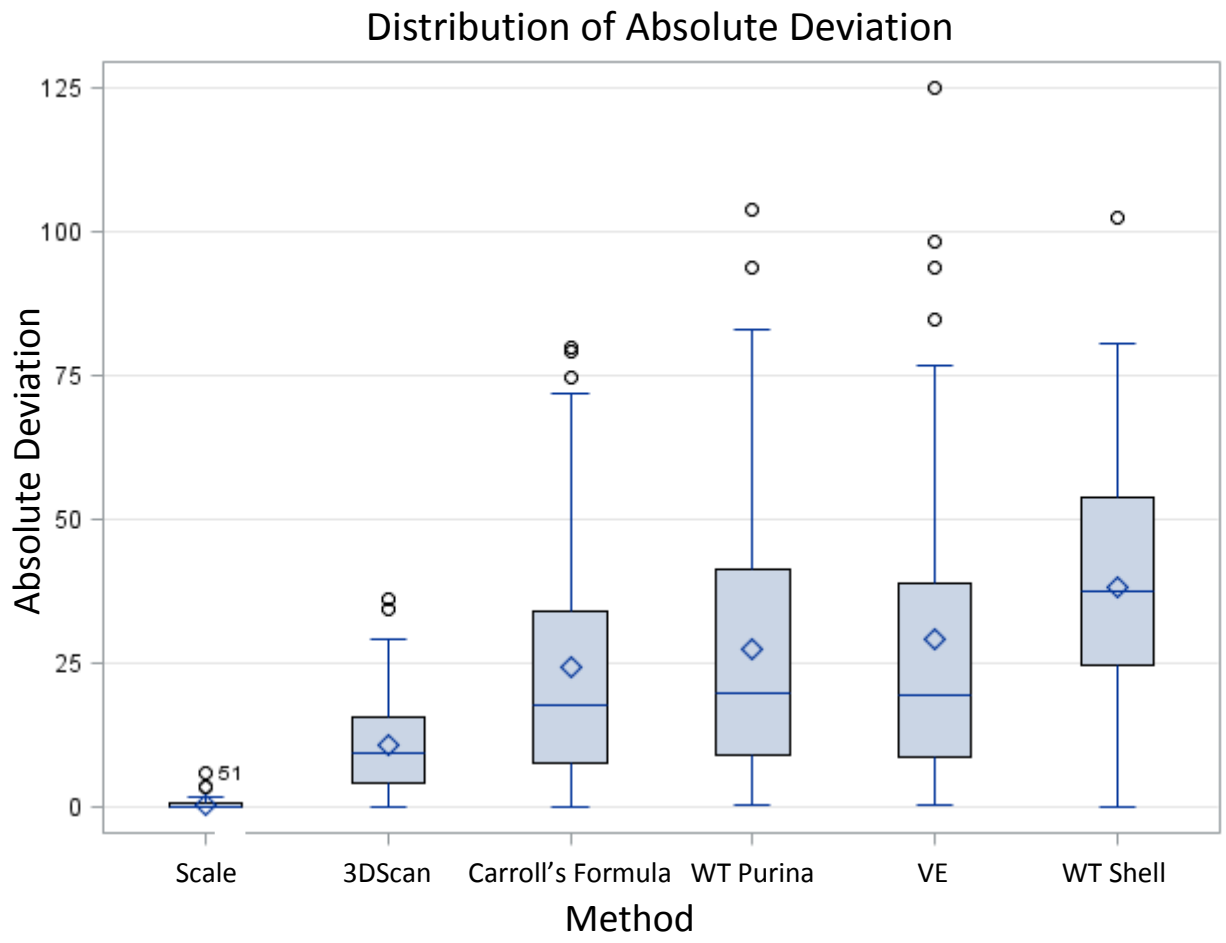

Figure 3.1. Distribution of absolute deviations (AbsDev) of six equine BW estimation methods: large animal scale, 3DScan, Carroll's formula, WT Purina, WT Shell, and VE.

A box and whisker plot. The opposite ends of the box are 25th percentile and 75th percentile. A horizontal line in the middle of the box is the median. Diamond shaped dot in the box is the mean. Whiskers are from 5th percentile to 95th percentile. In X-axis, the BW estimation methods were organized from the method of the smallest mean AbsDev (left) to the largest mean AbsDev (right). Y-axis is the value of AbsDev in kg.

3.2.a

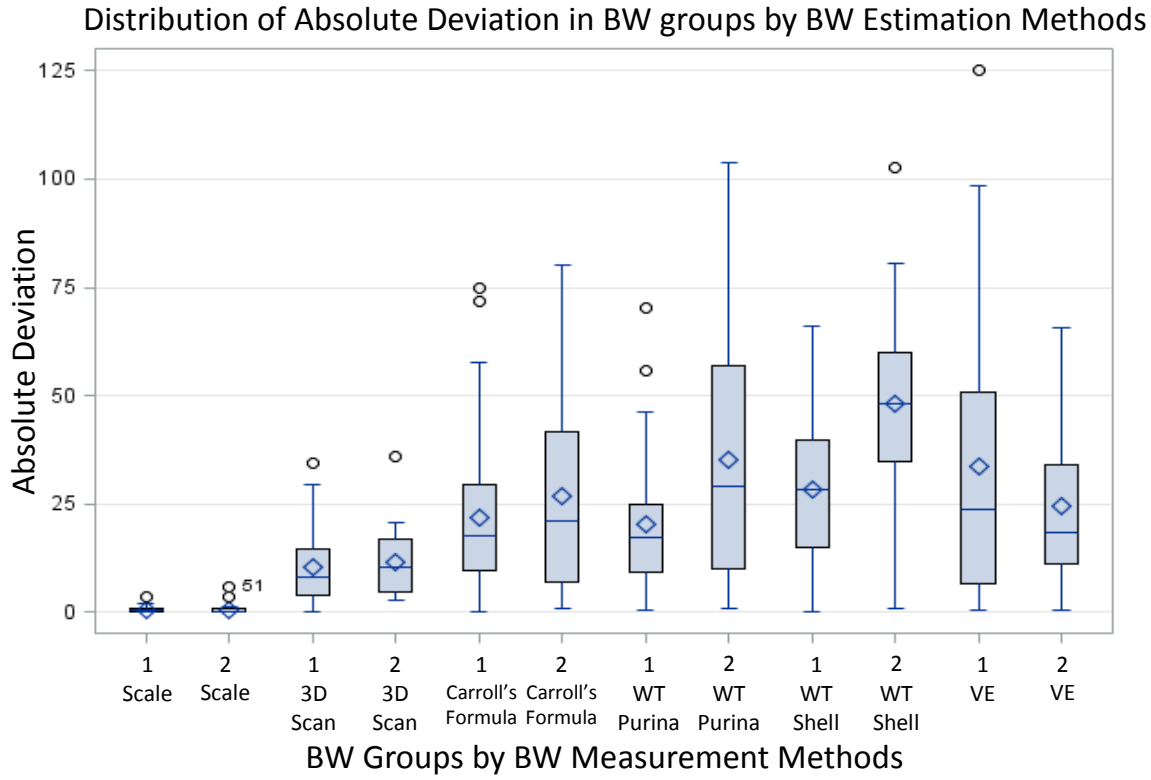

3.2.b

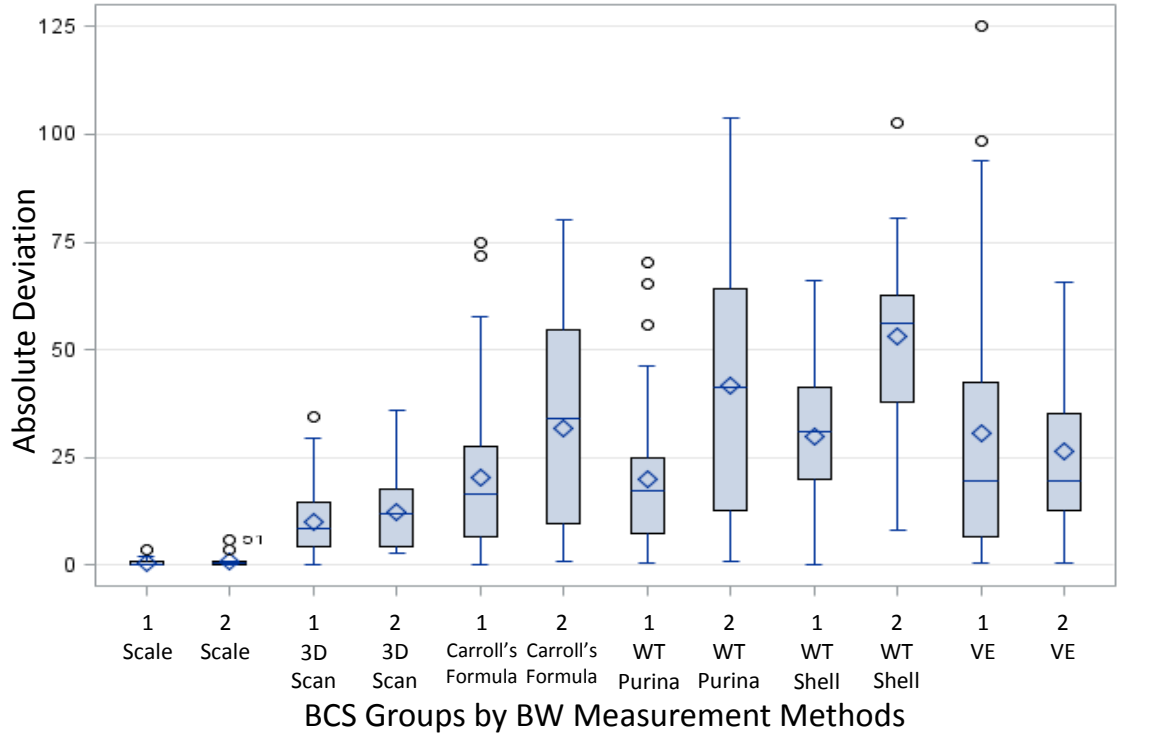

Figure 3.2. Distribution of AbsDev of BW groups and BCS groups.

REFERENCES

Box, G. E. 1953. Non-normality and tests on variances. Biometrika: 318-335.

Carroll, C., and P. Huntington. 1988. Body condition scoring and weight estimation of horses. Equine Vet. J. 20: 41-45.

Ellis, J., and T. Hollands. 1998. Accuracy of different methods of estimating the weight of horses. Vet. Rec. 143: 335-336.

Gharahveysi, S. 2012. Compare of Different Formulas of Estimating the Weight of Horses by the Iranian Arab Horse Data. JAVA 11: 2429-2431.

Gibbs, P., and D. Householder. Estimating Horse Body Weight with a Simple Formula. http://www.aspcapro.org/sites/pro/files/estimating_horse_body_weight.pdf (Accessed 4 April 2015). Texas A&M.

Henneke, D., G. Potter, and J. Kreider. 1981. Rebreeding efficiency in mares fed different levels of energy during late gestation. In: Proc 7th Eq Nutr Physiol Symp, Virginia State Univ. p 101-104.

Henneke, D., G. Potter, J. Kreider, and B. Yeates. 1983. Relationship between condition score, physical measurements and body fat percentage in mares. Equine Vet. J. 15: 371-372.

Katch, F., E. D. Michael, and S. M. Horvath. 1967. Estimation of body volume by underwater weighing: description of a simple method. J. Appl. Physiol. 23: 811-813.

Milner, J., and D. Hewitt. 1969. Weight of horses: improved estimates based on girth and length. Can. Vet. J. 10: 314.

Pagan J.D., J. S., Duren S. What does your horse weigh? www.ker.com/library/advances/113 (Accessed April 29 2015).

Rothman, K. J., S. Greenland, and T. L. Lash. 2008. Modern epidemiology. Lippincott Williams & Wilkins.

Seidel, D., F. Beyer, D. Hertel, S. Fleck, and C. Leuschner. 2011. 3D-laser scanning: A non-destructive method for studying above-ground biomass and growth of juvenile trees. Agr. forest Meteorol. 151: 1305-1311.

Sholts, S. B., S. K. Wärmländer, L. M. Flores, K. W. Miller, and P. L. Walker. 2010. Variation in the measurement of cranial volume and surface area using 3D laser scanning technology. J. Forensic Sci. 55: 871-876.

Tikuisis, P., P. Meunier, and C. Jubenville. 2001. Human body surface area: measurement and prediction using three dimensional body scans. Eur. J. Appl. Physiol. 85: 264-271.

Wakat, D. K., R. E. Johnson, H. J. Krzywicki, and L. I. Gerber. 1971. Correlation between body volume and body mass in men. Am. J. Clin. Nutr. 24: 1308-1312.

Wells, J. C., I. Douros, N. J. Fuller, M. Elia, and L. Dekker. 2000. Assessment of body volume using three-dimensional photonic scanning. Ann. N. Y. Acad. Sci. 904: 247-254.

CHAPTER IV.

EQUINE BODY WEIGHT MEASUREMENT USING PHOTOGRAMMETRY

4.1. Introduction

4.1.1. Background

Current development of 3D imaging technology makes it possible to estimate the important body indices such as body volume (BV), body weight (BW), body density and the distribution of body fat much easier than in the past (Wells et al., 2000; Istook and Hwang, 2001; Yu et al., 2003; Hasler et al., 2009). Traditional restrictions of 3D scanning, such as the requirement to maintain a rigid posture during the scanning, has limited past 3D studies on live subjects to humans only; however, our recent study revealed that 3D scanning of live animals is also possible and easy to accomplish.

The 3D scanning based equine BW estimation method (3DScan) showed that there is high correlation between equine BV and the BW, the correlation coefficient (R) being 0.94. Studies on human subjects showed stronger correlation between BV and BW (R=0.996-0.998) than our study (Katch et al., 1967; Ward, 1968; Wakat et al., 1971). The weaker R between BV and BW for horses compared to human subjects is attributed to the presence of hair, mane and tail, and the fact that most horses do to not maintain at a complete standstill during the entire 3D scanning procedure. The different type and number of 3D scanners used between the human and the equine study may have also have played a factor (Sansoni et al., 2009; Khoshelham, 2011; Polo and Felicísimo, 2012).

There is a diversity of available 3D imaging methods, e.g. structured light 3D scanning, laser triangulation 3D scanning, time-of-flight (ToF) 3D scanning, and photogrammetry, and each uses different algorithms and different technologies (Sansoni et al., 2009; Cui and Stricker, 2011; Cui et al., 2013). The accuracy, advantages, and disadvantages of those methods vary, and the advantage of one method can be a disadvantage in another method depending on the purpose of the 3D imaging. Decisions regarding which of the 3D scanning methods to use, therefore, should be made carefully (Baltsavias, 1999; Böhler and Marbs, 2004; Ozsoy et al., 2009).

Photogrammetry is a widely used 3D imaging method. Examples of the application of photogrammetry are geographic mapping, 3D mapping of historical buildings, 3D imaging of people, or statues (Siebert and Marshall, 2000; Tucci et al., 2001; Böhler and Marbs, 2004). An advantage of this method is that it only requires a photographing device, e.g. a camera, to obtain a 2D image that can then be converted to 3D image. Depending on the size of the object and the expected resolution of the obtained 3D image, an expensive photographing device or a specialized photogrammetry program may be required. For instance, large-scale geographic mapping such as of a mountain may require a state-of-the-art photographing device to maximize the accuracy and resolution (Sturzenegger and Stead, 2012). There have also been a few animal studies in which photogrammetry utilizing high quality photographing devices and specialized software was used to create 3D images of the animals, for example, sea lions or pigs (Wu et al., 2004; Waite et al., 2007). There has been, however, no currently available animal study where photogrammetry was accomplished using a commonly used low cost photographing device, e.g. a smart phone, and free-ware photogrammetry software (Pouliquen, 2011; Chandler and Fryer, 2013; Santagati and Inzerillo, 2013).

Cost is an important consideration in any type of industry in terms of application. Even a difference of $100 may bring about a different decision by the owners of small livestock facilities regarding use of a technology. In the equine industry, the majority of horse owners have only a small number of horses (Kilby, 2007), and this makes it difficult for them to justify the purchase of a basic management-related equipment such as a large animal scale. This study was therefore designed to develop a photogrammetry based equine BW measurement method using a smart phone[ee] and a free-ware photogrammetry application (Pouliquen, 2011). [ff] As most horse owners likely now have a smart phone, development of this method will provide even small equine facilities with the option to measure the BW of horses with little-cost.

4.1.2. Hypothesis

A. Photogrammetry can be used as a method to estimate the accurate equine BW

4.1.3. Objectives

A. To obtain photogrammetry based 3D images of horses using a smart phone and free photogrammetry software (123D Catch).

B. To develop a linear regression model to estimate the BW of horses based on BV as estimated from the photogrammetry based 3D images.

C. To compare the accuracy of photogrammetry based equine BW measurement method (2Dto3D) with other equine BW estimation methods.

[ee] iPhone 4, Apple Inc., Cupertino, CA, USA, https://www.apple.com/

[ff] 123D Catch, Autodesk, San Rafael, CA, USA

4.2. Materials and methods

4.2.1. Sample size and target population

Eleven horses were included in this study. These horses were selected from horses owned by Colorado State University (CSU). No random selection was done since complete list of the source population was lacking and different horses were available depending on the study date. Six were polo horses, four were therapeutic riding horses, and one was a dressage horse. Among those horses, eight were mares and three were geldings. Ten of the study horses were either American Quarter Horse or Thoroughbred-American Quarter Horse cross and one was a Hanoverian.

The study procedure was approved by the institutional animal care and use committee (IACUC) at CSU in 2014 and the study was conducted accordingly. All of the animal use part of this study was conducted in September 2014.

4.2.2. Measurement of BW, body volume (BV), trunk volume (TV), and body condition score (BCS)

4.2.2.1. Measurement of the gold standard body indices (true BW, true BV, true TV, and true BCS)

True BW of the study horses was measured using a digital large animal scale.[gg] In each measurement, a horse was brought on to the scale, stood square in the middle of it, and the BW was recorded after the value shown on the digital screen kept constant for 2-3 seconds. BW

[gg] Model 700, True-test, Mount Wellington, New Zealand, http://group.tru-test.com/en

measurement was conducted three times per horse, and for each measurement the horse was taken off the scale and led back on for the next measurement. The median value among the three measured weights was considered as the true BW (e.g. gold standard BW) of the horse.

True BV and TV were estimated based on the equations to estimate equine BW based on BV or TV, sex, and coat type of horses which were developed and described in chapter 2 of this thesis. As indicated below, the equations were re-written to calculate the predicted true BV and TV based on the true BW and sex of the horses. Coat type was excluded in these equations because all 11 horses in this study had summer coats, and the numeric value of a summer coat in the original multiple linear regression models was zero. The theory of these true BV and TV estimation methods was based on human studies by Wakat at al. (1971) and Katch at al. (1967) which showed that the R between BW and BV was between 0.996-0.998. Since the true BW of horses was measured using a digital large animal scale but measurement of the true BV and TV was not available for this study, we estimated the true BV and TV of the horses using two regression equations that were described in chapter two of this thesis. Each of these two regression equations used the true BW and sex status of each individual horse to estimate the true BV and TV respectively as demonstrated below.

$$\text{true BV} = \frac{\text{true BW} - 12.76284 - 14.22675 \times \text{sex}}{0.92984}$$

$$\text{true TV} = \frac{\text{true BW} - 52.2005 - 19.92913 \times \text{sex}}{0.9912}$$

Three people determined the BCS for each horse using Henneke's BCS estimation method (Henneke et al., 1981; Henneke et al., 1983). They were either experienced horse people or veterinarians, and their understanding of the procedure was refreshed through informational brochures before they conducted the BCS evaluation for this study.[hh] Each person evaluated the BCS once per horse, therefore each horse had independent BCS's provided by each three of the people. The median value among those three values was determined as the best estimate of the true BCS of the horse.

4.2.2.2. Measurement of predicted BW using six different equine BW measurement methods.

The BW of the study horses was measured using six different equine BW measurement methods: 3D scanning based equine BW measurement method using variables BV, sex, and coat type (3DScan BV); 3D scanning based equine BW measurement method using variables trunk volume (TV), sex, and coat type (3DScan TV); a formula developed by Carroll and Huntington (Carroll's formula)(Carroll and Huntington, 1988); weight tapes manufactured by Purina (WT Purina)[ii] and Shell (WT Shell)[ij]; and visual estimation (VE). These six alternative equine BW estimation methods are described in detail in chapter 3 of this thesis. All of the methods were repeated three times (three different people estimated the BW once per horse using the WT Purina, WT Shell, VE, and heart girth measurement and body length measurement to conduct Carroll's formula). Among the three repeated measurements in each BW estimation method, the median value was determined as the true estimated value of the method.

[hh] Equine body condition score poster, The Horse Media Group LLC, http://www.thehorse.com/free-reports/30154/equine-body-condition-score-poster

[ii] Purina, St. Louis, Missouri, USA

[ij] Shell, The Hague, Netherlands. Weight tape by Shell is no longer commercially available.

4.2.3. Photogrammetry

4.2.3.1. Preparation of the location and the horses

The space where the images were obtained was approximately 6 by 6 meters square. The floor was flat and finished with concrete. Initially the floor was cleaned and reference markers were placed on the floor as shown in figure 4.1. Two black 180cm long and 11cm wide linear reference markers were placed crossing each other in the middle of the floor. Four sheets of paper having the letters, C, S, U, and V in the middle were placed at the ends of the linear markers. The four letters were written in different colors: Yellow for C, green for S, blue for U, and red for V. The length×width of the paper was 27.94cm × 20.32cm and the size of each letter was approximately 17cm × 17cm.

A study horse was groomed and its tail wrapped using an elastic band. Sixteen 1.9 cm diameter flat circular stickers were placed on the body of the horse. The stickers were four different colors: green, yellow, blue, and red. Stickers were placed in four directions of the horse: frontal, caudal, right lateral, and left lateral, and four different color stickers were placed in each direction. In the frontal area, the stickers were placed on the points of the shoulders, forehead, and dorsal nostril. In the lateral area they were placed on the scapula, tuber coxae, at points of one thirds and two thirds of the lateral vertical midline of the trunk and also a point at two-thirds of that midline. In the caudal direction the stickers were placed on the points of the buttocks and the points of the hocks (Figure 4.2). Once all of these preparations were finished the horse was brought to the middle of the imaging area.

4.2.3.2. Photogrammetry

Photographs were obtained for the purpose of applying the photogrammetry. Two different methods were used to obtain the photographs, directly and through capturing images from a recorded video. Study horses were divided into two groups depending on the 2D imaging method, group P (photography group) and group V (video recording group). The number of study horses in each group was five and six, respectively, and there was no significant difference in the means of BW or BCS between the horses in these two groups ($P>0.05$) (Table 4.1).

For group P, photographs were obtained at three different heights (70-80cm, 140-150cm, and 200cm from the floor) and from 16 directions. Sixteen chairs with a seat height of approximately 50cm were placed in a circle around where the horse stood and photographs at the 200cm height were obtained on the top of chairs. The center of the circle was marked with a black cross, and the diameter of the circle was approximately 6 meters. The angle created by two neighboring chairs and the center point was approximately 22.5 degrees. Once the location was ready, a horse was led to the middle of the circle. The horse handler lightly restrained the horse using a halter and a lead and stood at the left side between the head and shoulder of the horse. Once the horse was calm and did not show any sudden movements, photographs were obtained using a cellular phone. Since the photographs were taken in 16 directions for each height and at three different heights, the total number of the photographs in one set of 2D images was 48. Photographing was conducted to include the horse and reference markers as much as possible. A set of the 48 photographs was obtained while there was no horse movement, but sometimes slight movement such as neck or leg movement was observed. Photographs were always retaken when there was any obvious horse movement such as shifting of the location of the entire body. Three sets of 48

photographs were obtained for each horse; therefore, a total of 144 photographs were obtained (48 photographs×3 set per horse).

For group V, video was recorded from only one height, 140-150cm from the floor. This time, a 6m diameter circle was drawn on the floor using chalk marker. An investigator recorded a video using a video tool in a cellular phone while he/she walked slowly along the chalked line around the horse. It took approximately 45-50 seconds to complete one circle of video recording. As with photographing, the video recording was retaken from the beginning when there was an obvious horse movement. A video file that was completed without any obvious horse movement was considered as a set. Video recording was continued until the investigator completed three sets. Horse movement or a change of posture between sets was allowed. Once the video recording was finished, 2D images were captured from the video file. An image was captured every second of the video run time. The number of photographs captured from a set video file was 50-60; therefore, a total of 150-180 images were captured from the three sets for each horse.

All of the 2D images were processed using a photogrammetry program to construct the horse 3D image. For group P, 48 photographs were processed, and for group V, 50-60 images were processed for photogrammetry. Three 3D images were obtained per horse in each group.

4.2.4. Volume measurement

The size of the 3D image obtained using photogrammetry was adjusted to represent the true size of each horse through the comparison of the lengths of reference markers in the 3D image with the true length of the markers. The length of the linear black markers or the paper sheet

reference markers in the 3D image was measured using Meshlab (Cignoni et al., 2008).[kk] The true lengths of the reference markers were divided by the mean value of the four-times-repeated measurements of the references in the 3D image. The size of the 3D image was then multiplied with the value of the division.

Any non-horse parts of the rescaled 3D image were then erased from the 3D image and Poisson reconstruction was conducted on the image. Body volume (BV) of the reconstructed 3D image was estimated using Meshlab at first, and the 3D image of the horse was trimmed using Netfabb basic[ll] so that only the trunk remained. The volume of the trunk (TV) was measured using either Meshlab or Netfabb. A total of three values for BV and TV were obtained from the three sets of 3D images of each horse. The median value among those three measurements was considered the true values of the photogrammetry based BV and TV.

4.2.5. Statistical analysis

A formula to estimate the equine BW using photogrammetry was developed using regression model stepwise selection. Regression model selection procedure in P and V groups was conducted independently. The dependent variable was true BW, and BCS, sex, and photogrammetry-based BV, as well as TV were potential independent variables in the model selection. Sex was not included as an independent variable in the V group because there was only one sex, mares, in this group. Once the linear regression models were determined, the BW

[kk] Meshlab, Istituto di Scienza e Tecnologie dell'Informazione (Institute of Information Science and Technology), Italian National Research Council (CNR), Pisa, Italy, http://meshlab.sourceforge.net/
[ll] Netfabb basic, Netfabb company, Lupburg, Germany, http://www.netfabb.com/

of horses was predicted using the developed formulas. The predicted equine BW was recorded as the Predicted BW of 2Dto3D method.

Lastly, the correlation between the true BW and predicted BW of seven different alternative equine BW estimation methods was analyzed. In addition, modified deviation (Dev) and modified absolute deviation (AbsDev) of the predicted BW of seven alternative equine BW estimation methods were calculated as follows: Dev=Predicted BW−True BW, AbsDev=|Predicted BW−True BW|. Dev and AbsDev of each method were compared using one-way ANOVA and pair-wise comparisons.

Criteria for the statistical significance of all analyses was $P<0.05$. All of the statistical analyses were conducted using a statistics package.[mm]

4.3. Results

4.3.1. BW, BV, and BCS measurement

The mean true BW and standard deviation (SD) (BW±SD) of the 11 study horses was 532.98±48 kg, the mean true BV±SD was 555.30±49.81 liters, and mean true TV±SD was 479.57±46.3 liters. The mean predicted BW and SD of alternative equine BW estimation methods are shown in Table 4.2. The difference of the means between the true BW and the estimated BW using alternative equine BW estimation methods was less than 10 kg in all the alternative equine BW estimation methods except for WT Shell. The average BW estimated by

[mm] SAS, version 9.3, SAS Institute Inc., Cary, NC, USA

WT Shell method underestimated the true BW by 32.38 kg. WT Shell was the only equine BW estimation method that showed a statistically significant mean difference with the true BW (paired t-test: P = 0.004). The mean true BCS±SD of the study horses was 6.0±1.

4.3.2. Photogrammetry

Photographing and video recording had to be restarted several times because the horses often had obvious body movement. Obtaining a set of 48 photographs without movement (a total 144 photographs, 48 times three sets) for group P group was especially time consuming. In group P, three sets of 48 photographs were obtained for three of the horses, but only two sets could be taken for one horse, and only one set for the remaining horse. Approximately 20-30 minutes was spent to obtain an acceptable set of 48 photographs, including the time required to obtain additional photographs because of the horse movement.

In contrast to photography, the video recording of group V horses was comparatively easier and less time consuming. Depending on the amount of movement and level of nervousness of the horses, it took 10-50 minutes to obtain three sets of short video clips per horse. Three short video clips of all six horses were obtained with little difficulty. Several images captured from the video files showed that the horse and background were slightly blurred. It was also observed that the resolution of the captured images of group V horses was lower than the resolution of the photographs of group P horses. The file size of a captured image for group V was only 20% of the size of the photograph files for group P.

The 3D images constructed using photogrammetry are shown in Figure 4.3. These images of group P horses were much more detailed than the 3D images of group V horses. Poor 3D construction was often observed in the head and neck region in the both groups (Figure 4.4).

Reference markers were easily identified in the constructed 3D images, but a little blurring of the markers was observed in group V images (Figure 4.5). Mean BV and TV of the study horses as measured using 2Dto3D 3D images were 591.3 liters and 505.29 liters, respectively. These values were 38.2 liters and 29.3 liters, respectively, larger than the true BV and TV.

4.3.3. Statistical analysis: linear regression model to estimate the BW of horses

TV and BV were selected as an independent variable in the P group and V group, respectively, in the linear regression model to estimate equine BW. The coefficient of determination (R^2) of the selected models was 0.82 and 0.78, respectively. Equations for the developed regression models are shown below. The mean BW and SD of the predicted BW of 11 study horses estimated using 2Dto3D was 532.98 kg$\pm$44.58 kg (Table 4.2.b). A graph of the predicted BW of 2Dto3D method and the true BW of 11 study horses is shown in Figure 4.6. The difference of the predicted BW estimated using the 2Dto3D method and the true BW of the horses was minus 35.11 kg-24.25 kg. The mean AbsDev of the 2Dto3D method was 14.24 kg and was 2.67% of the true BW.

$$\text{P group: BW} = -236.37757 + 1.5504 \times \text{TV (2Dto3D)}$$

$$\text{V group: BW} = -105.93233 + 1.05804 \times \text{BV (2Dto3D)}$$

4.3.4. Statistical analysis: Pair-wise comparisons of the equine BW measurement methods

The R between the true BW and predicted BW estimated using alternative equine BW estimation methods are described in Table 4.3. The highest R was shown in 3DScan BV (0.96), followed by VE (0.95), 3DScan TV (0.95), 2Dto3D (0.93), WT Purina (0.87), WT Shell (0.84), and Carroll's formula (0.82). Mean Dev and mean AbsDev of alternative equine BW estimation methods were

-32.38 kg – 9.35 kg and 11.62 kg-37 kg, respectively. The mean % errors ((mean AbsDev/mean true BW)×100) compared to the true BW of the alternative equine BW estimation methods were between 2.18-6.94%. The AbsDev of 3DScan BV method was 2.18% of the BW and it was the lowest among the seven methods. VE showed the second lowest absolute % error of 2.2% followed by 3DScan TV 2.46%, 2Dto3D 2.67%, WT Purina 3.64%, Carroll's formula 3.84%, and WT Shell 6.94% (Table 4.4, Figure 4.7).

A one-way ANOVA was conducted to compare the mean predicted BW, the mean Dev, and the mean AbsDev of the seven alternative equine BW estimation methods. The p-values were 0.4897, 0.0009, and <0.0001, respectively. Pair-wise comparisons of Dev and AbsDev were conducted. The result of the pair-wise comparisons showed that the mean Dev and AbsDev of six methods—2Dto3D, 3DScan BV, 3DScan TV, VE, Carroll's formula, and WT Purina—were not significantly different from each other, but the values for WT Shell were significantly different from the other six methods.

4.4. Discussion

Free–ware Photogrammetry can be a very useful tool to estimate the BW of horses due to it is essentially zero-cost (Chandler and Fryer, 2013; Santagati and Inzerillo, 2013). However, this method has several disadvantages which make it inconvenient to use compared to 3D scanning, e.g. photogrammetry does require more time to obtain the 3D image if only one 2D imaging device is used. In addition, it requires a reference material with known length to accurately measure the several indices of the subject. Lastly, the construction of the 3D image sometimes failed but, unfortunately, the operator does not know whether the 3D image construction will be

successful or not until the 2D images are processed using the photogrammetry software (Bartoš et al., 2014).

Since 3D images constructed using photogrammetry do not represent the true size of the object, we placed several reference materials around the horse so that it would be possible to estimate the volume of the horses using the obtained 3D images. The reference materials used in this study were a black 180 cm long cross and 27.94 cm long paper.

The black cross reference marker, however, caused unexpected disadvantages. The horses were often reluctant to stand on this marker. In addition, there was reflection of light from the surface of this marker. The reference marker was made of duct tape and the surface had a light coating of reflective material. The indoor arena where the 2D images were obtained had indirect light coming from the skylights. Since the photographs and the video were obtained from several different angles while the operator moved 360 degrees around the reference marker, the reflection of light on the reference marker changed as the angle of the 2D image changed. In consequence, the black cross often appeared grey in the 3D image, and sometimes was not clearly represented in the 3D image, making it difficult to measure length in the 3D image. Poor-representation of the reference markers in the constructed 3D image would probably be an even more serious problem if the photogrammetry images were obtained outdoors. Since not all equine owners have a barn or an arena, many of the 2Dto3D method will be conducted outdoors once this method is widely used. Development of reference markers without the light reflection is, therefore, required for the general application of 2Dto3D method.

In this study the markers and references were designed to improve the photogrammetry procedure itself. The photogrammetry software recognizes common points in overlapping part in

2D photographs obtained in different angles and determines the three-dimensional locations of those points in space by measuring their distance on the images from different angles. Several sets of these 3-D points were coordinated to build the 3D image from the the least sum of squares errors (Gruen and Akca, 2005; Pouliquen, 2011). An object of smooth shape, e.g., a monotone ball, makes this process difficult, thus the 3D construction commonly fails. Many horses have a smooth body shape and are a monotone color. The failure of the photogrammetry on this kind of object can be prevented if obviously recognizable markers are placed on or near the object. We therefore placed four letters of different colors and shapes, C, S, U and V, and also attached small circular markers of four different colors on the body of the horses to help the 3D image construction procedure of photogrammetry (Figure 4.1, 4.2).

Compared to the 3D scanning, more time was required for photographing or video recording of the horses. Even when we thought all the images were obtained without any horse movement, the constructed 3D image sometimes showed that there was actually subtle movement that induced a partial 3D imaging failure. Subtle movement of the head was observed most often, causing the 3D image of the head of some horses to appear much larger than the true size, and the shape of the head also looked abnormal. This might be the reason why TV, whereby volume was measured excluding the head and neck, was chosen as an independent variable in the linear regression model selection procedure in case of the group of horses that the 2D images were obtained through still photography.

Between two different methods which were used to obtain 2D images of the horse in this study, photography and video recording, Photography required more time to obtain enough 2D images for photogrammetry then video recording. On average, it took 20 to 30 minute to obtain a set of photographs in P group, but V group required only a half the amount of time to obtain a set of an

appropriate video file for photogrammetry. Since video recording took less time, it was more convenient and less horse movement was observed while the image was being obtained. However, later it was observed that the resolution of the captured 2D images from the video file was much lower than the resolution of the pictures obtained from the photography method. Video recording also required a time consuming video file editing procedure in order to obtain the needed 2D captures of a horse from the file. Approximately an hour was required to review the video file and obtain the 50-60 2D captures from a set of video file. Average file size of the captured 2D image from the video file was approximately 400 kb and was only 20% of the size of the photographs images. The low resolution of the group V images caused a loss of detail in the constructed 3D images. Even though the image resolution of V group was much lower than P group, R^2 difference between regression models of the P and V groups was only 0.04.

The lower resolution and larger 3D imaging error of the video recording method than photography method would likely be overcome if a high-resolution video recording device were used. The video recording method has a great advantage compared to the photography method because it greatly decreases the imaging time. Decreasing the time requirement for acquiring 2D images of live animals means higher accuracy in the end due to the less chance of animal movement while the images are obtained. It would be worthwhile to compare the different results of the video recording-based photogrammetry depending on the resolution of the video-recording devices.

The 2Dto3D method of equine BW estimation showed the same level of accuracy as other equine BW estimation methods. No statistically significant error (AbsDev) difference among 3DScan BV, 3DScan TV, 2Dto3D, VE, Carroll's formula, and WT Purina was observed, but it was observed when compared to the WT Shell method. One of the reasons for the lack of the

statistical significance on the AbsDev comparisons could be because of the low number of horses in each of the study groups. One of the interesting observations in this study is the fact that conventional equine BW estimation methods (Carroll's formula, WTs, and VE) showed higher levels of accuracy compared to our previous pair-wise comparison study described in chapter 3 of this research. There were eleven horses in this study compared to twenty two reported in chapter 3, and these eleven horses had an even more normal BW and BCS distribution than the horses used in chapter 3. Mean BW of these eleven horses was 532.98 kg and the SD was only 48 kg. This means 95% of the study horses had less than 96 kg of BW variation. As discussed in chapter 3 of this thesis, the accuracy of the BW estimation of the conventional equine BW estimation methods is stronger when the horse has an average or normal BW and BCS (Gibbs and Householder). If our 2Dto3D method has the same strength as the 3DScan method, the difference of the accuracy between the 2Dto3D method and conventional equine BW estimation methods would be more obvious if the comparison was conducted on a larger horse population with greater variability in the BW and BCS's.

In this chapter, the VE showed the same level of high accuracy as the 3DScan. It was surprising that VE in this group of horses showed better accuracy than majority of other equine BW estimation methods. This result was, however, somewhat expected because most of the horses in this study were of average BW with BCS variance being very small. Based on the findings in our study in chapter 3, people have a tendency to assume the BW of a horse close to the BW of average horses.

One could thus ask if the VE is more accurate than Carroll's formula or WTs if the estimation of BW is of a horse of normal BW and BCS. Further study will be necessary to clarify if this is a consistent finding. What we should take into consideration is the accuracy of VE appears to

depend on various factors such as the horse's BW or BCS. The % error of the VE compared to the true BW was 5.57% in the study reported in chapter 3 of this thesis, but was only 2.2% in the study reported in this chapter. VE was the method for which the % error fluctuated the most among all of the equine BW estimation methods that were evaluated in this thesis.

In conclusion, an equine BW measurement method using photogrammetry showed the same level of accuracy with other equine BW estimation methods evaluated. Horses used in this study were in the narrow BW variance and moderate BCS and thus the conventional methods showed a higher level of accuracy than they showed in the study reported in chapter 3 of this thesis that was conducted on a larger number of horses with greater BCS and BW variances. It is highly likely that 2Dto3D method will show higher accuracy than WT, Carroll's formula, or VE if the same study is conducted on the larger number of horses with greater variance of physical characteristics than those included in the present study since the margin of error of the estimated BW of the 2Dto3D method is expected to not increase as the BW and BCS variance of the study horses get larger but the margin of error of WT, Carroll's formula, and VE does. 2Dto3D has some disadvantages for the equine BW estimation compared to the 3DScan, but is still worthy of further study since the application of photogrammetry requires little to no financial investment beyond equipment that most equine owners would already own for other purposes, and thus has great potential to be widely used.

4.5. Tables and figures

Table 4.1. The comparison of BW, BV, TV, and the error of the 2Dto3D volume measurement of Group P and V. The unit of weight is kg and volume is liter. # Obs = number of observations, Std Dev = standard deviation. No significant variance or mean difference was observed between group P and V for the listed variables. The error of the volume measurement of these two groups was also compared to each other. No statistically significant variance or mean difference was observed.

Variables	Group	# Obs	Mean	Std Dev	Median	Minimum	Maximum	P-values	
								Levene's test	T-test
True BW	sum	11	532.98	48	537.96	443.16	620.5	0.4777	0.0747
	group P	5	560.94	48.37	553	496.68	620.5		
	group V	6	509.69	36.1	520.95	443.16	538.87		
True BV	sum	11	555.3	49.81	564.83	462.87	638.29	0.4322	0.1336
	group P	5	580.36	53.67	566.48	505.13	638.29		
	group V	6	534.42	38.83	546.53	462.87	565.8		
True TV	sum	11	479.57	46.31	485.14	394.43	553.24	0.4081	0.168
	group P	5	501.19	51.29	491.63	428.32	553.24		
	group V	6	461.55	36.42	472.91	394.43	490.99		
BV (2Dto3D)	sum	11	591.3	33.82	576.61	541.89	635.83	0.4657	0.3356
	group P	5	602.64	37.85	622.34	549.2	635.83		
	group V	6	581.85	30.09	575.66	541.89	620.87		
TV (2Dto3D)	sum	11	505.29	28.69	505.85	452.88	546.54	0.8625	0.3706
	group P	5	514.27	28.19	517.18	471.72	546.54		
	group V	6	497.8	29.36	504.27	452.88	531.84		
BV (2Dto3D) - True BV	sum	11	-1.11	15.67	-3.74	-21.86	31.54	0.4266	0.3726
	group P	5	-5.99	13.15	-10.54	-21.86	9.27		
	group V	6	2.96	17.58	-2.98	-16.75	31.54		
TV (2Dto3D) - True TV	sum	11	-1.8	17.11	-6.83	-24.52	37.3	0.3533	0.4494
	group P	5	-6.35	12.91	-8.23	-24.52	8.1		
	group V	6	2	20.34	-4.99	-18.73	37.3		

Table 4.2. True BW, true BV, and true TV of study horses (Table 4.2.a) and mean predicted BW, standard deviation, median, minimum and maximum of equine BW measurement methods evaluated in this study (Table 4.2.b). The predicted BW using alternative equine BW estimation methods were similar to the true BW. The exception was WT Shell which underestimated the true BW by 32.38 kg.

4.2.a. Summary of the true BW, BV, and TV of 11 study horses.

Variable	Mean	Std Dev	Median	Minimum	Maximum
True BW (kg)	532.98	48.0	537.96	443.16	620.5
True BV (liter)	555.3	49.81	564.83	462.87	638.29
True TV (liter)	479.57	46.31	485.14	394.43	553.24

Ste Dev = standard deviation.

$\text{true BV} = \frac{\text{true BW} - 12.76284 - 14.22675 \times \text{sex}}{0.92984}$, $\text{true TV} = \frac{\text{true BW} - 52.2005 - 19.92913 \times \text{sex}}{0.9912}$

4.2.b. Summary of the predicted BW (kg) estimated by using various equine BW measurement methods.

Method	Mean	Std Dev	Median	Minimum	Maximum
2Dto3D	532.98	44.58	543.12	467.41	610.97
3DScan BV	531.95	39.58	527.69	472.48	600.17
3DScan TV	531.17	38.39	528.67	480.13	596.09
Carroll's formula	524.09	38.54	538.72	464.9	584.57
WT Purina	542.33	50.25	539.77	460.4	621.42
WT Shell	500.6	26.91	496.68	468.56	547.03
VE	527.58	46.02	521.63	453.59	635.03

Table 4.3. R between the true BW and predicted BW of various equine BW estimation methods.

Method	True BW	2Dto3D	3DScan (BV)	3DScan (TV)	VE	Carroll's formula	WT Purina	WT Shell
True BW	1	0.92881	0.96278	0.94698	0.95096	0.81529	0.86501	0.8415
2Dto3D	0.92881	1	0.9477	0.95152	0.81243	0.872	0.83676	0.88915
3DScan BV	0.96278	0.9477	1	0.9952	0.89826	0.86931	0.81081	0.8359
3DScan TV	0.94698	0.95152	0.9952	1	0.88172	0.8877	0.81805	0.86035
VE	0.95096	0.81243	0.89826	0.88172	1	0.70908	0.85016	0.8094
Carroll's formula	0.81529	0.872	0.86931	0.8877	0.70908	1	0.85792	0.87939
WT Purina	0.86501	0.83676	0.81081	0.81805	0.85016	0.85792	1	0.94872
WT Shell	0.8415	0.88915	0.8359	0.86035	0.8094	0.87939	0.94872	1

Table 4.4. Predicted BW, Dev and AbsDev of various equine BW measurement methods.

Method	Predicted BW	Predicted BW-True BW				|Predicted BW-True BW|			
		mean	% error*	95% Confidence Limits		mean	% error*	95% Confidence Limits	
2Dto3D	532.98	0.0	0.0	-12.23	12.23	14.24	2.67	5.76	22.73
3DScan (BV)	531.95	-1.03	-0.19	-13.26	11.2	11.62	2.18	3.14	20.11
3DScan (TV)	531.17	-1.81	-0.34	-14.04	10.42	13.12	2.46	4.63	21.61
VE	527.58	-5.4	-1.01	-17.63	6.83	11.72	2.2	3.24	20.21
Carroll's formula	524.09	-8.9	-1.67	-21.13	3.33	20.46	3.84	11.97	28.95
WT Purina	542.33	9.35	1.75	-2.88	21.58	19.42	3.64	10.94	27.92
WT Shell	500.6	-32.38	-6.08	-44.61	-20.16	37	6.94	28.52	45.49

Dev = Predicted BW-True BW, AbsDev=|Predicted BW-True BW|

* Percent error compared to the true BW

4.1.a

4.1.b.

Figure 4.1. The preparation of the location of photogrammetry application. Two linear black reference markers were placed crossing each other on the floor of the study area (Figure 4.1a). The length of each marker was 180 cm. At the ends of the black markers a paper sheet with letters C, S, U, and V, were placed (Figure 4.1.a). To obtain photographs of group P horses, 16 chairs with a seat height of approximately 50 cm were placed to surround the area where the horse stood (Figure 4.1.b).

4.2.a

4.2.b

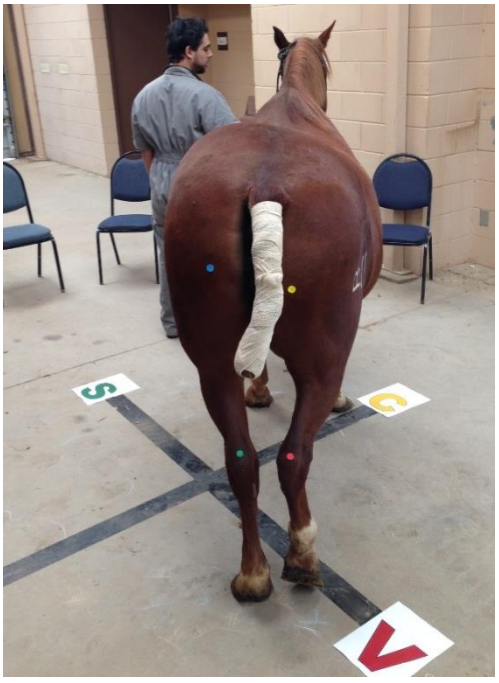

4.2.c

Figure 4.2. Location of the markers on the body of the horse. Circular markers were placed on 16 locations on the body of each horse. Frontal view (Figure 4.2.a), caudal view (Figure 4.2.b), and lateral view (Figure 4.2.a-c).

4.3.a.

4.3.b.

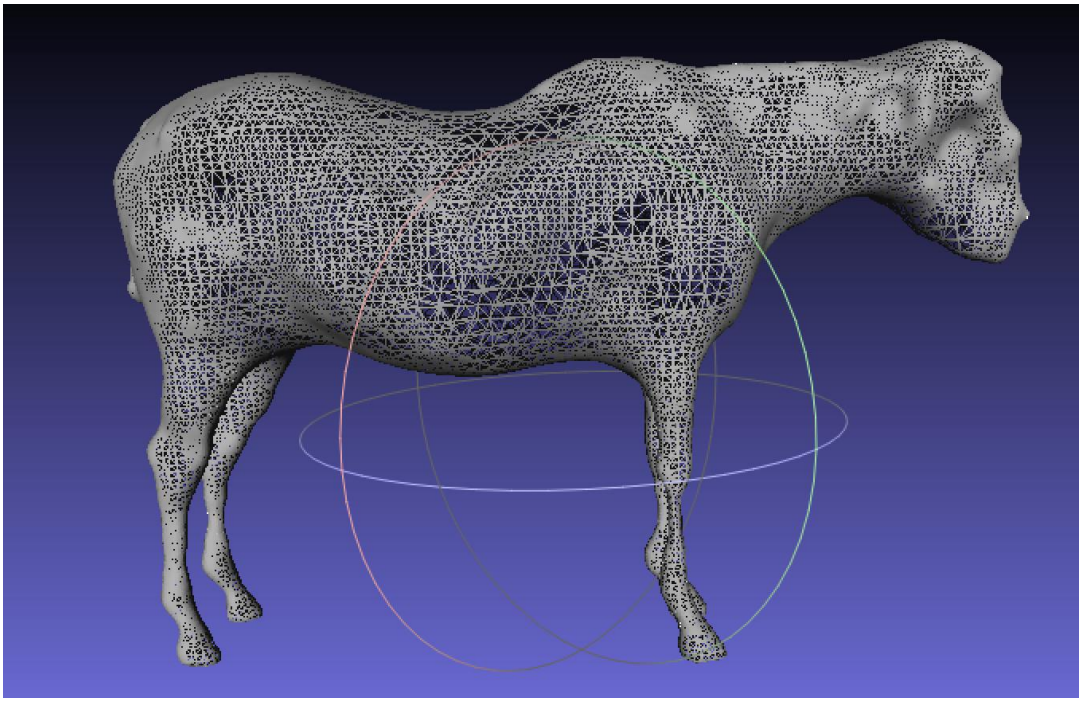

4.3.c.

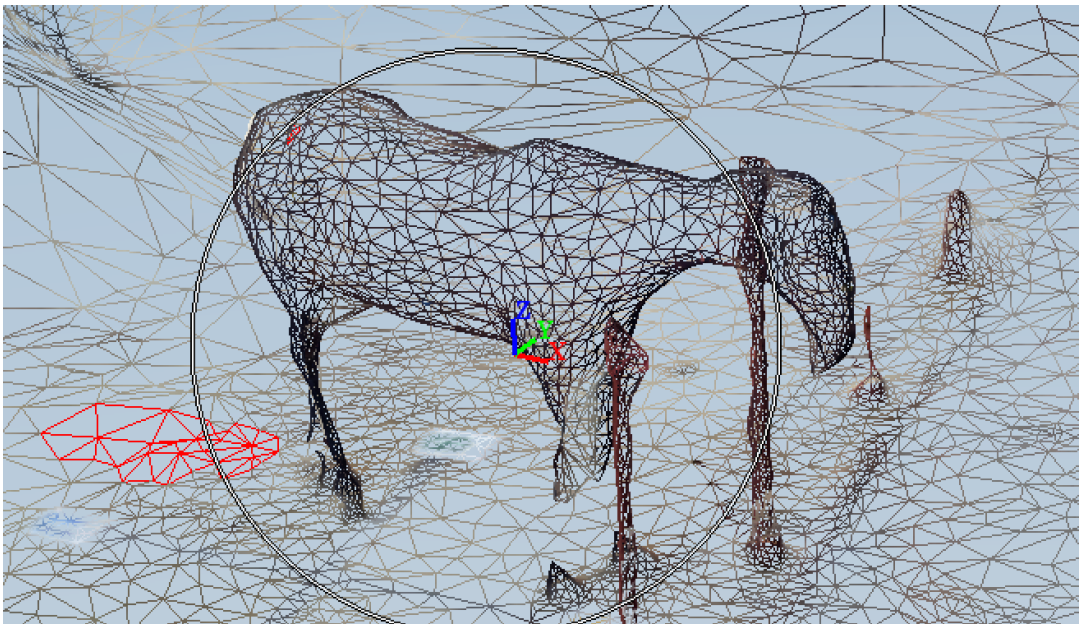

4.3.d

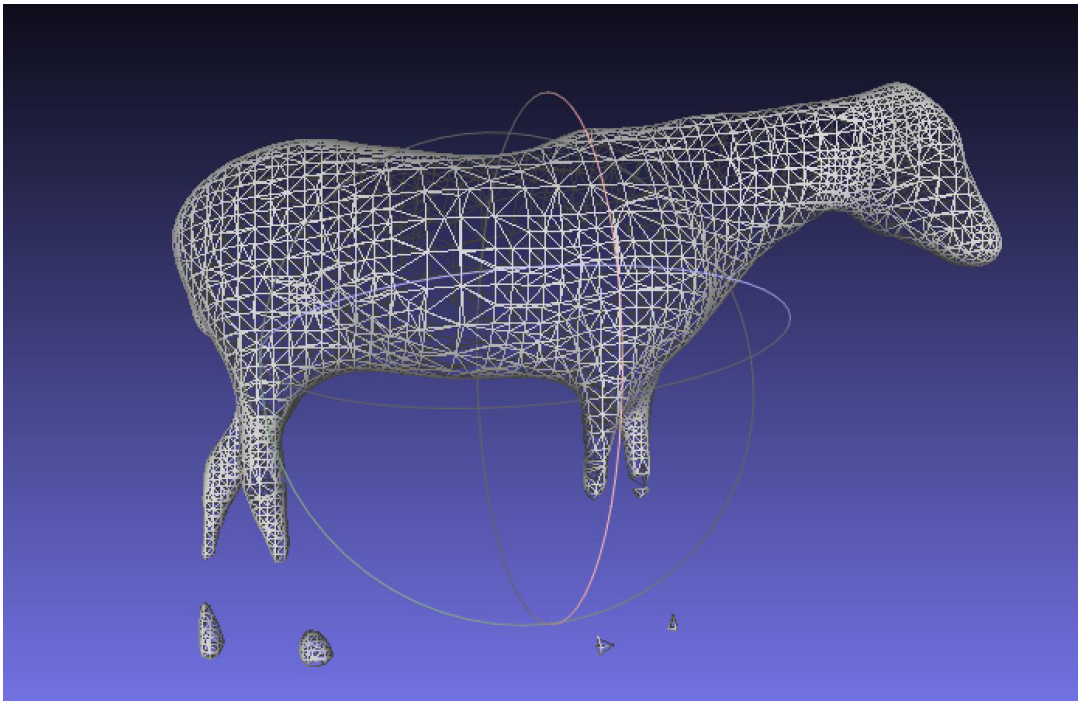

Figure 4.3. 3D images obtained using photogrammetry. Figures 4.3.a and 4.3.c are raw 3D images constructed using photogrammetry, 4.3.a from group P and 4.3.c from group V. Figures 4.3.b and 4.3.d are horse 3D images after the trimming of non-horse part and Poisson reconstruction were conducted on the images of figure 4.3.a and 4.3.c, respectively. Group P horse 3D images (Figure 4.3.a, 4.3.b) were more detailed than those from group V (Figure 4.3.c, 4.3.d).

4.4.a

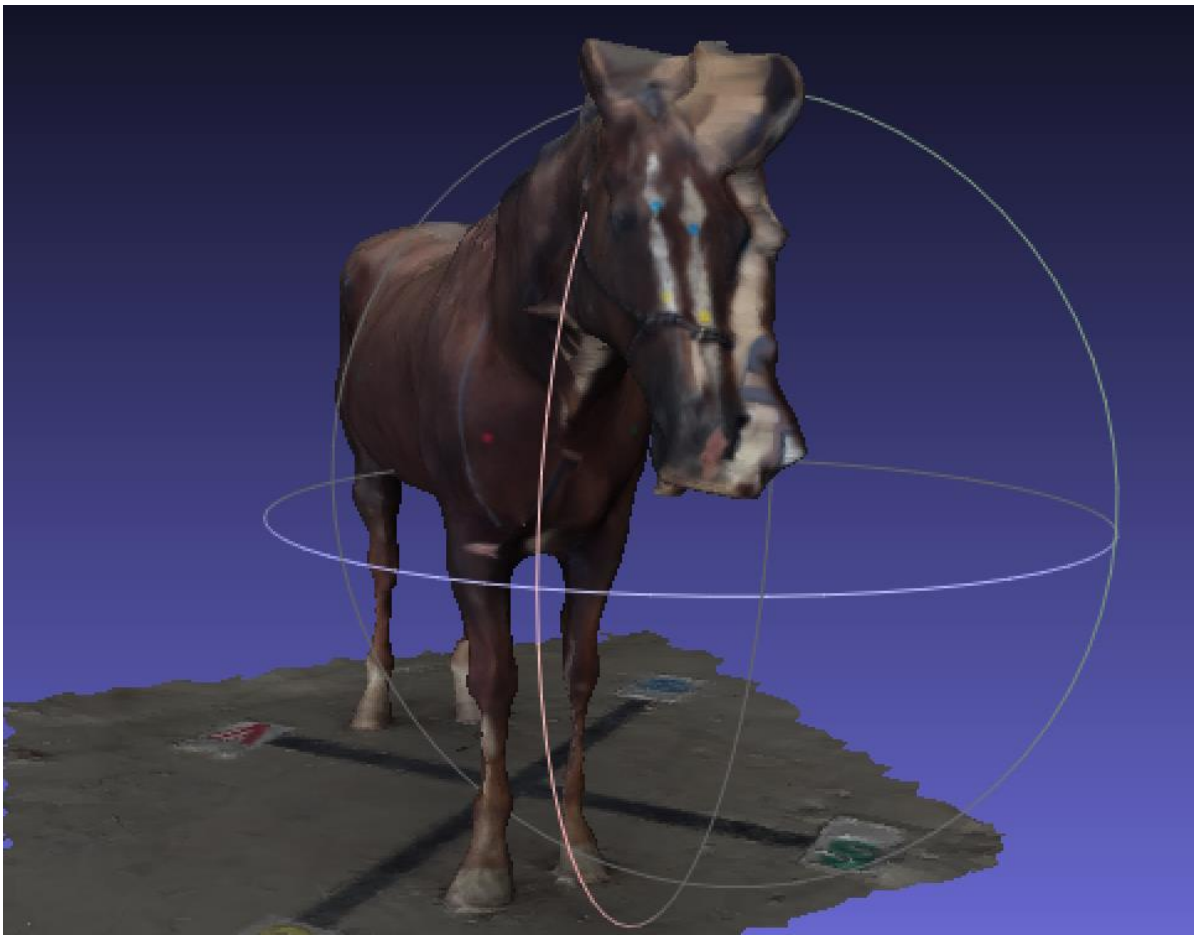

4.4.b

4.4.c

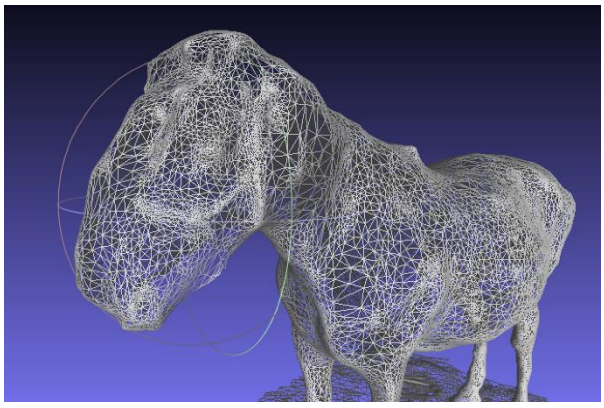

Figure 4.4. Poorly-constructed 3D image of the head and neck of a P group horse. 3D imaging error was induced by subtle movement of the horses during the 2D imaging. In figure 4.4.a, subtle horizontal head movement induced error in the constructed 3D image. Neither the horse handler nor the photographer recognized the horse movement at the time of 2D imaging because the movement was so subtle, but recognized it only after the photogrammetry was finished. In consequence, the constructed 3D image of the head and neck was larger and distorted compared to the true head (Figure 4.4.b and 4.4.c).

4.5.a

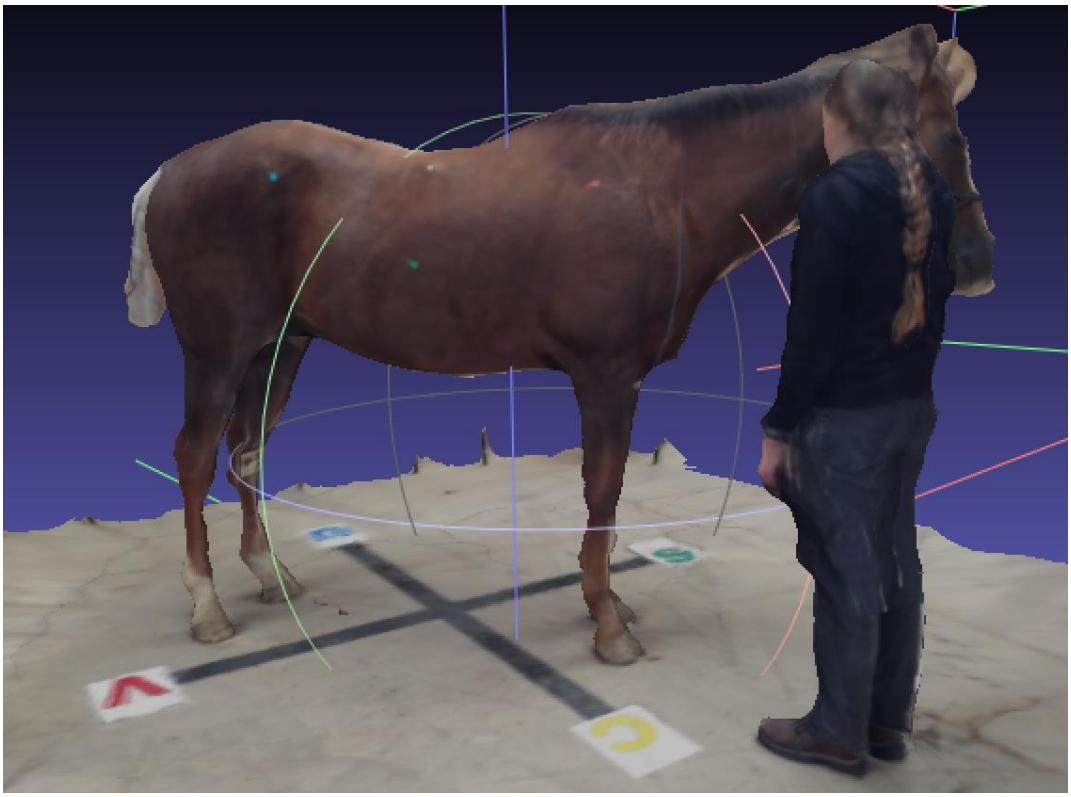

4.5.b

4.5.c

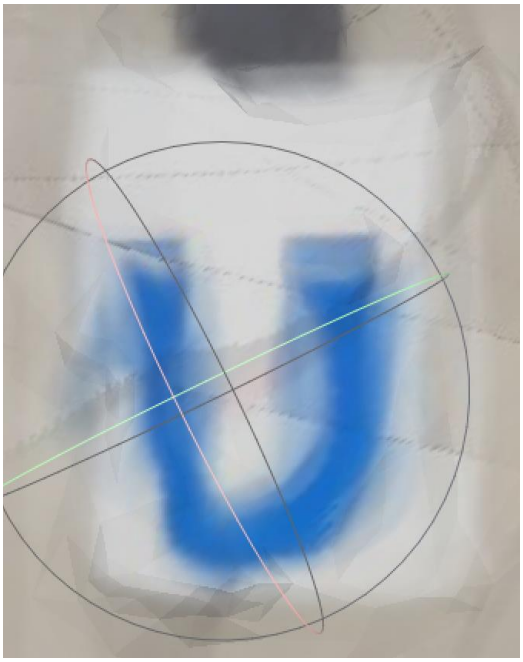

Figure 4.5. Reference markers represented in the constructed 3D image. Reference markers were clearly shown in the 3D image (Figures 4.5.a and 4.5.b) but slight blurring of the reference markers was sometimes observed (Figure 4.5.c).

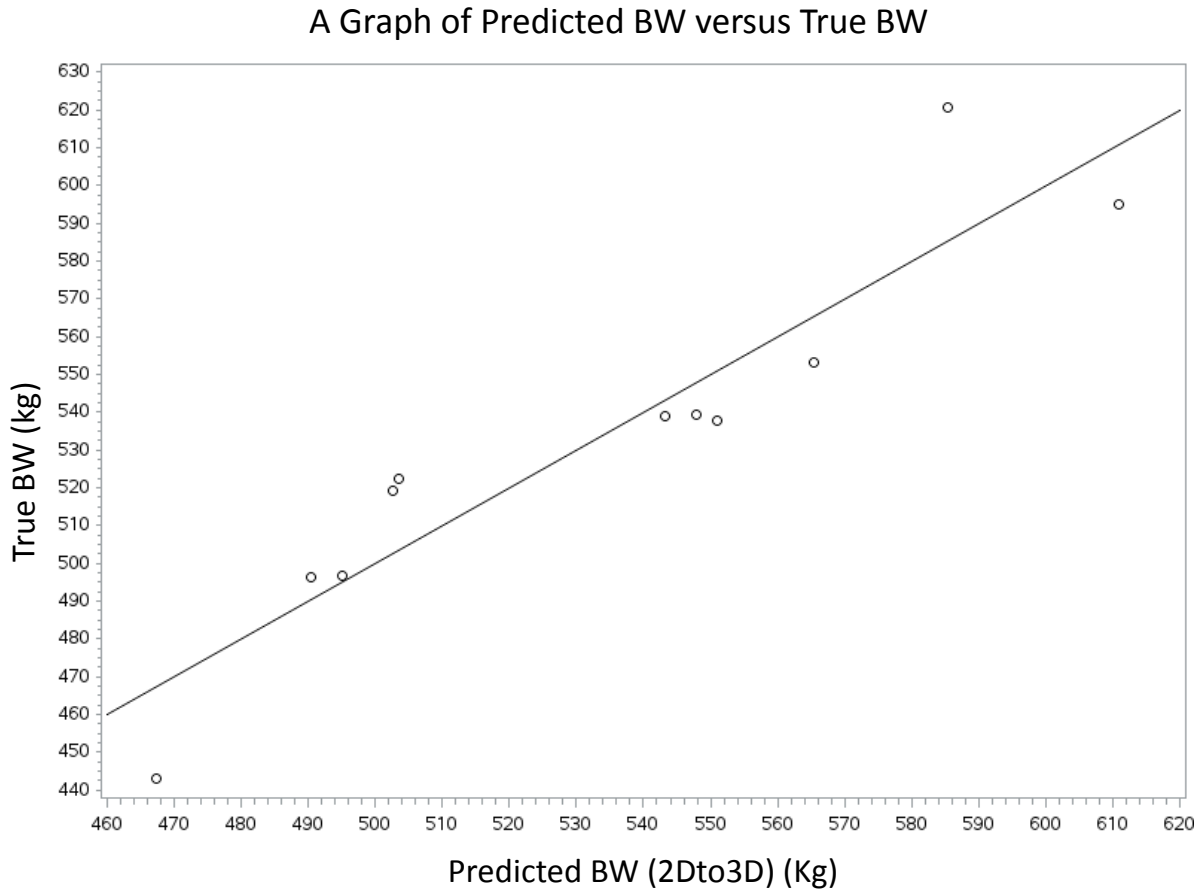

Figure 4.6. The plot of predicted BW using 2Dto3D method versus the true BW.

4.7.a.

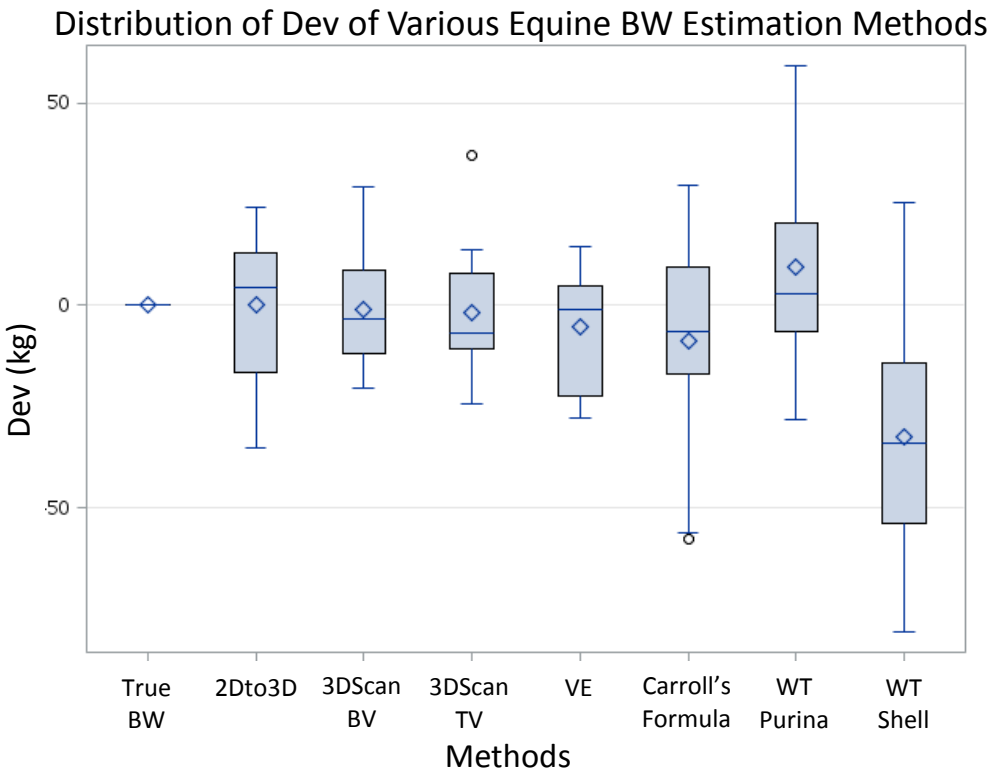

4.7.b.

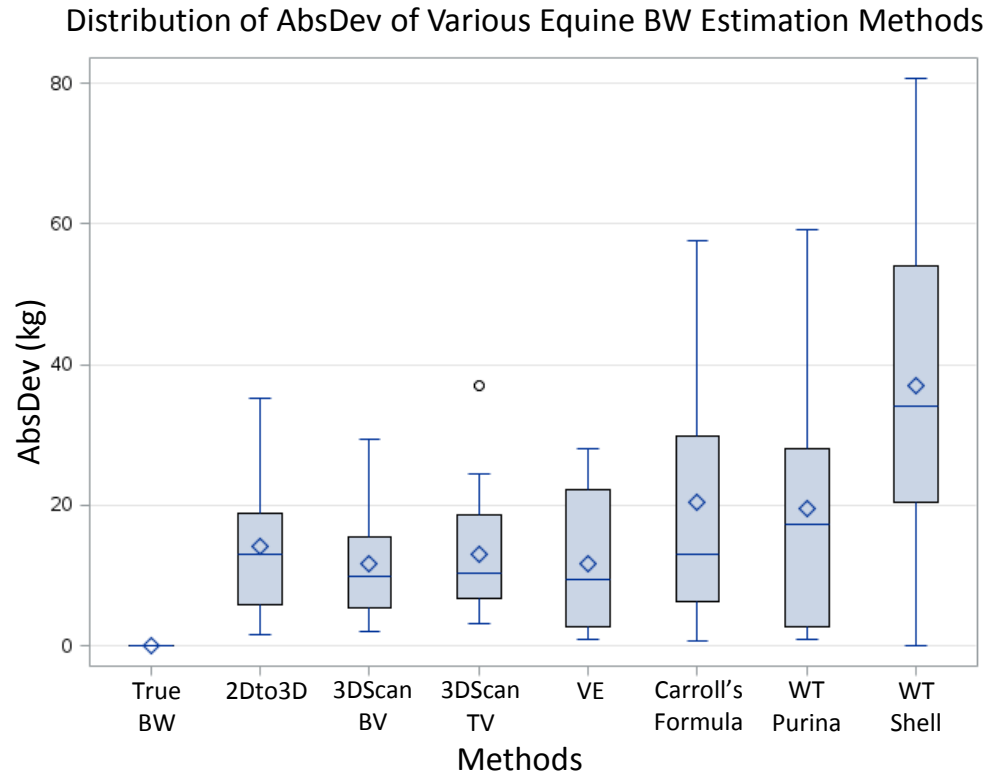

Dev = Predicted BW-True BW, AbsDev=|Predicted BW-True BW|

Figure 4.7. Distribution of Dev and AbsDev of equine BW estimation methods

REFERENCES

Baltsavias, E. P. 1999. A comparison between photogrammetry and laser scanning. ISPRS Journal J. Photogramm. Remote Sens. 54: 83-94.

Bartoš, K., K. Pukanská, and J. Sabová. 2014. Overview of available open-source photogrammetric software, its use and analysis. Int. J. Innov. Educ. Res 2: 62-70.

Böhler, W., and A. Marbs. 2004. 3D scanning and photogrammetry for heritage recording: a comparison. Proc. 12th International Conference on Geoinformatics. p 291-298.

Carroll, C., and P. Huntington. 1988. Body condition scoring and weight estimation of horses. Equine Vet. J. 20: 41-45.

Chandler, J., and J. Fryer. 2013. Autodesk 123D catch: how accurate is it. Geomatics World 2: 28-30.

Cignoni, P., M. Corsini, and G. Ranzuglia. 2008. Meshlab: an open-source 3d mesh processing system. Ercim news 73: 45-46.

Cui, Y., S. Schuon, S. Thrun, D. Stricker, and C. Theobalt. 2013. Algorithms for 3d shape scanning with a depth camera. IEEE Trans. Pattern. Anal. Mach. Intell. 35: 1039-1050.

Cui, Y., and D. Stricker. 2011. 3d shape scanning with a kinect. ACM SIGGRAPH 2011 Posters. p 57.

Gibbs, P., and D. Householder. Estimating Horse Body Weight with a Simple Formula. http://www.aspcapro.org/sites/pro/files/estimating_horse_body_weight.pdf (Accessed 4 April 2015). Texas A&M.

Gruen, A., and D. Akca. 2005. Least squares 3D surface and curve matching. ISPRS J. Photogramm. Remote Sens. 59: 151-174.

Hasler, N., C. Stoll, B. Rosenhahn, T. Thormählen, and H.-P. Seidel. 2009. Estimating body shape of dressed humans. Computers & Graphics 33: 211-216.

Henneke, D., G. Potter, and J. Kreider. 1981. Rebreeding efficiency in mares fed different levels of energy during late gestation. In: Proc 7th Eq Nutr Physiol Symp, Virginia State Univ. p 101-104.

Henneke, D., G. Potter, J. Kreider, and B. Yeates. 1983. Relationship between condition score, physical measurements and body fat percentage in mares. Equine Vet. J. 15: 371-372.

Istook, C. L., and S.-J. Hwang. 2001. 3D body scanning systems with application to the apparel industry. JFMM 5: 120-132.

Katch, F., E. D. Michael, and S. M. Horvath. 1967. Estimation of body volume by underwater weighing: description of a simple method. J. Appl. Physiol. 23: 811-813.

Khoshelham, K. 2011. Accuracy analysis of kinect depth data. ISPRS workshop laser scanning. 133-138.

Kilby, E. R. 2007. The demographics of the US equine population. http://www.humanesociety.org/assets/pdfs/hsp/soaiv_07_ch10.pdf (Accessed 26 December 2014). The humane society of the United States.

Ozsoy, U., B. M. Demirel, F. B. Yildirim, O. Tosun, and L. Sarikcioglu. 2009. Method selection in craniofacial measurements: advantages and disadvantages of 3D digitization method. J Craniomaxillofac. Surg. 37: 285-290.

Polo, M.-E., and Á. M. Felicísimo. 2012. Analysis of uncertainty and repeatability of a low-cost 3d laser scanner. Sensors 12: 9046-9054.

Pouliquen, D. 2011. It's a Snap! Take a photograph and create a 3D. https://www.thingiverse.com/download:75082 (Accessed 4 April 2015). Autodesk University.

Model. https://thingiverse-production.s3.amazonaws.com/assets/8a/3e/e6/60/19/catchManual.pdf (Accessed May 1 2015).

Sansoni, G., M. Trebeschi, and F. Docchio. 2009. State-of-the-art and applications of 3D imaging sensors in industry, cultural heritage, medicine, and criminal investigation. Sensors 9: 568-601.

Santagati, C., and L. Inzerillo. 2013. 123D Catch: efficiency, accuracy, constraints and limitations in architectural heritage field. Int. J. Herit. Digit. Era. 2: 263-290.

Siebert, J. P., and S. J. Marshall. 2000. Human body 3D imaging by speckle texture projection photogrammetry. Sensor Review 20: 218-226.

Sturzenegger, M., and D. Stead. 2012. The Palliser rockslide, Canadian rocky mountains: characterization and modeling of a stepped failure surface. Geomorphology. 138: 145-161.

Tucci, G. et al. 2001. Photogrammetry and 3D scanning: Assessment of metric accuracy for the digital model of Danatello's Maddalena. NRC Canada.

Waite, J. N., W. J. Schrader, J.-A. E. Mellish, and M. Horning. 2007. Three-dimensional photogrammetry as a tool for estimating morphometrics and body mass of Steller sea lions (Eumetopias jubatus). Can. J. fish Aquat. Sci. 64: 296-303.

Wakat, D. K., R. E. Johnson, H. J. Krzywicki, and L. I. Gerber. 1971. Correlation between body volume and body mass in men. Am. J. Clin. Nutr. 24: 1308-1312.

Ward, C. L. 1968. Obese or overweight?. Aerosp. Med. 39: 680-682.

Wells, J. C., I. Douros, N. J. Fuller, M. Elia, and L. Dekker. 2000. Assessment of body volume using three-dimensional photonic scanning. Ann. N. Y. Acad. Sci. 904: 247-254.

Wu, J. et al. 2004. Extracting the three-dimensional shape of live pigs using stereo photogrammetry. Comput. Electron. Agr. 44: 203-222.

Yu, C.-Y., Y.-H. Lo, and W.-K. Chiou. 2003. The 3D scanner for measuring body surface area: a simplified calculation in the Chinese adult. Appl. Ergon. 34: 273-278.

CHAPTER V.

CONCLUSIONS FROM RESEARCH PERFORMED AND FUTURE DIRECTIONS

5.1. Introduction

Application of 3D imaging technology on live animals has been studied minimally in spite of the growth of 3D scanning technology in the past decades. Our study described in chapter 2-4 of this thesis, however, showed easy applications of equine 3D image construction and the usage in the equine BW estimation. Low-cost 3D imaging technologies have advantages due to the price of equipment, easy application, and the accuracy. These technologies, however, still have some limitations in terms of the minimally restrained live animal 3D image construction.

In this chapter, limitations and obstacles that we were faced with during the accomplishment of this project, developed solutions to obstacles, and possible future applications of 3D imaging technology in horses and other animals are described.

5.2. Key take-home messages from the research performed

5.2.1. Lessons learned, modifications made to acquire equine 3D images

5.2.1.1. 3D scanning

Impact of environmental light intensity

A preliminary study using a small plastic horse model[nn] and a laser 3D scanner[oo] was conducted to determine the practicality of 3D scanning of a horse-shaped object. 3D scan was conducted under different levels of environmental light (50 lux: dark indoor, 500 lux: light indoor, 10,000 lux: under direct sunlight). The constructed 3D image showed surface irregularity when the 3D scanning was conducted under 10,000 lux light strength. This finding indicates the strong light reflection on the surface of the plastic horse model interfered with the projected laser of the 3D scanner. In addition, under a strong light, any shadowed area (e.g. under the abdomen) also resulted in a poor 3D image.

The laser projection pattern, laser type and data acquisition methods are different Depending on the 3D scanner (Sansoni et al., 2009). The pattern of error affected by environmental light, therefore, would be varied depending on the type of the 3D scanner. In our study, all of the equine 3D scanning was successfully conducted regardless of the difference in environmental light strength. Comparison of error (difference between the true body weight (BW) and predicted BW using 3DScan) between indoors and outdoors 3D scan was not conducted in this study because only two horses were scanned outdoors. The influence of light strength on 3D imaging

[nn] 13713 (item #), Schleich, Schwäbisch Gmünd, Germany
[oo] 3D Scanner HD, NextEngine Inc., 401 Wilshire Blvd., Ninth Floor, Santa Monica, California 90401.

should be addressed in future studies. Once the 3DScan method is applied in the equine industry, scans are highly to be performed outside under varying light intensity.

It is interesting to note that the 3D scanning ability of a structured light 3D scanner is not affected even if the location of scanning is in the dark. This might be because the projected light from the scanner is an infrared laser. The 3D scanning result itself would probably be better if the scanning was conducted at night rather than in the daytime. If the 3D scanning performed outside during the day is proven to have the same level of accuracy as indoor 3D scanning, it would indicate that 3D scanning can be used under any environmental light strength, dark or bright light.

Adjustment of the scanning method due to the movement of the horse

Obtaining an intact horse 3D image as a single image using the structured-light 3D scanner was not easy because even subtle movement of the horse may result in errors in the 3D image. Movement of the study horses during 3D scanning was most often observed in the head and neck area and occasionally in the lower limbs. It resulted in destruction of the overall image. Obtaining segmental body 3D images minimized body movement during 3D scanning and satisfactory 3D images were obtained.

Three-dimensional markers were attached on the body to facilitate the point alignment procedure of segmental 3D images to construct an entire body 3D image of the horse. Subsequent to the completion of our study, color acquisition function was added to the 3D scanning software. Due to the color acquisition function, markers such as color stickers, now, may be enough for the point alignment. If the color markers are found to be adequate, then preparation for 3D scanning

and the point alignment procedure will be much easier than it was at the time this study was conducted.

In terms of the horse movement, the advancement in the 3D scanning technology in the near future would make it available to obtain an accurate horse 3D image regardless its movement (Izadi et al., 2011). Once 3D imaging of a moving object is possible, segmental 3D image acquisition will no longer be required. In addition, BW estimation of a herd of animals in the field will also be possible. The potential for this technology is enormous since it will decrease the labor and time required for BW estimation of domestic or wild animals.

Options for minimizing the negative effect of subtle body movement while 3D image is being obtained

While 3D scanning was conducted, it was observed that the order in which the 3D image was obtained affected the quality of the 3D image of sections of the body that had slight regular external movement, e.g. respiration. When the 3D scanning of the trunk was conducted so that one lateral part was completely finished, and then the scan was continued in another direction, sometimes a large gap between the scanning start point and end point was observed. In contrast, when a 360-degree silhouette of the trunk was scanned rapidly at first and detailed imaging including the dorsal and ventral areas of the trunk was conducted later, the gap was minimized or did not exist. This difference might be because of the combined effect of horse respiration and intrinsic error of the structured-light 3D scanner (Cui and Stricker, 2011). When the trunk 3D scanning was conducted slowly from one part to next, surface movement of the trunk due to the horse's respiration induces distortion of the 3D image. On the contrary, when the silhouette of the trunk was obtained first, the slight geometric change of the trunk due to respiration might not

change the 3D image if the change is less than the detection level of the 3D scanner. The gap between the dotted laser projection patterns was described in chapter 1 of this thesis as a limiting factor in the structured-light 3D scanner. However when performing 3D scanning of a horse's truck area, this intrinsic error might minimize the distortion of the 3D image of the trunk due to respiration. Once the frame 3D image of the trunk was rapidly obtained, slight changes to the trunk geometry while adding details in the 3D image is negated especially when the change is within the range of detection of the error of the 3D scanner. Consequently, an accurate trunk 3D image was obtained. In addition, 3D scanning software must be designed to allow for some level of geometric change in the object.

3D image construction from the 3D scanner is conducted based on the geometric relationship between the previously scanned body part and the body part that is going to be scanned. This allows the operator to move around the object while obtaining the 3D image. We made interesting observations regarding this characteristic. When a horse moved his head and neck up and down quickly several times while 3D scanning of the head and neck was being conducted, the partially completed head and neck segmental 3D image was not corrupted but was observed to move on the screen following the horse movement. In addition, when we once tried to 3D scan the forelimbs and hindlimbs together, it was failed because tracking of the horse's limbs ceased during the procedure. This may be due to the too small scanned part of the horse (part of forelimbs and hindlimbs) to continue the tracking since there was a large gap in the middle of the scanning field between the forelimbs and hindlimbs in the image.

Rescaling and reconstruction of equine3D images, and suggestions for simple and easy 3D image acquisition

Size of the 3D image was exactly 1:1,000 smaller than the size of the true object in our study when the measurement was conducted using computer 3D software (Jecić and Drvar, 2003; Sansoni et al., 2009). The reason for this problem is uncertain but the problem was solved by simply multiplying the size of the 3D image times a 1,000. Details of the 3D image were not changed even if the image size is magnified, so there was no file size change after the multiplication of the size of the 3D image.

Conversely, the file size was changed dramatically in the image editing process. The size of the horse 3D image on the scanner was between 3-5 megabytes, and the size was increased in each image-editing step (e.g. alignment, cleaning, Poisson reconstruction), making the final file size approximately 200 megabytes. Image editing was conducted with Ply formatted 3D images and it must be one of the reasons that the file size was increased. The second reason was because we used high level of octree depth in Poisson reconstruction (Wilhelms and Van Gelder, 1992; Kazhdan et al., 2006; Zhou et al., 2011). A high level of octree depth increases the number of vertices and faces. After the Poisson reconstruction, the number of faces was increased to almost 1 million and the number was ten times that of the original 3D image.

Prior to the next step, decimation was applied to decrease the file size. Decimation is a procedure that decreases the number of vertices with minimal effect on the shape of the 3D image (Schroeder et al., 1992; Alciatore and Wohlers, 1996). In our study, the level of decimation was designated as the point where the volume change was under one liter compared to the original

image. After several preliminary assessments, the number of faces of the 3D model was decimated to 100,000.

Average time required to 3D scan a horse was 1 minute per segmental 3D image when the horse did not move very much. It took average an hour to obtain three sets of four intact segmental 3D images of a horse including the time required to prepare a horse (grooming, turned-in and –out from the paddock) and to repeat the 3D scanning when a 3D scanning was failed due to the horse movement. An additional hour on average was required to construct an entire horse 3D image using point alignment, Poisson reconstruction, and decimation. Occasionally more time was needed to make the necessary correction on a slightly distorted 3D image due to subtle movement of the horse during scanning.

The main reasons complicated image processing procedures were conducted in our study were because, at first, we tried to estimate the BW of horses based on the 3D image of the entire body, and, secondly, we believed that it was required to make a water tight 3D image to estimate the volume of the 3D imaged object. However, two interesting but important observations were made while the study was conducted:

1. Equine BW estimation was possible using only trunk 3D images.
2. Accurate volume measurement was obtainable even when there were small gaps in the 3D image.

These observations indicate that neither the point alignment nor the Poisson reconstruction may be required for equine BW estimation. This open a probability to develop a simple mobile device-based software to directly estimate the BW of horses using a structured light 3D scanner.

Equine BW estimation regression model

Our study showed a lower correlation coefficient between BW and BV of horses compared to human studies (Katch et al., 1967; Wakat et al., 1971). This may be due to the diverse physical characteristics of horses, such as the existence of body hair, mane, and tail and the hair length differences on these body parts. The error induced by hairiest parts of the body may significantly affect the accuracy of the 3DScan method if it is applied to breeds of horses with more hair than those used in our study or on horses with diseases that may affect the hair length, e.g. Cushing's disease. In addition, in our study, the tail was wrapped with an elastic band to minimize the error; therefore it is highly likely that BV measured from horses without the same preparation will be slightly different from our study. It is still quite likely that even with these factors that may induce errors in 3D scanning based equine BW estimation, the accuracy of this method would be significantly higher than other equine BW estimation methods.

5.2.1.2. Photogrammetry

Reference marker

Reference marker was designed as a grid form at first, but it was observed that the grid pattern interfered with reconstruction of the limbs. Next a black cross shape reference material was designed. This design made it easy to recognize the center of the imaging location and thus helped in locating chairs and other materials in their accurate positions. It was, however, observed that, for some horses, it was difficult to lead them onto the reference materials because they were fearful and were unwilling to step on the designated site. At one point, we tried using reference material that did not stick to the floor as we thought it would be helpful to be able to move the photographing location in order to calm down a nervous horse. It was easy to move the

material, however the use of non-stick material proved to be a bad idea because the paper slipped when a horse stepped on it, and this frightened the horse even more. If photogrammetry is applied to a large equine population in the future, a redesign of the reference materials will be required.

Adjustment made for the 2D image acquisition

At least three photographs are required for the desktop photogrammetry software and at least sixteen photographs for the mobile device software according to the photogrammetry manufacturer's instruction (Pouliquen, 2011). Sixteen photographs of a plastic horse model were obtained in three environmental light settings (50 lux, 500 lux, and 10,000 lux) in the first preliminary study but all of them failed to create a complete 3D image of the model. The number of photographs were changed to 24 and the 3D image was obtained when the photographs were taken in 500 lux, but failed when the photographs were taken in 50 lux and 10,000 lux environmental light strength areas. Next we obtained 36 photographs at the three heights; the carpus, the withers, and the height 1.5 times higher than the withers. 3D images were successfully constructed without failure using this method.

In a live horse, however, 3D image construction using photogrammetry with 36 photographs failed. The constructed 3D image showed that only half of the body, the right lateral side, showed as a complete 3D image, while the other half of the body, the left lateral side, failed to be completely constructed as a 3D image (Figure 5.1). Direction of the body where the 3D image construction failed was the same as where the assistant stood. Sometimes the assistant changed her/his position while the photographs were being taken. We hypothesized that movement by the assistant induced the corruption of the 3D image in the same direction. However, the true reason

is not known since there were several other different factors between right and left sides of the study horses, for example, the background wall color and the light strength. More photographs were added to the protocol; total 48 photographs taken at 3 heights; 16 at the carpus, 16 at the withers, and 16 at a height of 1.5 times higher than the withers. No further failures of 3D image construction was observed.

A disadvantage of photogrammetry is it is not possible to know whether the 3D image reconstruction will be successful or failed until the photographs are processed by the software. It is, therefore, important to obtain enough photographs of the horse to make it possible to build the 3D image without failure. Forty-eight photographs resulted in successful photogrammetry, and so this number was used throughout our study.

2D image acquisition and the 3D image construction

Only one person used the photographing device to more closely represent a horse owner obtaining all of the images by him- or herself Substantial amount of time was required for the 2D imaging. Movements of the horse while obtaining the photographs negatively impacted the construction of the 3D image. In order to improve the accuracy of photogrammetry of live animals, it will be necessary to enhance the quality of 2D images, minimize the required number of 2D images, and also decrease the time required to obtain 2D images.

The head and neck were the areas of the horse that most commonly moved during photography. There was a concern about the probability of total corruption of the 3D image construction due to the intervention by the head and neck movement. Fortunately, 3D images of the trunk of the horse were obtained without failure even when there was subtle head and neck movement. In photogrammetry, several identical points are recognized and the locations of those points are

constructed in three-dimensional space in such a way that the sum of the square errors due to the disagreement among points from multiple photographs was minimized. Even if the location of a small part of the object changes while photographs are obtained, so the sum of the square error is increased due to the disagreement of some points aligned in the 3D space, among points from photographs obtained before the location change and after the change, the construction of the 3D image can still be accomplished without the total corruption of the image as long as the largest part of the object is held standstill during the photography. This is because the sum of the square error increase due to the movement of the small part cannot be larger than the potential increase of the sum of the error that will occur if the major part of the object is slightly distorted in 3D space (Figure 5.2).

In the present study, photographs or video obtained during subtle head and neck movement of the horse were included in creation of the 3D image. The error induced by head and neck movement did not overwhelm the other body parts that were held constant thus the 3D image construction was well accomplished except the body part where there was the movement. We do not know if extreme segmental body movements would induce total failure of the 3D imaging or not because photographs or video containing extreme head and neck movement was not used for photogrammetry in this study. If the 3D image construction is successful even with 2D images obtained during extreme head and neck movement, photogrammetry based BW estimation of horses would be feasible with little concern about movement of the horse. This would make photogrammetry an easy and fast method for estimating the approximate BW of horses. It would be, therefore, worthwhile to answer the effect of the extreme body extremity movement on equine 3D image construction using photogrammetry in follow-up studies.

The detail of the 3D image constructed using photogrammetry was not as good as it was for 3D scanning. The volume measurement showed that the volume of the 3D images constructed using photogrammetry was larger than volume from the 3D scanning method. The loss of image detail might induce the overall volume increases, especially between the abdomen and limbs (Figure 5.3). In addition, the Poisson reconstruction itself resulted in a worsening of the image detail. 3D image reconstruction without the loss of the image detail might be possible if the image reconstruction were conducted using a simple hole filling function or using another 3D image reconstruction algorithm (Hoppe et al., 1992; Curless and Levoy, 1996; Amenta et al., 2001; Carr et al., 2001; Dey and Goswami, 2004; Ohtake et al., 2005; Kazhdan et al., 2006).

Regression model

Prior to the regression analysis procedure, it was hypothesized that the regression model developed from V group must have much lower R^2 than the P group since 3D image quality of the V group was much worse than the P group. The regression analysis showed that the R^2 of the equine BW estimation regression model of P group was a little higher than the V group, but the difference in R^2 was only 0.04. In addition, there was no significant difference in the error of the predicted BW compared to the true BW of the horses between these two groups. This illustrated obtaining 2D images in the shortest time possible eventually increases the accuracy of the constructed 3D image based equine BW estimation method.

2Dto3D method showed a lower mean error than weight tapes and Carroll's formula. 2Dto3D method is expected to have better result in the near future since the quality of cameras in mobile devices is improving quickly, and Photogrammetry technology is getting improved and being

more convenient to use. There is, therefore, a high probability that the 2Dto3D method will be the principle method used to accurately estimate equine BW in the near future.

5.3. Future applications

5.3.1. Equine medicine and equine sciences

Equine 3D scanning has the potential to be used in various areas of equine medicine beyond its utility in estimating BW. For example, the volumetric function and BSA measurements are useful in pharmacology, e.g. pharmacokinetics and pharmacodynamics of a drug (DuBois and DuBOIS, 1915; Benet et al., 1996; Sawyer and Ratain, 2001). Due to the difficulty of obtaining accurate BV and BSA measurements, the majority of pharmacologic studies have been conducted using approximated values based on other body indices such as BW or height (DuBois and DuBOIS, 1915). Since BV and BSA can be easily and accurately measured using 3D scanning, application of 3D scanning technology in pharmacologic studies can be a revolutionary step that may improve the understanding of metabolism of veterinary drugs. In addition, BSA measurement is important in oncology because it represents the distribution of body fluid better than BW and is used to determine the dose for chemotherapeutic agents whose margin of safety is very low (Peterson et al., 1996). This measurement can also be used for skin graft procedure since 3D scanning makes it easy to accurately estimate the surface area where the transplant is needed.

Volume measurement can be used to monitor a patient that is in danger of dehydration or developing edema (Sukul et al., 1993; Sander et al., 2002). Also, 3D scanning based volume

measurement can be an accurate and non-invasive method to measure the volume of tissue required for tissue transplant (Robb et al., 1996; Ji et al., 2002). In human medicine, medical use of 3D imaging technology is rapidly being developed. For example, 3D scanning and 3D printing technology are used in combination to make customized prosthetics, body supporting devices such as an exoskeleton for the patient who has scoliosis, producing artificial bones for orthopedics, in plastic surgery, and for educational programs such as 3D image based anatomy or virtual surgery programs (Morgan et al., 1995; Alciatore and Wohlers, 1996; Rengier et al., 2010; Ransley, 2014).

In equine medicine, this technology has applicability in the management of foals with angular limb deformities. Application of 3D imaging could be used to produce a customized limb exoskeleton of a foal with severe angular limb deformities, and then an assistance device could be used to correct the abnormal angle of the limbs by daily adjusting the angle. Customized exoskeleton can also be used for horses with limb fractures. The limbs of a horse support a large amount of weight, particularly in the adult. Due to the weight-bearing load, many horses with limb fractures develop secondarily problems such as laminitis in the opposite support limb. If an exoskeleton can be made for these horses that eases the weight bearing, the prognosis will be greatly improved.

Carroll's formula was reported to have better accuracy than weight tapes in other studies, but in our study Carroll's formula showed the same accuracy as use of a weight tape (Carroll and Huntington, 1988; Ellis and Hollands, 1998). One possible explanation of this comparatively lower accuracy of Carroll's formula than weight tape is that a mistake may have occurred during the measurement of body length or heart girth in our study. It is possible that a slight amount of slack in the measurement tape went undetected, resulting in an error of BW estimation.

The 3D images can be used for the accurate measurement of diverse body indices (Wu et al., 2004; Wang et al., 2006a). This characteristic of 3D scanning could be used to produce customized equestrian products. Measurement of the length and circumference of the head and nose of a horse, for example, would provide information needed to design a customized halter or bridle. Measurement of the back width and length, and analysis of the shape of the back could be used in the design of an optimal fitting saddle. For some horses there may be a need to have a customized saddle, saddle pad or blanket made. The 3D image of the horse would allow for these tack items to be produced to best fit the horse. Good saddle fit is very important in maximizing the performance of horses and also in preventing development of a chronic sore back. All of these potential applications of 3D imaging technology could improve athletic capability and quality of life of horses by preventing exercise related diseases.

Another advantage of the 3D imaging technology is that the entire body of the horse can be observed at a glance from any direction (Wang et al., 2006a). The 3D imaging of the 22 study horses allowed us to look at several body parts from directions we had not previously observed them, for example, from the dorsal view. The ability to observe the horse 3D images on a computer screen provided a great opportunity to compare the diversity of horse conformations. Even among horses with the same BCS and similar BW, diversity exists in their body conformation. The distribution of muscle mass and fat accumulation were different in each horse. Equine 3D image is a useful tool for body conformation analysis. The results of the analysis can then be used for planning an exercise regimen to improve the contour of the horse through strength and balance exercises and then assess the impact of the exercises by comparing 3D images obtained at prescribed time periods (Ross et al., 2000). In consequence, equine 3D

scanning can be used not only in the veterinary field, but also to improve the general management and welfare of horses.

5.3.2. Wild animals and other large animals

In the present study, BW estimation using 3D scanning was applied on live horses without any restraint or sedation (Wu et al., 2004; Waite et al., 2007), and this shows the potential of 3D scanning based BW estimation method for use on wild animals. BW estimation of wild animals is difficult, dangerous, and currently requires a lot of labor to sedate and manipulate the animals. To measure the BW of elephants or hippopotamuses, for example, several people have to work together to sedate the animal and move it by use of a crane onto a specially designed scale. Not only is the BW measurement difficult, but also the sedation process itself is risky, as miscalculation of the dosage of sedative drug commonly occurs, and results in either over or under dosing that is dangerous to the animal and the handlers (Arnemo et al., 2006; Jamieson, 2014). This is not only true for the huge wild animals such as the elephant or hippopotamus, but also is true for the BW measurement of comparatively small animals, often causing the death of the animal due to extreme stress, trauma during manipulation of the sedated animal or medication overdose.

BW estimation is required to properly monitor the health status of individual wild animals and herd health status. For zoo animals, record keeping of BW is important for monitoring health status and when treatment is required, e.g. deworming. BW measurement of these animals using a conventional method such as requiring them to move onto a scale frightens the animals and may result in injury or even death of the animal, or injury to their caretakers. 3D scanning based BW measurement can be applied without touching the animal, an advantage that can minimize

any potential distress to the animal and improving worker safety. In addition, the 3D scanning method does not require the use of an expensive equipment such as a crane. Decreased cost and increased safety for the BW estimation using 3D imaging method will make it possible to monitor the BW of the animals more frequently. The frequent BW estimation of the animals, especially sick animals or animals undergoing treatment, will provide more information regarding the animal health status and treatment adequacy.

The 3D image based BW measurement method does, however, require species- and sex-specific adjustment because 3D scanning only represents the silhouette of the object. Different species of animals have different body composition, and differing body surface characteristics such as hair length and type. In the case of lions, for example, their hair length and distribution is different between sexes, so the BW estimation formula based on the BV between male and female lions would be expected to be very different. Moreover, the limitation of 3D scanning field size also restricts the availability of 3D image based BW estimation. Currently, the maximum field size of the structured light 3D scanner that was used in our study is approximately 4m. 3D scanning of larger animals, therefore, would require segmental scanning which may make the procedure more difficult and complicated. Structured-light 3D scanning requires under 4 m distance between the scanning object and the scanner and this is also a limitation of the 3D scanning of zoo or wild animals.

There is also a possibility that movement of the scanning operator causes the animal to feel insecure. In our project, a few horses showed constant alertness to the location of the operator as they walked around the animal to obtain the image. Such a movement pattern might terrify the tied animal because the operator’s movement resembles that of some hunting predators. If a 3D scan is obtained far away from the animal, for example, using terrestrial 3D scanners, this would

not be a problem, but those 3D scanners are expensive[pp] and would only be available to those who could afford this equipment. If the approximation of the BW using the partial body 3D scanning is available, it will be useful since it will decrease not only the scanning time but also the distress of the animals being scanned.

5.3.3. Animal identification and breed association's registration process

Currently the American Quarter Horse Association (AQHA) requires five photographs for horse registration. Photographs, however, are restricted in their ability to represent the true shape and conformation of the horse. Even a slight change of the angle while photographing the horse gives a very different impression to the observers about the size and conformation of the horse. In addition, it is difficult to tell the true height and length of the horse from photographs. In contrast, 3D scanning makes it possible to observe the horse from every angle and from the bottom to the top. This method also gives accurate size information including height and body length. If equine 3D images were used in horse registration, it would help interested persons observe the horses in a much more accurate manner than with 2D images. This technology would also have utility in equine sales. In terms of the equine registration information, 3D images can also be added to the hard copy paper certification form using means such as QR code.[qq] People who are interested in the horse can scan the QR code using their mobile device and then view the 3D images of that horse on their device.

Several distinctive points on the horse that are represented in the 3D image can also be used to improve verification of the identity of the scanned horse. This method would be useful when a

[pp] Example of terrestrial 3D scanners are FARO laser tracker (FARO, Lake Mary, FL, USA) and Leica Scan Station (Leica, Wetzlar, Germany). The price of these 3D scanners is around $100,000 or more.
[qq] QR code: Quick Response Code

specific horse in a large herd needs to be identified or the identity of a horse which is being moved interstate or internationally needs to be verified. Since the 3D image of horses provides not only the color or partial shape information, but also the geometric body shape and accurate body indices such as height and body length, use of 3D images in registration and identification would decrease the labor needed to identify a horse in a large herd, and also prevent potential fraud when horses are sold, raced or moved interstate or internationally. 3D image based animal registration would have similar benefits if used for identification of other types of animals.

5.3.4. Equine conformation and body condition score evaluation

3D images of horses could be a useful tool to evaluate health and body conformation/condition status. Periodic 3D imaging of a horse in training would be a good way to evaluate and categorize the training status of the horse as poor, optimal, or excessive. In addition, 3D image of the horse would also provide the conformation information of a specific body part thus the trainer can modify the training strategy based on the acquired 3D image due to improving the quality of the body conformation analysis. When 3D images are obtained regularly and compared, they could provide information about body soreness since pain changes the overall contour or stance of the horse. If computer software to compare serially obtained 3D images of a horse was developed, the evaluation procedure would be more efficient and accurate. 3D image based horse evaluation will provide accurate information about the fitness and comfort level of a horse.

3D technology could be used to determine the BCS of the horse. BCS determination requires evaluation of six different area of the horse's body through visual examination or by manual palpation. The BCS system was developed to make the outcome more reproducible across

evaluators however this method remains very subjective. Each person may give a different BCS result on the same horse at any given point in time. In our study, there was up to a 2.5 level difference out of 9 levels between BCS evaluators who were all experienced horse people when they examined the same horse. This finding illustrates how much the BCS estimation can differ depending on the operator. This difference among experienced equine people can sometimes bring about a legal conflict. In many states in the USA, horse abuse such as emaciation due to negligence, can result in confiscation of the horses by the local authorities, but sometimes the confiscation stimulates a legal conflict between the owner and law enforcement. Documentation of horse's body condition based on the BCS of the horse(s) can be challenged based on differing opinions among experienced equine people about the score, giving rise to a challenge of the validity of the confiscation. If 3D imaging was used to document the horse's body condition then the body conformation and shape of the horse would be recorded in an accurate and objective way resulting in more objective defensible recording of the horse's body condition status for legal proceedings, e.g. shape of the ribcage and fat accumulation on the withers, neck, behind the shoulder, and over the buttocks. Since the 3D image provides accurate geometric distribution information for every body part of the horse, it will be possible to automatically determine the BCS by interpreting its 3D image. Once this automatic BCS determination method is developed, conflicts between law enforcement and horse owners and also disagreement among experienced equine people will be decreased.

In conclusion, 3D images of the animals have the potential to be used in diverse areas of veterinary medicine and animal science. Fast developing 3D scanning technology soon will make the imaging process easier and faster, and also widely expand the areas where it can be applied. The application of low-cost 3D imaging technology on horses will allow us to more

deeply understand their physical characteristics, diversity, and needs. In consequence, this method will contribute to improving the general welfare and soundness of horses.

5.4. Tables and figures

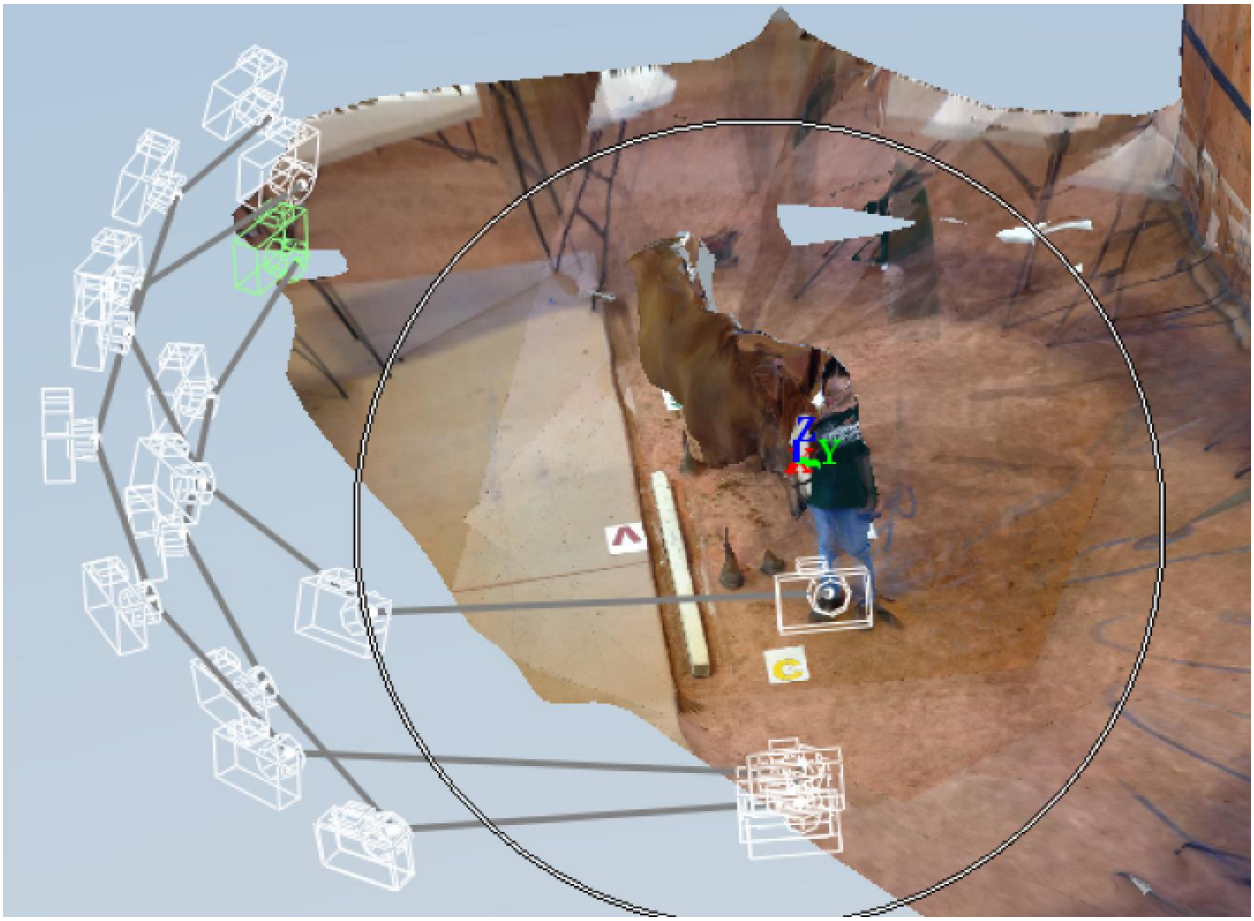

Figure 5.1. A photo enhancement that illustrates the incompleteness of the photogrammetry method when it was conducted with 36 photographs as a part of the preliminary study. The camera figures show the locations where the photographs were taken that lead to a successful photogrammetry procedure. Photographs were obtained from all directions around the horse but only photographs obtained on the right lateral side were successfully used for a complete 3D image construction. Photographs obtained on the left lateral side failed to be useable. Therefore, only the right lateral part of the horse was fully constructed in the resulting 3D image. This captured image shows that the left trunk of the horse is blank.

Figure 5.2.a. Photogrammetry based 3D image construction.

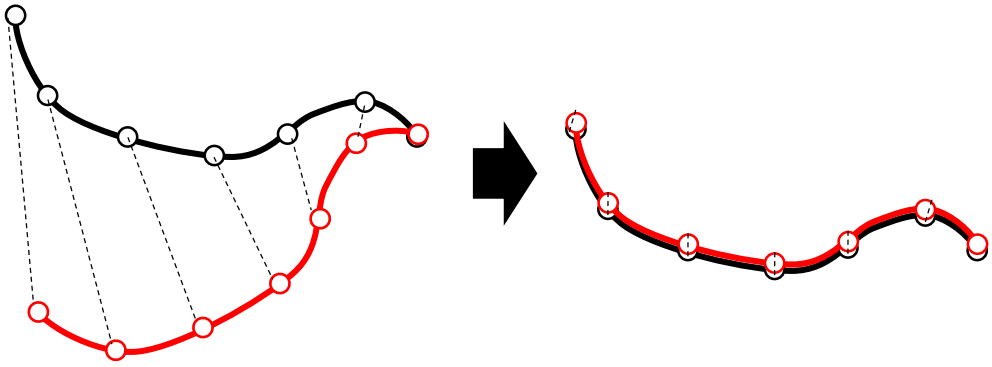

Figure 5.2.b. Photogrammetry based 3D image construction when there was a slight movement of the object.

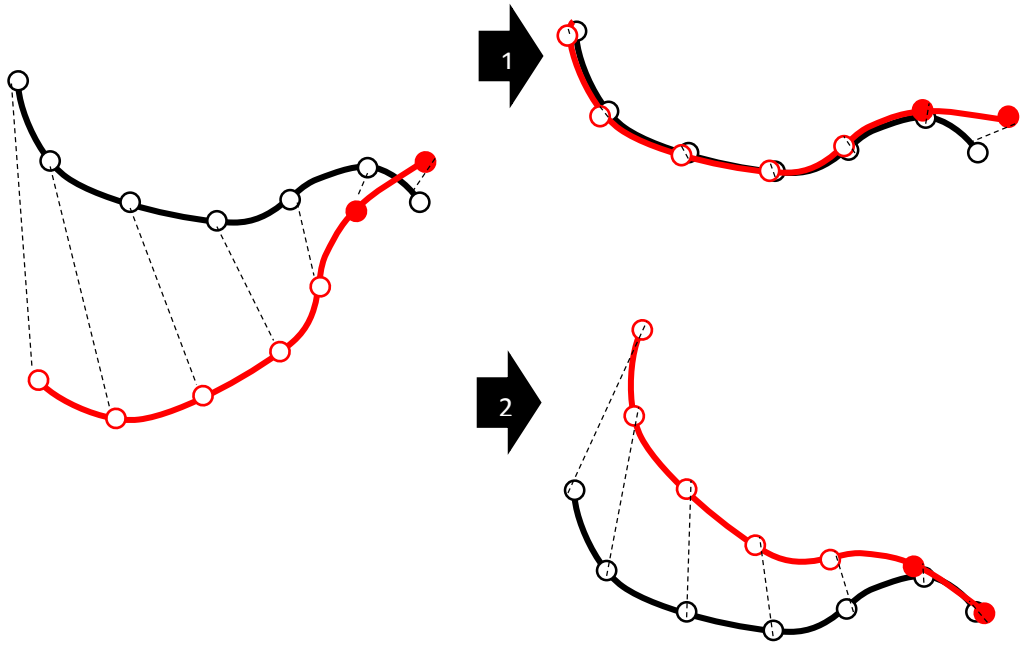

Figure 5.2. 3D image construction in photogrammetry. Black and red lines are silhouettes of an object photographed in different directions. Circles on the silhouettes represent the recognized point agreements. Dotted line is error of point agreement. The sum of the length of the dotted lines is an overall error of the point agreements (sum of the square error in 3D space). In photogrammetry, the 3D image of an object is constructed to minimize the error (minimize the sum of the length of the dotted lines) (Figure 5.2.a). In the case that there was a partial movement of the object (Figure 5.2.b) (Moved area is marked as red filled circles), error must increase in photogrammetry. 3D image is still constructed to minimize the sum of the error. If the area of movement is minimal, 3D image is still well constructed except the part where there was movement. The reason was the error due to the point disagreement of the areas of movement (Figure 5.2.b. arrow 1) was still smaller than the potential error increase when the point disagreement of unmoving part of the object increased due to the effect of the moving part (Figure 5.2.b. arrow 2).

Figure 5.3.a. Mesh of part of a 3D image of a horse constructed using photogrammetry.

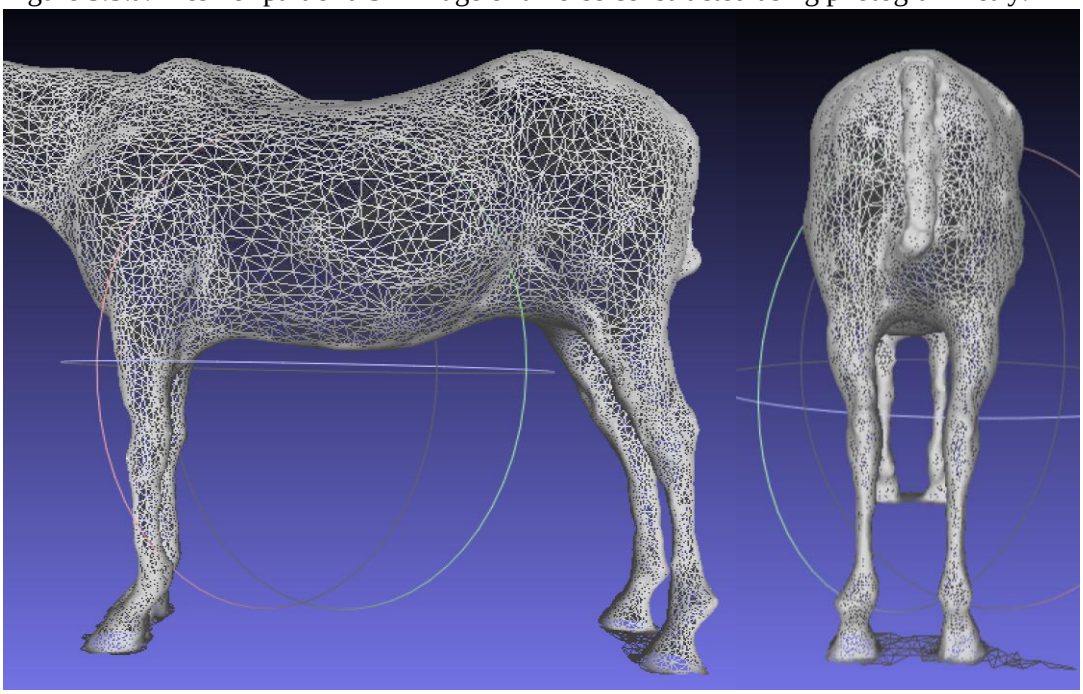

Figure 5.3.b. Part of an equine 3D image that was constructed using 3D scanning.

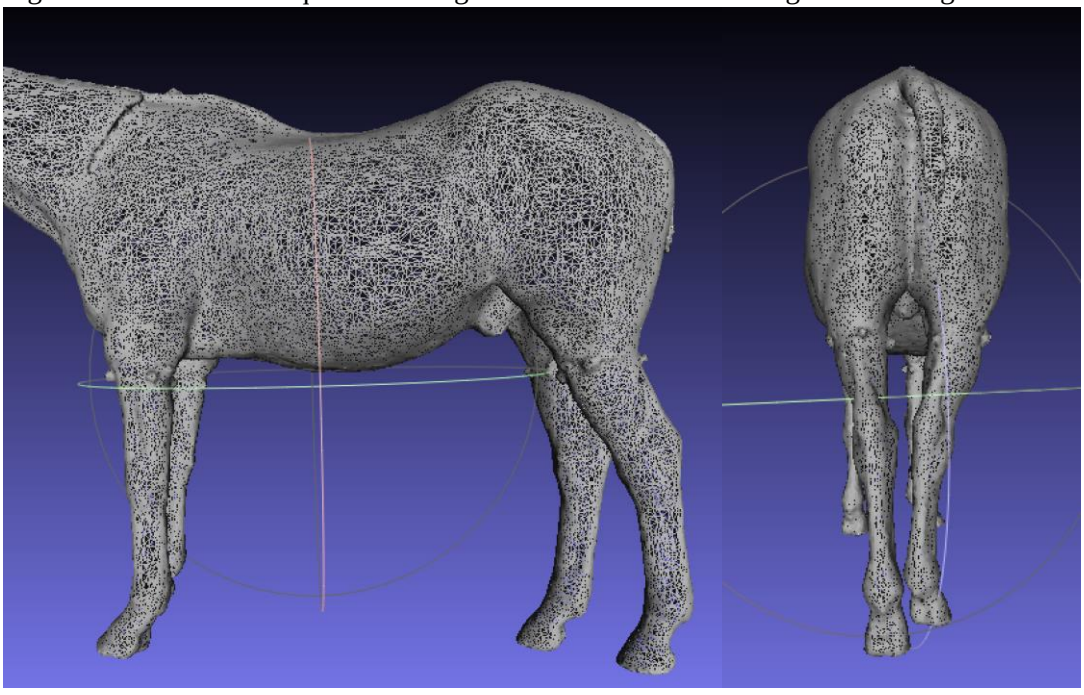

Figure 5.3. Comparison of the 3D images obtained using photogrammetry based equine 3D image construction (Figure 5.3.a) and 3D scanning (Figure 5.3.b). The boundaries of abdomen and limbs lacked detail in the 3D image and might induce the increase in the volume of the 3D image in photogrammetry based equine 3D image construction method compared to 3D scanning.

REFERENCES

AQHA, Register a Foal: Make your new foal a part of the world's largest breed registry. http://aqha.com/register (Accessed 8 June 2015).

Alciatore, D. G., and T. T. Wohlers. 1996. Importing and reshaping digitized data for use in rapid prototyping: a system for sculpting polygonal mesh surfaces. Rapid Prototyping J. 2: 13-23.

Alford, P. et al. 2001. A multicenter, matched case-control study of risk factors for equine laminitis. Prev. Vet. Med. 49: 209-222.

Allen, B., B. Curless, and Z. Popović. 2003. The space of human body shapes: reconstruction and parameterization from range scans. In: ACM Transactions on Graphics (TOG). p 587-594.

Amenta, N., S. Choi, and R. K. Kolluri. 2001. The power crust, unions of balls, and the medial axis transform. Comp. Geom. 19: 127-153.

Arnemo, J. M. et al. 2006. Risk of capture-related mortality in large free-ranging mammals: experiences from Scandinavia. Wildlife Biology 12: 109-113.

Baltsavias, E. P. 1999. A comparison between photogrammetry and laser scanning. ISPRS J. Photogramm. Remote Sens. 54: 83-94.

Bartoš, K., K. Pukanská, and J. Sabová. 2014. Overview of available open-source photogrammetric software, its use and analysis. Int. J. Innov. Educ. Res 2: 62-70.

Behnke, A., B. Feen, and W. Welham. 1942. The specific gravity of healthy men: body weight÷ volume as an index of obesity. JAMA 118: 495-498.

Benet, L. Z., D. Kroetz, L. Sheiner, J. Hardman, and L. Limbird. 1996. Pharmacokinetics: the dynamics of drug absorption, distribution, metabolism, and elimination. Goodman and Gilman's the pharmacological basis of therapeutics: 3-27.

Biaggi, R. R. et al. 1999. Comparison of air-displacement plethysmography with hydrostatic weighing and bioelectrical impedance analysis for the assessment of body composition in healthy adults. Am. J. Clin. Nutr. 69: 898-903.

Böhler, W., and A. Marbs. 2004. 3D scanning and photogrammetry for heritage recording: a comparison. In: Proceedings of the 12th International Conference on Geoinformatics. p 291-298.

Box, G. E. 1953. Non-normality and tests on variances. Biometrika: 318-335.

Brown, B. J., and S. Rusinkiewicz. 2007. Global non-rigid alignment of 3-D scans. ACM Transactions on Graphics (TOG) 26: 21.

Burkholder, W. J. 2000. Timely Topics in Nutrition. Use of body condition scores in clinical assessment of the provision of optimal nutrition. JAVMA 217: 650-654.

Carr, J. C. et al. 2001. Reconstruction and representation of 3D objects with radial basis functions. In: Proceedings of the 28th annual conference on Computer graphics and interactive techniques. p 67-76.

Carroll, C., and P. Huntington. 1988. Body condition scoring and weight estimation of horses. Equine Vet. J. 20: 41-45.

Chandler, J., and J. Fryer. 2013. Autodesk 123D catch: how accurate is it. Geomatics World 2: 28-30.

Christie, J. L. et al. 2006. Management factors affecting stereotypies and body condition score in nonracing horses in Prince Edward Island. Can. Vet. J. 47: 136.

Cignoni, P., M. Corsini, and G. Ranzuglia. 2008. Meshlab: an open-source 3d mesh processing system. Ercim news 73: 45-46.

Clauser, C. E., J. T. McConville, and J. W. Young. 1969. Weight, volume, and center of mass of segments of the human body, DTIC Document.

Cui, Y., S. Schuon, S. Thrun, D. Stricker, and C. Theobalt. 2013. Algorithms for 3d shape scanning with a depth camera. IEEE Trans. Pattern. Anal. Mach. Intell. 35: 1039-1050.

Cui, Y., and D. Stricker. 2011. 3d shape scanning with a kinect. In: ACM SIGGRAPH 2011 Posters. p 57.

Curless, B., and M. Levoy. 1996. A volumetric method for building complex models from range images. In: Proceedings of the 23rd annual conference on Computer graphics and interactive techniques. p 303-312.

Daubenspeck, J. A., A. Li, and E. E. Nattie. 2008. Acoustic plethysmography measures breathing in unrestrained neonatal mice. J. Appl. Physiol. 104: 262-268.

Deltombe, T. et al. 2007. Reliability and Limits of Agreement of Circuferential, Water Displacement, and Optoelectronic Volumetry in the Measurement of Upper Limb Lymphedema. Lymphology 40: 26-34.

Dempster, P., and S. Aitkens. 1995. A new air displacement method for the determination of human body composition. Med. Sci. Sports Exerc. 27: 1692-1697.

Dey, T. K., and S. Goswami. 2004. Provable surface reconstruction from noisy samples. In: Proceedings of the twentieth annual symposium on Comp. geom. p 330-339.

DuBois, D., and E. F. DuBOIS. 1915. Fifth paper the measurement of the surface area of man. Arch. Intern. Med. 15: 868-881.

Ellis, J., and T. Hollands. 1998. Accuracy of different methods of estimating the weight of horses. Vet. Rec. 143: 335-336.

Geor, R. J. 2008. Metabolic predispositions to laminitis in horses and ponies: obesity, insulin resistance and metabolic syndromes. J. equine Vet. Sci. 28: 753-759.

German, A. J. 2006. The growing problem of obesity in dogs and cats. J. Nutr. 136: 1940S-1946S.

Gharahveysi, S. 2012. Compare of Different Formulas of Estimating the Weight of Horses by the Iranian Arab Horse Data. JAVA 11: 2429-2431.

Gibbs, P., and D. Householder. Estimating Horse Body Weight with a Simple Formula. http://www.aspcapro.org/sites/pro/files/estimating_horse_body_weight.pdf (Accessed 4 April 2015). Texas A&M.

Gibbs, P. G., G. D. Potter, and M. Vogelsang. 2005. Nutritional and Feeding Management of Broodmares. http://scholar.google.com/scholar?q=Nutritional+and+Feeding+Management+of+Broodmares&btnG=&hl=en&as_sdt=0%2C6 (Accessed 4 April 2015).

Giles, S. L., S. A. Rands, C. J. Nicol, and P. A. Harris. 2014. Obesity prevalence and associated risk factors in outdoor living domestic horses and ponies. Peer J. 2: e299.

Gnaedinger, R. et al. 1963. DETERMINATION OF BODY DENSITY BY AIR DISPLACEMENT, HELIUM DILUTION, AND UNDERWATER WEIGHING*. Ann. N. Y. Acad. Sci. 110: 96-108.

Goldman, R., and E. Buskirk. 1961. Body volume measurement by underwater weighing: description of a method. Techniques for measuring body composition: 78-89.

Gruen, A., and D. Akca. 2005. Least squares 3D surface and curve matching. ISPRS J. Photogramm. Remote Sens. 59: 151-174.

Hardman, A. C. L. 1980. Equine nutrition. Michael Joseph.

Hasler, N., C. Stoll, B. Rosenhahn, T. Thormählen, and H.-P. Seidel. 2009. Estimating body shape of dressed humans. Computers & Graphics 33: 211-216.

Hatcher, D. C., and C. L. Aboudara. 2004. Diagnosis goes digital. Am. J. Orthod. Dentofacial Orthop. 125: 512-515.

Henneke, D., G. Potter, and J. Kreider. 1981. Rebreeding efficiency in mares fed different levels of energy during late gestation. In: Proc 7th Eq. Nutr. Physiol. Symp. Virginia State Univ. p 101-104.

Henneke, D., G. Potter, J. Kreider, and B. Yeates. 1983. Relationship between condition score, physical measurements and body fat percentage in mares. Equine Vet. J. 15: 371-372.

Henry, P., M. Krainin, E. Herbst, X. Ren, and D. Fox. 2012. RGB-D mapping: Using Kinect-style depth cameras for dense 3D modeling of indoor environments. Int. J. Robot. Res. 31: 647-663.

Hile, M. E., H. F. Hintz, and H. N. Erb. 1997. Predicting body weight from body measurements in Asian elephants (Elephas maximus). J Zoo. Wildl. Med.: 424-427.

Hoppe, H., T. DeRose, T. Duchamp, J. McDonald, and W. Stuetzle. 1992. Surface reconstruction from unorganized points. ACM.

Huang, Q.-X., S. Flöry, N. Gelfand, M. Hofer, and H. Pottmann. 2006. Reassembling fractured objects by geometric matching. ACM Transactions on Graphics (TOG) 25: 569-578.

Hubert, H. B., M. Feinleib, P. M. McNamara, and W. P. Castelli. 1983. Obesity as an independent risk factor for cardiovascular disease: a 26-year follow-up of participants in the Framingham Heart Study. Circulation 67: 968-977.

Istook, C. L., and S.-J. Hwang. 2001. 3D body scanning systems with application to the apparel industry. JFMM 5: 120-132.

Izadi, S. et al. 2011. KinectFusion: real-time 3D reconstruction and interaction using a moving depth camera. Proc. 24th ACM symposium on User interface software and technology. p 559-568.

Jamieson, D. 2014. Against zoos. Revista Brasileira de Direito Animal 3.

Jecić, S., and N. Drvar. 2003. The assessment of structured light and laser scanning methods in 3D shape measurements. Proc. 4th International Congress of Croatian Society of Mechanics. p 237-244.

Ji, Y., F. Zhang, J. Schwartz, F. Stile, and W. C. Lineaweaver. 2002. Assessment of facial tissue expansion with three-dimensional digitizer scanning. J. Craniofac. Surg. 13: 687-692.

Johnson, E., R. Asquith, and J. Kivipelto. 1989. Accuracy of weight determination of equids by visual estimation. Proc. 11th ENPS. Stillwater, Oklahma. p 240.

Jones, R., T. Lawrence, A. Veevers, N. Cleave, and J. Hall. 1989. Accuracy of prediction of the liveweight of horses from body measurements. Vet. Rec. 125: 549-553.

Katch, F., E. D. Michael, and S. M. Horvath. 1967. Estimation of body volume by underwater weighing: description of a simple method. J. Appl. Physiol. 23: 811-813.

Kaushal, R. et al. 2001. Medication errors and adverse drug events in pediatric inpatients. JAMA 285: 2114-2120.

Kazhdan, M., M. Bolitho, and H. Hoppe. 2006. Poisson surface reconstruction. Proc 4th Symp. Geom. Process.

Khoshelham, K. 2011. Accuracy analysis of kinect depth data. ISPRS workshop laser scanning. 133-138.

Kilby, E. R. 2007. The demographics of the US equine population. http://www.humanesociety.org/assets/pdfs/hsp/soaiv_07_ch10.pdf (Accessed 26 December 2014). The humane society of the United States.

King, T. I. 1993. The effect of water temperature on hand volume during volumetric measurement using the water displacement method. J. Hand Ther. 6: 202-204.

Levoy, M. et al. 2000. The digital Michelangelo project: 3D scanning of large statues. Proc. 27th annual conference on Computer graphics and interactive techniques. p 131-144.

Liu, Y., and J. Kang. Application of Photogrammetry: 3D Modeling of a Historic Building. Construction Research Congress 2014 at Construction in a Global Network. p 219-228.

Magnusson, M., A. Lilienthal, and T. Duckett. 2007. Scan registration for autonomous mining vehicles using 3D-NDT. J. field Robot. 24: 803-827.

Martín, S., H. Uzkeda, J. Poblet, M. Bulnes, and R. Rubio. 2013. Construction of accurate geological cross-sections along trenches, cliffs and mountain slopes using photogrammetry. Computers & Geosciences 51: 90-100.

McCrory, M. A., T. D. Gomez, E. M. Bernauer, and P. A. Molé. 1995. Evaluation of a new air displacement plethysmograph for measuring human body composition. Med. Sci. Sports Exerc. 27: 1686-1691.

McDonnell, S. M. 2005. Techniques for Extending the Breeding Career of Aging and Disabled Stallions. Clin. Tech. Equine. Pract. 4: 269-276.

Mendell, C. A Better “Weigh”. http://homesforhorses.org/wp-content/uploads/BCS.pdf (Accessed on April 4 2015).

Milner, J., and D. Hewitt. 1969. Weight of horses: improved estimates based on girth and length. Can. Vet. J. 10: 314.

Morgan, K., R. Satava, H. Sieburg, R. Mattheus, and J. Christensen. 1995. Virtual reality assisted surgery program. St. Heal. T. 18: 309.

Munkelt, C., B. Kleiner, T. Torhallsson, P. Kühmstedt, and G. Notni. 2014. Handheld 3D Scanning with Automatic Multi-View Registration Based on Optical and Inertial Pose Estimation. Fringe. 2013. p 809-814. Springer.

Ohtake, Y., A. Belyaev, M. Alexa, G. Turk, and H.-P. Seidel. 2005. Multi-level partition of unity implicits. ACM SIGGRAPH. 2005. Courses. p 173.

Ozsoy, U., B. M. Demirel, F. B. Yildirim, O. Tosun, and L. Sarikcioglu. 2009. Method selection in craniofacial measurements: advantages and disadvantages of 3D digitization method. J Craniomaxillofac. Surg. 37: 285-290.

Pagan J.D., J. S., Duren S. What does your horse weigh?. www.ker.com/library/advances/113 (Accessed April 29 2015).

Peterson C.M., Lu J.M., Sun Y., Peterson C.A., Shiah J.G., Straight R.C., and Kopeček J. 1996. Combination chemotherapy and photodynamic therapy with N-(2-hydroxypropyl) methacrylamide copolymer-bound anticancer drugs inhibit human ovarian carcinoma heterotransplanted in nude mice. Cancer Res. 56: 3980-3985.

Polo, M.-E., and Á. M. Felicísimo. 2012. Analysis of uncertainty and repeatability of a low-cost 3d laser scanner. Sensors. 12: 9046-9054.

Pouliquen, D. 2011. It's a Snap! Take a photograph and create a 3D. https://www.thingiverse.com/download:75082 (Accessed 4 April 2015). Autodesk University.Model. https://thingiverse-production.s3.amazonaws.com/assets/8a/3e/e6/60/19/catchManual.pdf (Accessed May 1 2015).

Powers, J. H. 2009. Risk perception and inappropriate antimicrobial use: yes, it can hurt. Clin. Infect. Dis. 48: 1350-1353.

Ramos, E. 2012. Kinect Basics Arduino and Kinect Projects. p 23-34. Springer.

Ransley, M. 2014. Developing Wearable Assistive Materials for Orthopaedic Applications-3 Month Report.

Rathbun, E. N., and N. Pace. 1945. Studies on body composition I. The determination of total body fat by means of the body specific gravity. J. Biol. Chem. 158: 667-676.

Rengier, F. et al. 2010. 3D printing based on imaging data: review of medical applications. Int. J. Comput. Assist. Radiol. Surg. 5: 335-341.

Robb, R. A., D. P. Hanson, and J. J. Camp. 1996. Computer-aided surgery planning and rehearsal at Mayo Clinic. Computer 29: 39-47.

Ross, R., J. A. Freeman, and I. Janssen. 2000. Exercise alone is an effective strategy for reducing obesity and related comorbidities. Exerc. Sport Sci. Rev. 28: 165-170.

Rothman, K. J., S. Greenland, and T. L. Lash. 2008. Modern epidemiology. Lippincott Williams & Wilkins.

Runciman, B., and M. Walton. 2007. Safety and ethics in healthcare: a guide to getting it right. Ashgate Publishing, Ltd.

Sander, A. P., N. M. Hajer, K. Hemenway, and A. C. Miller. 2002. Upper-extremity volume measurements in women with lymphedema: a comparison of measurements obtained via water displacement with geometrically determined volume. Phys. Ther. 82: 1201-1212.

Sansoni, G., M. Trebeschi, and F. Docchio. 2009. State-of-the-art and applications of 3D imaging sensors in industry, cultural heritage, medicine, and criminal investigation. Sensors. 9: 568-601.

Santagati, C., and L. Inzerillo. 2013. 123D Catch: efficiency, accuracy, constraints and limitations in architectural heritage field. Int. J. Herit. Digit. Era. 2: 263-290.

Sawyer, M., and M. J. Ratain. 2001. Body surface area as a determinant of pharmacokinetics and drug dosing. Invest. New Drugs. 19: 171-177.

Schroeder, W. J., J. A. Zarge, and W. E. Lorensen. 1992. Decimation of triangle meshes. ACM Siggraph Computer Graphics. p 65-70.

Seidel, D., F. Beyer, D. Hertel, S. Fleck, and C. Leuschner. 2011. 3D-laser scanning: A non-destructive method for studying above-ground biomass and growth of juvenile trees. Agr. forest Meteorol. 151: 1305-1311.

Sheng, H.-P., A. L. Adolph, and C. Garza. 1988. Body volume and fat-free mass determinations by acoustic plethysmography. Pediatr. Res. 24: 85-89.

Sholts, S. B., S. K. Wärmländer, L. M. Flores, K. W. Miller, and P. L. Walker. 2010. Variation in the measurement of cranial volume and surface area using 3D laser scanning technology. J. Forensic Sci. 55: 871-876.

Siebert, J. P., and S. J. Marshall. 2000. Human body 3D imaging by speckle texture projection photogrammetry. Sensor Review 20: 218-226.

Sillence, M., G. Noble, and C. McGowan. 2006. Fast food and fat fillies: the ills of western civilisation. Vet. J. 172: 396-397.

Slater, M. R., D. Hood, and G. Carter. 1995. Descriptive epidemiological study of equine laminitis. Equine Vet. J. 27: 364-367.

Smisek, J., M. Jancosek, and T. Pajdla. 2013. 3D with Kinect Consumer Depth Cameras for Computer Vision. p 3-25. Springer.

Sturzenegger, M., and D. Stead. 2012. The Palliser rockslide, Canadian rocky mountains: characterization and modeling of a stepped failure surface. Geomorphology. 138: 145-161.

Sukul, D. K., P. T. den Hoed, E. Johannes, R. Van Dolder, and E. Benda. 1993. Direct and indirect methods for the quantification of leg volume: comparison between water displacement volumetry, the disk model method and the frustum sign model method, using the correlation coefficient and the limits of agreement. J. Biomed. Eng. 15: 477-480.

Taylor, M. W. 2012. 3D surface modeling of a giant redwood trunk The magazine of the native tree society No. 2. p 101.

Tikuisis, P., P. Meunier, and C. Jubenville. 2001. Human body surface area: measurement and prediction using three dimensional body scans. Eur. J. Appl. Physiol. 85: 264-271.

Tong, J., J. Zhou, L. Liu, Z. Pan, and H. Yan. 2012. Scanning 3d full human bodies using kinects. Visualization and Computer Graphics, IEEE Trans. Pattern. Anal. Mach. Intell. 18: 643-650.

Tucci, G. et al. 2001. Photogrammetry and 3D scanning: Assessment of metric accuracy for the digital model of Danatello's Maddalena. NRC Canada.

Uyar, R., and F. Erdoğdu. 2009. Potential use of 3-dimensional scanners for food process modeling. J. Food Eng. 93: 337-343.

Waite, J. N., W. J. Schrader, J.-A. E. Mellish, and M. Horning. 2007. Three-dimensional photogrammetry as a tool for estimating morphometrics and body mass of Steller sea lions (Eumetopias jubatus). Can. J. fish Aquat. Sci. 64: 296-303.

Wakat, D. K., R. E. Johnson, H. J. Krzywicki, and L. I. Gerber. 1971. Correlation between body volume and body mass in men. Am. J. Clin. Nutr. 24: 1308-1312.

Wang, J. et al. 2006a. Validation of a 3-dimensional photonic scanner for the measurement of body volumes, dimensions, and percentage body fat. Am. J. Clin. Nutr. 83: 809-816.

Wang, Y.-C., M.-S. Wei, Y.-Y. Jiang, Y.-H. Chang, and Y.-H. Fan. 2006b. Automatic Measurement System using a Laser Scan Instrument for Ceramic Bearings. 8th International Conference on Laser and Fiber-Optical Networks Modeling. p 66-69.

Ward, C. L. 1968. Obese or overweight? Aerosp. Med. 39: 680-682.

Wells, J. C., I. Douros, N. J. Fuller, M. Elia, and L. Dekker. 2000. Assessment of body volume using three-dimensional photonic scanning. Ann. N. Y. Acad. Sci. 904: 247-254.

Wilhelms, J., and A. Van Gelder. 1992. Octrees for faster isosurface generation. ACM Transactions on Graphics (TOG) 11: 201-227.

Wu, J. et al. 2004. Extracting the three-dimensional shape of live pigs using stereo photogrammetry. Comput. Electron. Agr. 44: 203-222.

Wulf, O., and B. Wagner. 2003. Fast 3D scanning methods for laser measurement systems. International conference on control systems and computer science (CSCS14). p 2-5.

Wylie, C. E., S. N. Collins, K. L. Verheyen, and J. R. Newton. 2012. Risk factors for equine laminitis: a systematic review with quality appraisal of published evidence. Vet. J. 193: 58-66.

Wyse, C., K. McNie, V. Tannahil, J. Murray, and S. Love. 2008. Prevalence of obesity in riding horses in Scotland. Vet. Rec. 162: 590.

Yu, C.-Y., Y.-H. Lo, and W.-K. Chiou. 2003. The 3D scanner for measuring body surface area: a simplified calculation in the Chinese adult. Appl. Ergon. 34: 273-278.

Zhou, K., M. Gong, X. Huang, and B. Guo. 2011. Data-parallel octrees for surface reconstruction. Visualization and Computer Graphics, IEEE Trans. Pattern. Anal. Mach. Intell. 17: 669-681.

APPENDIX

Appendix 1. Definition of terms

Ambulatory care: Medical care provided on the farm. The care includes diagnosis of disease, preventative care, consultation, rehabilitation, and treatment.

American Quarter Horse: An American breed of horse. The name originated from a characteristic of this breed that has a great strength and speed in a quarter mile race.

Bias (epidemiology): The result of the unmeasured factor (e.g. confounder) that negatively affects the understanding of the true relationship between two factors or the risk and the disease.

Coefficient of determination: The strength of correlation between the dependent variable and a regression equation made by single or multiple independent variable(s). If there is a complete correlation, the coefficient of determination is 1. In the situation of no correlation, the value is 0.

Conformation (horse): The shape and body structure of horses. The conformation of a horse is used to evaluate the athletic potential of the horse.

Conventional method (equine BW estimation): Equine BW estimation methods that have been already developed and used in the equine industry, e.g., weight tape, visual estimation, or a large animal scale.

Cook's distance: A statistical method of testing an outlier among observations. Generally, the sample was considered as an outlier if Cook's distance is larger than 1.

Correlation coefficient: The strength of correlation between two numeric variables. If there is a complete correlation between the two variables, correlation coefficient is 1. In the situation of no correlation, the value is 0.

Dependent variable: In a regression analysis, the dependent variable is a variable of interest that the numeric value can be predicted by the measurement of other easily measurable variables (independent variables).

Deworm: Treat an animal to remove parasites.

Dosage: An amount of drug or medicine prescribed for a patient.

Dystocia: Difficult parturition/birthing.

Epidemiology: A study of the cause of a disease and the pattern in a population and development and application of a strategy to prevent the disease based on the study of the cause and pattern.

Face (3D): A triangle shaped surface made by 3 vertices. Combinations of faces create a 3D image.

Global non-rigid alignment: A method to assemble several partial 3D images into one. This alignment method makes it available to create a combined 3D image even when there is a slight difference between some of the partial 3D images. Low-frequency non-rigid deformation can occur even among 3D images of the same object due to device nonlinearities of calibration error.

Hanoverian: A warmblood horse originating from Germany. Commonly used for English riding, dressage, or carriage driving.

Infrared (IR) projector/IR camera: A light source and light reflection recording device used in structured-light 3D scanner. Infrared light pattern is not detectable by human eyes.

Iterative closest point (ICP) algorithm: A surface reconstruction algorithm when two or more 3D images with partially overlapped areas are combined. The images are combined together so the direction of the differences between two point clouds are minimized.

Laminitis: An equine disease when the laminae in the hoof are inflamed and, in a severe cases, separation of hoof from the coffin bone occurs. Laminitis is caused by severe inflammation and result in hoof pain in the horse.

Levene's test: A statistical test used to confirm the equality of variances of two or more groups of comparisons. Generally, if the p-value is less than 0.05, it means the distribution of variances are not equal between (among) groups.

Mane: A long continuously growing hair along the top of the neck of a horse between the forehead and the withers.

Natural logarithm: A logarithm to the base e; e=2.71828.

Octree depth: The depth of the 3D image subdivision. One octree increase represents 8 times of image subdivision.

One-way ANOVA: A statistical method to compare the means of more than two groups.

Osteochondrosis: A type of developmental orthopedic disease. Developing cartilage is usually affected and, in affected horses, the joint margins are changed, and a cartilage flap is created. It is believed to occur from a focal disturbance in endochondral ossification. In horses, rapid growth, over-nutrition, and mineral imbalance are known risk factors.

Pair-wise comparison: A statistical method to compare the means of more than two groups in pair-wise way. For example, there are a total of 6 comparisons in the comparison of 4 groups.

Pharmacodynamics: A study of the action and the effect of a drug in the body.

Pharmacokinetics: A study of the drug absorption, distribution, metabolism, and the excretion in the body.

Point based gluing alignment: A 3D image construction method. This method is commonly used to construct an intact entire 3D image of an object by using several segmental 3D images of the object. Usually, a minimum of 4 identical locations in different segmental 3D images are designated by the user and the partial 3D images are assembled based on those manually recognized points.

Point of buttock: The most caudal point of the horse's rump. The tuber ischii is ventral to this point.

Point of shoulder: A spot in the front of the horse trunk that is the cranial point of the shoulder joint.

Poisson surface reconstruction: A 3D image surface reconstruction method which was developed by M. Kazhdan. This reconstruction method is known to minimize the noise of 3D data and makes it available to achieve a highly detailed surface reconstructed 3D image.

Power: A probability of correctly rejecting the null hypothesis when the alternative hypothesis is the truth.

Predictor variable (independent variable): Numeric variables in a regression model that can predict the value of the dependent variable.

Preliminary study: A study which is conducted prior to the main study. A preliminary study is usually conducted when there is not enough currently available information (e.g. published research papers) to determine the methods to include in main study.

Quadric edge collapse decimation: A method to decrease the number of vertices and faces of the 3D image. Decimation may induce the decrease of the 3D image detail.

Reconstruction (3D image): A 3D image defect correction procedure to construct a true 3D image that does not have any hole that connects inside and outside of the 3D image.

Regression model: A statistical model to analyze the linear correlation between (among) numerical variables.

Residual: A difference between the predicted value and the observed value.

Studentized residual: A value where the residual is divided by the standard deviation. This method is commonly used to detect an outlier. When the value of studentized residual is bigger than 3, the sample is considered as an outlier.

Thoroughbred: A breed of the horse most commonly used worldwide in racing.

Tidal volume: The lung air volume difference between normal inhalation and exhalation without an extra effort of respiration.

T-test: A statistical method of mean comparisons of two groups.

Volumetric reconstruction: A 3D image surface reconstruction method which was developed by Curless et al.

Withers (horse): The highest point on the top line of the horse. This is the point where the tallest spinous process of thoracic vertebraees is located underneath